Abstract Volume
10th Swiss Geoscience Meeting

Bern, 16th – 17th November 2012

3. Mineralogy, Petrology, Geochemistry

sc | nat
Swiss Academy of Sciences
Akademie der Naturwissenschaften
Accademia di scienze naturali
Académie des sciences naturelles

UNIVERSITÄT
BERN

3. Mineralogy, Petrology, Geochemistry &
4. Tracing magmatic systems from the petrological, geochemical and isotopic perspective &
5. Low-Temperature Isotope Geochemistry

Eric Reusser, Bernard Grobéty, Benjamin Heredia, Sebastien Pilet, Thomas Nägler,
Elias Samankassou, Andrea R. Voegelin

Swiss Society of Mineralogy and Petrology (SSMP)

TALKS:

3.1 Cochrane R., Spikings R., Chew D., Wotzlaw J. F., Chiaradia M., Tyrrell S., Schaltegger U., Van der Lelij R.: Extracting accurate high temperature thermal histories from crustal rocks

3.2 Cooper L., Reubi O., Dungan M., Bourdon B., Langmuir C., Turner S., Schaefer J.: Using U-series and beryllium isotopes to reveal the occurrence and relative timing of crustal and mantle processes in the Southern Volcanic Zone of Chile

3.3 El Korh A.: Ablation behaviour of titanite and constraints for U–Th–Pb geochronology using LA-ICP-MS

3.4 Ferreiro Mählmann R., Bozkaya Ö., Potel S., Le Bayon R., Segvic B., Nieto García F.: The pioneer work of Bernard Kübler and Martin Frey in very low-grade metamorphic terranes: Paleo-geothermal potential of variation in Kübler-Index/organic matter reflectance correlations – a review

3.5 Greber N.D., Neubert N., Nägler T.F.: Do Mo isotope fractionation processes accompany the dissolution of molybdenites? Studying the interface of water, molybdenite and their weathering products.

3.6 Luginbühl S., Ulmer P., Pettke T.: The geochemistry of aqueous fluids and hydrous melts in subduction zones

3.7 Mattsson, H.B.: Ascent and fragmentation in volcanic eruptions involving CO_2-rich silicate magmas

3.8 Moeller K., Schoenberg R., Grenne T, Thorseth I.H., Pedersen, R.B.: Fe stable isotope fractionation in modern and ancient hydrothermal Fe-Si deposits

3.9 Nandedkar R., Ulmer P., Müntener O., Hürlimann N.: Trace element partitioning along the liquid line of descent from olivine-tholeiite to granite

3.10 Ortelli M., Kouzmanov K., Dilles J.H., Rusk B.G.: Fluid inclusion study in ore and gangue minerals from Main Stage veins at Butte, Montana.

3.11 Pinget M. MC., Dold B., Fontboté L.: Exotic mineralization at Chuquicamata, Chile: focus on the copper wad enigma

3.12 Pretet C., Nägler T.F., Reynaud S., Samankassou E.: First results of Barium isotope fractionation in scleractinian coral skeleton

3.13 Tran T.D., Audiguier M., Cojean R.: Experimental study of the sensitivity to shrink/swell behaviour of clayey soils in the Paris Basin

3.14 von Niederhäusern B., Engi M., Rubatto D.: HP metamorphism in the Sesia Zone (Western Alps, Italy): Constraints on subduction dynamics of continental crust from in-situ U-Th-Pb dating of accessory minerals

POSTERS

P 3.1 Galster F., Othmar M.: Accessory mineral thermometry, a case study from the Ivrea Verbano Zone

P 3.2 von Niederhäusern B., Manzotti P., Cenki-Tok B., Zucali M., Engi M., Rubatto D., Darling J.: The Permian evolution of the internal Austroalpine units (Sesia Zone, Dent Blanche tectonic system): Constraints from in-situ U-Pb geochronology

P 3.3 Negro F., Bousquet R., Vils F., Pellet C.M., Schaub J.: Thermal structure and metamorphic evolution of the Piemont-Ligurian metasediments in the northern Western Alps

P 3.4 Vogel M., Früh-Green G.,Schwarzenbach E., Boschi C.: Serpentinization and fluid-rock interaction in mafic and ultramafic seafloor: Constraints from Ligurian ophiolite sequences

P 3.5 Hauser A., Bussy F.: Residual liquid segregation and rhythmic magmatic layering by syn-magmatic shear in the Punta Falcone intrusion (Sardinia, Italy)

P 3.6 Tornare E., Bussy F.: Origin and emplacement of a clinopyroxenite body in the feeder-zone of an ocean island volcano (Fuerteventura, Canaries)

P 3.7 Rochat L., Pilet S.: Alkaline melts –peridotite reaction as the process responsible for the nephelinite-alkali basalt transition

P 3.8 Suter D., Franz L., de Capitani C.: PT-t evolution of migmatites from the region of Todtnau (southern Schwarzwald, southwest Germany)

P 3.9 Hunziker D., Reusser E., Grolimund D., Lottermoser W., Burg J-P.: Fe^{3+}/Fe^{2+} ratios in minerals and bulk of metamorphic rocks: Mössbauer spectroscopy, wet chemistry and high resolution XANES on the blueschists of Syros and Sifnos (Cyclades, Greece)

P 3.10 Müller F., Mullis J.: Geochemical investigation of fluid inclusions in fissure-quarzcrystals of the Meta-dolomites in the Binn-Valley, Wallis, Switzerland

P 3.11 Wolf M., Mullis J.: Retrograde fluid evolution and its impact on mineral precipitation. An example from an Alpine fissure of the Gotthard rail base tunnel between Amsteg and Sedrun, external part of the Central Alps.

P 3.12 Dolder F., Mäder U.K., Jenni, A.: Experimental characterization of cement-bentonite interaction using core infiltration techniques coupled with 4D X-ray tomography

P 3.13 Bader T., Zhang L., Franz L., Ratschbacher L., de Capitani C.: The enigmatic Songshugou complex (Qinling orogen, central China): mélange of high-pressure and (ultra) high-temperature metamorphic rocks?

P 3.14 Beridze G., Tedliashvili K.: Naw data about regional metamorphism and magmatism of Khrami crystalline massif (the Caucasus, Georgia)

P 3.15 Kayani, S.: Elemental composition of a bangle shard from Harrappa, an Indus valley settlement

P 3.16 Novroozi Z., Moosavi Harami R., Mahboubi A., Mahmoodi Gharaie M. H., Ghaemi F.: Geochemistry of Silurian Niur sandstones in Tabas Block, Central Iran

P 3.17 van der Lelij R., Spikings R., Gerdes A., Ulianov A.: Early Palaeozoic tectonic process in north-western Gondwana as revealed by zircon hafnium isotope analysis: tectonic switching along an active margin

P 3.18 Grakova O.: Accessory ilmenorutile of diamondiferous terrigenous rocks of South Timan in the north-east borderland of the East-European platform.

P 3.19 Vardanashvili K., Maisuradze N.: Exocontact metamorphism in Klich gabbro-diorite intrusive

P 3.20 Ulyasheva N.: Metamorphism of the polarural precambrian rocks

P 3.21 Gialli S., Moritz R., Popkhadze N., Gugushvili V., Migineishvili R., Spangenberg J.: The Madneuli polymetallic deposit, Bolnisi district, Georgia: Evidence for a magmatic input in a submarine, transitional hydrothermal system.

P 3.22 Hemon P., Moritz R., Ramazanov V.: The Gedabek epithermal Cu-Au deposit, Lesser Caucasus, Western Azerbaijan: geology, alterations, petrography and evolution of the sulfidation fluid states.

P 3.23 Lambiel F., Dold B., Fontboté L.: Present copper-rich “gel” formation in the giant porphyry copper deposit of Chuquicamata (northern Chile)

P 3.24 Rezeau H., Moritz R., Beaudoin G., Gobeil C.: New mineralogical and fluid inclusion genetic constraints for Archean batholith-hosted gold veins at the Lac Herbin deposit, Val-d’Or, Canada

P 3.25 Saintilan N., Stephens M.B., Fontboté L., Lundstam E.: Reactivation of fault zones in Precambrian crystalline basement and the location of stratabound, sandstone-hosted Pb-Zn deposits along the front of the Scandinavian Caledonides.

P 3.26 Decrouy L., Bourquard M., Vennemann T.: Isotope composition of lacustrine vapour of Lake Geneva

P 3.27 Naumenko M.O., Mezger K., Nägler T.F., Villa I.M.: Thermal ionisation mass spectrometric determination of the $^{40}K/^{39}K$ ratio

3.1

Extracting accurate high temperature thermal histories from crustal rocks

Ryan Cochrane[1], Richard A Spikings[1], David Chew[2], Jörn-Frederik Wotzlaw[1], Massimo Chiaradia[1], Shane Tyrrell[3], Urs Schaltegger[1], Roelant Van der Lelij[1]

[1] *Section of Earth and Environmental Sciences, University of Geneva, Switzerland (ryan.cochrane@unige.ch)*
[2] *Department of Geology, School of Natural Sciences, Trinity College Dublin, Ireland*
[3] *UCD School of Geological Sciences, University College Dublin, Ireland*

Thermochronological studies assume that daughter isotopes (e.g. ^{206,207}Pb and ^{40}Ar) are redistributed within minerals and ultimately lost to an infinite reservoir by thermally activated, volume diffusion (Watson & Baxter, 2007). This fundamental assumption is central to hundreds of scientific publications which have focussed on the thermal history of the Earth's crust since the 1970's. However, some studies (Lee, 1995; Villa, 1998) challenge this assumption, suggesting that the physical mechanisms controlling isotope transport in minerals over geological time-scales are dominated by aqueous fluid flow along specific mineral pathways and that volume diffusion is a secondary process. An experimental verification of the role played by Fickian volume diffusion in mechanisms of daughter isotope loss over geological time-scales is therefore vital in validating the accuracy of existing and future thermochronological studies.

We present high precision single and multi-grain isotope-dilution thermal ionization mass spectrometer (ID-TIMS) apatite U-Pb dates (~81 – 137 My) extracted from an early Triassic (~247 Ma) migmatite of southern Ecuador. These data are used to generate theoretical thermal history solutions assuming that Pb was lost by volume diffusion. A comparison of these solutions with i) intra-grain apatite U-Pb date profiles, and ii) independent geological constraints demonstrates that volume diffusion governed the displacement of Pb. Inverse-modelling has permitted the generation of several million time(t)-temperature(T) path iterations. The large quantity of iterations and measured intra-grain U-Pb profiles provide an opportunity to test whether or not Mesozoic (approximately 250 – 65 Ma) apatite U-Pb dates can be used to differentiate between fundamentally contrasting t-T paths, which reflect significantly different high temperature (375 - 570 °C) tectonic processes.

This study has demonstrated that the dispersion of whole grain U-Pb dates and core-rim intra-grain U-Pb variation can be used to differentiate between gradual cooling and reheating with respect to the Pb partial retention zone (PRZ) using only the ^{206}Pb /^{238}U chronometer. This permits the application of this procedure to Mesozoic (approximately 250 – 65 Ma) rocks which have resided at temperatures of ~375-570°C, providing geologists with a unique tool for studying the high-temperature thermal evolution of the Earth's crust.

REFERENCES

Lee, J. K. W. 1995. Multipath diffusion in geochronology. Contributions to Mineralogy and Petrology, 120(1): 60-82.
Villa, I. M. 1998. Isotopic closure. Terra Nova, 10(1): 42-47.
Watson, E. B., & Baxter, E. F. 2007. Diffusion in solid-Earth systems. Earth and Planetary Science Letters, 253(3-4): 307-327.

3.2

Using U-series and beryllium isotopes to reveal the occurrence and relative timing of crustal and mantle processes in the Southern Volcanic Zone of Chile

Cooper Lauren[1,2], Reubi Olivier[1], Dungan Michael[2], [3], Bourdon Bernard[4], Langmuir Charles[5], Turner Stephen[5], Schaefer Joerg[6]

[1] *Institute of Geochemistry and Petrology, ETH Zürich, Clausiusstrasse 25, CH-8092 Zürich (lauren.cooper@erdw.ethz.ch)*
[2] *Départment de Minéralogie, University of Geneva, Rue de Maraîchaire 13, CH-1205 Genève*
[3] *Department of Geological Sciences, University of Oregon, 1275 East 13th Avenue, US-97403 Eugene, Oregon*
[4] *Laboratory of Geology, ENS de Lyon and CNRS, 46 Allee d'Italie, FR-69364 Lyon*
[5] *Department of Earth and Planetary Sciences, Harvard University, 20 Oxford Street, US-02138 Cambridge, Massachusetts*
[6] *Lamont-Doherty Earth Observatory, Columbia University, 61 Route 9W, US-10964 Palisades, New York*

Magmas erupted from subduction zone volcanoes represent the end products of multiple magmatic processes occurring in the asthenospheric mantle wedge and overlying lithosphere (i.e., fluid addition, melting, assimilation, and crystal fractionation). To resolve the contributions of diverse processes and components, and the relative timing of these events, we have determined U-series activities (U-Th-Ra-Pa) for 60 and ^{10}Be compositions for 20 historic or very young lavas carefully chosen on the basis of major and trace element analyses of 625 samples from six volcanoes in the Andean Southern Volcanic Zone of Chile (37.6-41.1°S: Nevados de Chillán, Antuco, Llaima, Lonquimay, Villarrica, and Osorno). Our dataset demonstrates that each of these volcanoes reflects a unique combination and sequence of magmatic processes that are only revealed through analysis of multiple samples spanning the extent of intra-volcano and intra-eruption chemical variation.

Sigmarsson et al. (1990; 2002) identified a regional trend using U-series and Be isotopes from mostly single samples, which they interpreted to represent along-strike variations in the flux of slab-derived fluid into the wedge [from ^{230}Th-excess plus ^{226}Ra-deficit plus low ^{10}Be/^{9}Be at Chillán towards progressively higher ^{238}U- and Ra-excesses and ^{10}Be/^{9}Be at Villarrica and Osorno]. These data fall within the much broader array defined by our results, but we infer the operation of assimilation (e.g., Llaima; Reubi et al., 2011) and aging of subduction zone components with variable compositions and proportions in the mantle prior to partial melting as important factors in generating the highly individualized and complex U-series systematics observed at each of these six volcanoes. All of the volcanoes exhibit evidence of assimilation, with the exception of Lonquimay which has undergone mostly closed-system fractional crystallization. At Llaima and Chillán the assimilant is crustal. At Villarica, flux-related melts that dominate in the main edifice have been mixed with magma compositions similar to those at surrounding minor eruptive centers (Hickey-Vargas et al., 2002). The latter appear to be decompression melts of enriched mantle which manifest moderate U-Th-Ra disequilibrium and substantial ^{231}Pa-excesses, whereas melts from Villarrica have substantial U- and Ra-excesses. Magmas from Osorno reflect a greater influence of sediments originating from the incoming slab. After discounting assimilated samples, all primary melts have uniformly high Pa-excesses (1.7-2.2) coincident with large variations in ^{238}U-^{230}Th disequilibria. Fluid addition-aging-melting successions at Antuco and Chillán may have led to compositions near U-Th equilibrium or with Th-excesses, respectively. Primary Ra-deficits at Chillán, Lonquimay, and Osorno are under investigation and potentially reflect melting of a cumulate body.

Forthcoming ^{10}Be data for select U-series samples will enable further clarification of the regional trend. Preliminary analyses of nine Llaima samples erupted between 1850 and 2009 confirm the successful elimination of a meteoric ^{10}Be component and produce a data array consistent with assimilation. The invocation of radioactive decay to produce U-Th equilibrium (duration of at least 380 ky) could also explain the low ^{10}Be/^{9}Be compositions (half-life of ^{10}Be=1,390 ky). Our comprehensive dataset may shed new light on melting processes in subduction zone systems.

REFERENCES

Hickey-Vargas, R., Sun, M., Lopez-Escobar, L., Moreno-Roa, H., Reagan, M.K., Morris, J.D. & Ryan, J.G. 2002: Multiple subduction components in the mantle wedge: Evidence from eruptive centers in the Central Southern volcanic zone. Geology, 30, 199-202.

Reubi, O. Bourdon, B., Dungan, M.C., Koornneef, J.M., Sellés, D., Langmuir, C.H., & Aciego, S. 2011: Assimilation of the plutonic roots of the Andean arc controls variations in U-series disequilibria at Volcan Llaima, Chile. Earth and Planetary Science Letters, 303, 37-47.

Sigmarsson, O., Chmeleff, J., Morris, J. & Lopez-Escobar, L. 2002: Origin of 226Ra-230Th disequilibria in arc lavas from southern Chile and implications for magma transfer time. Earth Planetary Science Letters, 196, 189-196.

Sigmarsson, O., Condomines, M., Morris, J. D. & Harmon, R. S. 1990: Uranium and 10Be enrichments by fluids in Andean arc magmas. Nature, 346, 163-165.

3.3

Ablation behaviour of titanite and constraints for U–Th–Pb geochronology using LA-ICP-MS

El Korh Afifé

Institut für Geologie, Universität Bern, Baltzerstrasse 1+3, CH-3012 Bern (afife.elkorh@geo.unibe.ch)

Titanite ($CaTiSiO_5$) is a common accessory mineral in magmatic and metamorphic rocks. It is commonly involved in reactions with other Ca- and Ti-bearing phases (e.g. rutile, perovskite), and element substitutions occurring in titanite enhance its stability. Titanite lattice can incorporate significant amounts of U and Th. In-situ age determination of titanite is crucial for metamorphic rocks, since different titanite generations can be assigned to different stages of the metamorphic P–T cycle.

U–Pb geochronology using laser ablation inductively coupled plasma mass spectrometry (LA-ICP-MS) has become a widespread and powerful tool for in-situ U–Pb dating of zircon in the last 10 years. The LA-ICP-MS technique has recently been developed for in-situ U–Th–Pb titanite geochronology and has become a rising technique (e.g. Storey et al. 2006; Simonetti et al. 2006). However, only few titanite standards are currently available for titanite geochronology: Khan, BLR-1, Fish Canyon Tuff and Grenville skarn titanite, and opinions diverge on the possibility of using non matrix-matched standards and samples (e.g. zircon and titanite). In order to understand the behaviour of U, Th and Pb with respect to Ti, Ca and Si in titanite, ablation experiments were carried out on the Khan titanite (522.2 ± 2.2 Ma; Heaman 2009) using a GeoLas Pro 193 nm ArF excimer laser ablation system (Lambda Physik, Germany) coupled to an Elan DRC-e quadrupole ICP-MS (Perkin Elmer, Canada). The $^{206}Pb/^{238}U$, $^{207}Pb/^{235}U$ and $^{208}Pb/^{232}Th$ ratios were also measured in the Plešovice zircon (337.13 ± 0.37 Ma; Sláma et al. 2008), as well. All analyses were carried out using a spot ablation mode.

Laser-induced elemental fractionation Si/Th, Si/U, Si/Ca, Pb/Ti and Si/Ti increase when increasing energy density and repetition rate conditions, while the Pb/Si, Ca/Ti, U/Ti, Th/Ti and U/Ca intensity ratios remain relatively constant during ablation. The temporal changes of the intensity ratios indicate a similar behaviour for Ca, Ti, U and Th, while Pb and Si share a similar behaviour to each other. With increasing ablation repetition rate and/or energy density, the fractionation of the $^{206}Pb/^{238}U$, $^{207}Pb/^{235}U$ and $^{208}Pb/^{232}Th$ ratios increases and becomes parabolic for both zircon and titanite. However, the laser-induced fractionation is weaker for titanite than for zircon at the same operating conditions. Matrix effects on the Pb/U and Pb/Th ratios between zircons and titanite can be tested by a comparison of the mass bias coefficients: e.g. for the $^{206}Pb/^{238}U$ system, KPb/U = $^{206}Pb/^{238}U$ known / $^{206}Pb/^{238}U$ measured

The mass bias coefficients calculated for the $^{206}Pb/^{238}U$, $^{207}Pb/^{235}U$, and $^{208}Pb/^{232}Th$ ratios in Khan titanite and Plešovice zircon generally decrease when decreasing the spot size from 44 to 32 µm, and when increasing the repetition rate and/or the energy density. The mass bias coefficients are higher for Khan titanite than for Plešovice zircon, at similar laser operating conditions. The $^{208}Pb/^{232}Th$ ratio in Plešovice zircon is more sensitive to fractionation than in Khan titanite due to the low Th/U content in Plešovice. The comparison of the mass bias coefficients between zircon and titanite indicates that comparable mass bias values are obtained between the two matrices, if Plešovice zircon is analysed at a larger spot size than Khan titanite with a similar repetition rate and energy density conditions.

A Khan titanite age was determined using Plešovice zircon as an external standard at a repetition rate of 4 Hz, and an energy density of 4.5 J/cm^2. The beam size for Plešovice zircon was fixed to 44 µm. At a beam size of 32 µm, the weighted average $^{206}Pb/^{238}U$ and $^{208}Pb/^{232}Th$ ages calculated for Khan titanite are within error to the reference ID-TIMS from Heaman (2009). At a beam size of 44 µm, the $^{206}Pb/^{238}U$ and $^{208}Pb/^{232}Th$ ages are c. 35–40 Ma younger than the reference value. The increase of the repetition rate for titanite has only a small effect on age accuracy. Still, the $^{206}Pb/^{238}U$ and $^{208}Pb/^{232}Th$ ages obtained for Khan are closer to the reference age, when using a spot size of 32 µm instead of 44 µm.

Even if matrix-matched standardisation is preferred for titanite dating, this various series of ablation experiments has shown that matrix effects can be minimised using a varying spot size for zircon standard and titanite samples.

REFERENCES

Heaman, L.M. 2009: The application of U–Pb geochronology to mafic, ultramafic and alkaline rocks: an evaluation of three mineral standards. Chemical Geology, 261, 43-52.

Simonetti, A., Heaman, L.M., Chacko, T., Banerjee, N.R. 2006: In situ petrographic thin section U–Pb dating of zircon, monazite, and titanite using laser ablation MC-ICP-MS. International Journal of Mass Spectrometry, 253, 87-97.

Sláma, J., Košler, J., Condon, D.J., Crowley, J.L., Gerdes, A., Hanchar, J.M., Horstwood, M.S.A., Morris, G.A., Nasdala, L., Norberg, N., Schaltegger, U., Schoene, B., Tubrett, M.N., Whitehouse, M.J., 2008: Plesovice zircon – a new natural reference material for U–Pb and Hf isotopic microanalysis. Chemical Geology, 249, 1-35.

Storey, C.D., Jeffries, T.E., Smith, M. 2006: Common lead-corrected laser ablation ICP-MS U–Pb systematics and geochronology of titanite. Chemical Geology, 227, 37-52.

3.4

The pioneer work of Bernard Kübler and Martin Frey in very low-grade-metamorphic terranes: Paleo-geothermal potential of variation in Kübler-Index/organic matter reflectance correlations – a review

Rafael Ferreiro Mählmann[1,2], Ömer Bozkaya[3], Sébastien Potel[2,4], Ronan Le Bayon[1,2], Branimir Šegvić[1] and Fernando Nieto García[5]

1 Technical and Low Temperature Petrology, Institut für Angewandte Geowissenschaften, Technische Universität Darmstadt, Schnittspahnstraße 9, D–64287 Darmstadt, Germany
2 Mineralogisch-Petrographisches Institut, Universität Basel, Bernoullistrasse 30, CH–4056 Basel, Switzerland.
3 Department of Geological Engineering, Cumhuriyet University, TR–58140 Sivas, Turkey
4 Institut Polytechnique LaSalle Beauvais, Equipe B2R, 19 rue Pierre Waguet, BP 30313, F–60026 Beauvais Cedex, France
5 Departamento de Mineralogía y Petrología and IACT. Universidad de Granada, CSIC. Av. Fuentenueva, E-18002 Granada, Spain

Abstract Low-temperature metamorphic petrology occupies theP-T field between sedimentary and metamorphic petrology. Two important pillars of low-temperature metamorphism are coal petrology and clay mineralogy. When low temperature petrology was established bridging a hiatus between the two classical geological disciplines of sedimentary geology and metamorphic petrology, geologists faced a need for the usage of different terminology tenets. Martin Frey and Bernard Kübler were two pioneers in low-grade metamorphic petrology. They focused their research on clarifying the relationships of clay mineralogy and organic petrology to metamorphic pressure (P) and temperature (T) conditions.. The ultimate aim of M. Frey and B. Kübler was to establish a correlation between clay indices and organic parameters for different geodynamic setting and therefore for various pressure-temperature (P–T) conditions occurring in low grade metamorphic terranes. For this purpose, a special attention was addressed to the correlation between the Kübler-Index (KI) and vitrinite reflectance (VR). All these efforts are dedicated to estimate the P–T conditions and thus to gain insight into the geodynamic evolution of low-grade metamorphic terranes.

B. Kübler and M. Frey honored here concentrated their studies to the Helvetic Central Alps area. The very low-grade Helvetic domain is therefore of basic interest of this paper. Ensuing the extensive compilation of data from the Helvetic domain, a reinterpretation of Kübler and Frey's research is presented in the light of last decade's scientific progress. A comprehensive dataset avaliable enables to discriminate many factors influencing the Kübler-Index and organic-matter reflectance alongside to time, temperature and pressure. The correlation is restricted to the KI and organic matter reflectance (mostly VR) because most of the studies used both methods. Organic matter reflectance (OMR) includes data from vitrinite reflectance and bituminite reflectance measurements.

Geodynamics has important control on the KI/VR (OMR) correlation. Tectonic units having a similar geodynamic evolution are featured by the comparable KI/OMR trends, related to the particular paleo-geothermal conditions. Obviously the KI/OMRcorrelations provide a mean to characterise geothermal gradients and metamorphic very-low-grade pressure–temperature conditions. In terranes where high deformations rates are reported, exceeding the high anchizone conditions, strain promotes the kinetic effects of temperature and pressure on the KI versus OMR ratio.

3.5

Do Mo isotope fractionation processes accompany the dissolution of molybdenites? Studying the interface of water, molybdenite and their weathering products.

Nicolas D. Greber[1], Nadja Neubert [1,2] and Thomas F. Nägler[1]

[1] Institut für Geologie, Universität Bern, Balzerstrasse 3, CH-3012 (greber@geo.unibe.ch)
[2] Institut für Mineralogie, Leibniz Universität Hannover, Callinstr.3, D-30167 Hannover

The element molybdenum (Mo) is redox sensitive and the most abundant transition metal in the ocean. In todays oxidized surface waters, Mo is predominantly present as molybdate anion (MoO_4^{2-}; Mo^{6+}). Its isotope ratios in marine sediment records are used as proxy to reconstruct the redox history of the ocean. However, the knowledge about the sources of the ocean Mo cycle is limited. It is known, that changes in the Mo-complex (coordination number) or the redox state of Mo may lead to isotope fractionation. Molybdenite (MoS_2; Mo^{4+}) is not only an ore mineral, it is also quite common as an accessory mineral phase in granites and pegmatites (Audétat et al. 2011), making it even more important to investigate. In addition, earlier studies have shown that sulfide melt inclusions play a crucial role during the weathering of Mo (Voegelin et al. 2012). Its dissolution comes along with a change in the redox state of Mo from 4+ to 6+, which bears the potential of Mo isotope fractionation. Therefore, the dissolution of molybdenite has been investigated at the Alpjahorn, where different molybdenite weathering products and the access to water samples flowing through a talus with molybdenite bearing handspecimens produces a perfect natural laboratory to investigate small scale Mo dissolution and accompanying isotope fractionation processes.

A heavy (centered around 1.1‰) and a light (centered around 0.2‰) molybdenite group can be identified based on their δ^{98}Mo isotope composition. The mean Mo isotope composition of all measured molybdenites is around 0.42‰. The secondary Mo minerals powellite ($CaMoO_4$) and ferrimolybdite ($Fe_4(MoO_4)_3 \cdot 8H_2O$) are very common. Both incorporating Mo as the oxidized molybdate anion complex. Powellite and ferrimolybdite are either grown directly on top of molybdenite or a bit farther away covering the granite or pegmatite. In addition, also amorphous Fe-hydroxide crusts exist. Their Mo content is very high, resulting in a low Fe:Mo ratio of ~5:1. Water was collected directly inside the talus, outside the mineralized area and below the enriched zone.

The water samples have different δ^{98}Mo values and Mo concentrations. The sample outside the molybdenite-mineralized zone has a low concentration (0.2ppb) and a δ^{98}Mo value of 0.75‰. The one below the talus has an intermediate concentration (5ppb) and the highest Mo isotope composition of 0.83‰. The sample deriving from the mineralized zone has by far the highest concentration (380ppb) but with 0.63‰ the lowest δ^{98}Mo.
The isotopic signatures of the molybdate weathering products (ferrimolybdite and powellite) show two different signatures. Either, the Mo isotope composition is very close to the one of the molybdenite from the same sample, or they lie very close to the water deriving from the talus. A closer look reveals that all the molybdate minerals with a similar composition to the water sample are situated on the surrounding rock and not on top of molybdenites. On the other hand, molybdate minerals always show values identical δ^{98}Mo to those of associated molybdenites, if they crystallized on top of these. In contrast, the Mo isotope composition of the Fe-Hydroxides is always lighter than of the corresponding molybdate mineral or molybdenite, indicating the expected preferential adsorption of light Mo isotopes onto Fe-hydroxide phases.

This results lead to the following three conclusions.

1. During the precipitation of molybdate minerals from a water source, no Mo isotope fractionation is observed and the mineral keeps the signature of the water. This can be explained, as no change in the Mo-complex (coordination number) occurs during the precipitation process.
2. Fe-Hydroxides adsorb light Mo isotopes, an actually well known fact. Combining those two results is a further argument that a change of the Mo-complex (tetrahedral to octahedral) is the reason for the isotope fractionation during the adsorption of Mo on Fe-Hydroxides.
3. No net Mo isotope fractionation is observed in the case of a direct transformation and recapture of Mo4+ to Mo6+ (the case when molybdate minerals are on top of molybdenite). This is considered to indicate a batch process, i.e. that no significant amount of Mo is removed from the system.

The δ^{98}Mo value of 0.63‰ of the creek water sample deriving from the talus fan is 0.21‰ higher than the mean Mo isotope composition of the molybdenites. This difference may derive from a non-representative sampling, or it is the effect of the adsorption of light isotopes on Fe-hydroxides. Another explanation may be that it results from a Mo isotope fractionation during molybdenite dissolution. A Bachelor Thesis at our Institute will experimentally investigate this latter hypothesis.

REFERENCES

Voegelin A.R., Nägler T.F., Pettke T., Neubert N., Steinmann M., Pourret O. and Villa I.M. 2012: The impact of igneous bedrock weathering on the Mo isotopic composition of stream waters: Natural samples and laboratory experiments, Geochimica et Cosmochimica Acta, Volume 86(1), 150-165

Audétat A., Dolejš D., and Lowenstern J.B., 2011: Molybdenite Saturation in Silicic Magmas: Occurrence and Petrological Implications, Journal of Petrology, 52(5), 891-904

3.6

The geochemistry of aqueous fluids and hydrous melts in subduction zones

Stefanie Luginbühl[1], Peter Ulmer[1], Thomas Pettke[2]

[1] *Institute of Geochemistry and Petrology, ETH Zürich, Clausiusstrasse 25, CH-8092 Zürich (stefanie.luginbuehl@erdw.ethz.ch)*
[2] *Institute of Geological Sciences, University of Bern, Baltzerstrasse 1+3, CH-3012 Bern*

Aqueous fluids and silicate melts released from dehydrating slabs play a crucial role in mass transfer in subduction zones. Therefore, it is important to quantify the nature and composition of these mobile phases in order to understand elemental transport from the slab to the mantle wedge and the consequences for arc magmatism. We performed experiments at 2 and 3 GPa and temperatures between 700 and 1100°C on a K-free, H_2O-saturated and trace element-doped basaltic composition representing altered, oceanic crust. This pressure-temperature range corresponds to a depth in subduction zones where hydrous phases, most prominently epidote group minerals and amphibole, are stable and constitute hosts for a number of trace elements like REE, HFSE, some LILE as well as U and Th.

Due to experimental and analytical difficulties in measuring the composition of fluids and melts directly and quantitatively, a “freezing stage” (Kessel et al., 2004, Aerts et al., 2010) is employed to determine compositions of frozen liquids and fluids by Laser ablation ICP-MS. By applying this method, the loss of any potential precipitates and unquenchable solutes upon preparation for subsequent analyses is prevented. We employed diamond traps in the experiments which allow mobile phases to be collected in the trap and being analysed by Laser ablation ICP-MS. Coexisting eclogitic residual mineral assemblages are likewise measured by EMPA and LA-ICP-MS in order to obtain partition coefficients between fluids/melts and solid residual phases.

At 2 GPa preliminary results show hydrous phase assemblages with amphibole and epidote stable at lower temperatures (700 and 800°C), that are replaced by dominantly anhydrous phase assemblages with omphacitic clinopyroxene and garnet coexisting with trondhjemitic melt at higher temperatures. Accessory minerals are titanite (at 700°C) and rutile, the latter stable up to 1000°C. We observe the hydrous phase staurolite at 3 GPa and 700°C coexisting with garnet, clinopyroxene and rutile, additionally, kyanite is stable at 800°C. H_2O contents of the liquid phase indicate an aqueous fluid being stable up to 800°C and hydrous melts coexisting with eclogite above 850°C at 2 GPa. At 3 GPa we observe aqueous fluids up to 900°C. Liquids show (strongly) peralkaline character at lower temperatures and evolve towards metaluminous compositions with increasing temperature.

Partition coefficients between hydrous mobile phases and the solid residue indicate epidote controlling (Light) REE, as well as Th and U, below 800°C. Garnet is the principal control for Heavy REE; its composition is temperature dependent. Titanite and rutile are the principal hosts for HFSE.

REFERENCES

Kessel, R., Ulmer, P., Pettke, T., Schmidt, M.W. and Thompson, A.B. 2004: A novel approach to determine high-pressure high-temperature fluid and melt compositions using diamond trap experiments. American Mineralogist, 89, 1078-1086.

Aerts, M., Hack, A.C., Reusser, E. and Ulmer, P. 2010: Assessment of the diamond-trap method for studying high-pressure fluids and melts and an improved freezing stage design for laser ablation ICP-MS analysis. American Mineralogist, 95, 1523-1526.

3.7

Ascent and fragmentation in volcanic eruptions involving CO_2-rich silicate magmas

Mattsson Hannes B[1]

[1] Institute of Geochemistry and Petrology, Swiss Federal Institute of Technology (ETH Zurich), Clausiusstrasse 25, 8092 Zürich (hannes.mattsson@erdw.ethz.ch)

A common feature of many volcanic eruptions involving CO_2-rich silicate magmas is the formation of landforms normally attributed to explosive interactions between the rising magma and an external water source (i.e., phreatomagmatic fragmentation building maar volcanoes and tuff cones). However, on closer inspection, many of these landforms lack the typical features diagnostic of phreatomagmatism and instead produce fine-grained and well-rounded pyroclasts (Fig. 1). The mechanisms driving the ascent and fragmentation of CO_2-rich silicate magmas thus need to be revised.

It is generally accepted that melilititic magmas form by small degrees of partial melting at mantle depths and that the magmas can hold a significant amount of CO_2 dissolved within the melt structure (15-18.5 wt.% at 1.2-2.0 GPa; Brooker et al., 2001). The high CO_2 solubility in melilititic magmas can thus have a significant effect on the ascent and fragmentation of such magmas. It has previously been shown that the melilitites ascend rapidly from the source region to the surface (i.e., at 10-30 m s^{-1}; Mattsson, 2012), exsolving volatiles and frequently carrying abundant mantle debris intermixed with the juvenile material. In the East African Rift of northern Tanzania melilititic eruptions form maar-diatreme volcanoes, while the less volatile-rich nephelinitic magmas predominantly form scoria cones. This region is arid with evaporation greatly exceeding rainfall on an annual basis, and thus a potential water source required to drive the postulated phreatomagmatic fragmentation is not obvious.

Analyzes of pyroclast shapes, vesicle size distributions (VSD), vesicle density numbers (VDN) were carried out on pyroclasts from the Loolmurwak maar. These pyroclasts are representative of the different depositional facies and show considerable differences. Stereologically corrected 2D-vesicularities range from 15.3 to 43.0 vol. %. It appears that larger pyroclasts (cm-sized) have higher overall vesicularities (up to 43 vol. %), while pelletal lapilli (>0.5 cm) have considerably lower vesicularities (typically <20 vol.%). The spread in VDN's is surprisingly small, only varying from 1.48 x103 to 1.52x103 mm^{-3}, which is overlapping with values previously reported from both phreatomagmatic eruptions as well as Hawaiian-style fountaining. Therefore it is difficult to distinguish between different fragmentation mechanisms solely based on textural analyses.

However, when combined there are many indications suggesting that the CO_2-rich melilititic eruptions in Tanzania were dry and only involve magmatic fragmentation. These include: (1) absence of features typically found in phreatomagmatic deposits (such as accretionary lapilli, plastering and vesiculated tuffs), (2) the strong similarities between the fluidal-shaped melilititic pyroclasts and those produced in Hawaiian-type fountaining, (3) the arid climate, in combination with the fact that the maar-diatreme volcanoes occur on top of horst-structures and not in the lake basins, (4) only melilititic magmas form maar-diatreme volcanoes while nephelinites predominantly form scoria cones. In addition to this, the fast ascent rates of the melilititic magmas would leave very little time for magma-water interactions to occur, especially considering the lack of a obvious water source in the vicinity. Moreover, the dominance of near-spherical pelletal lapilli in the deposits suggest that most of the fragmentation was driven by gas-exsolution, and that if water was at all involved in the eruptions this could only have had a minor effect on the fragmentation process.

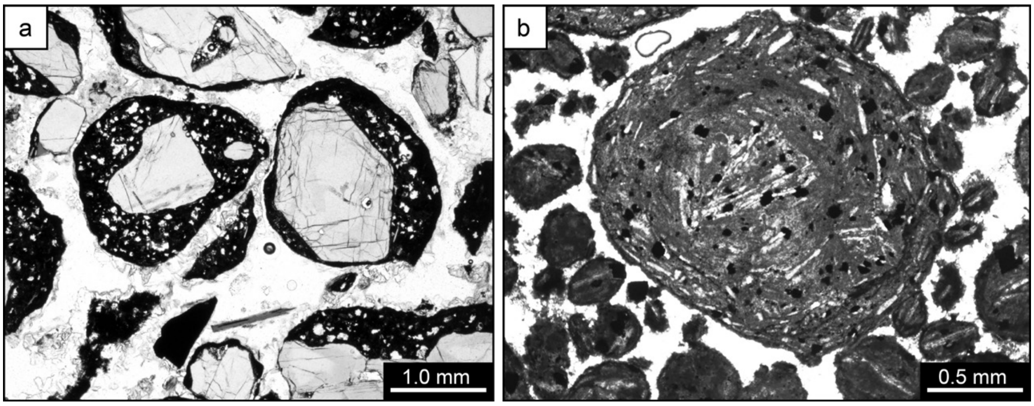

Figure 1. Typical morphologies of melilititic pyroclasts. (a) Moderately vesicular pelletal lapilli with clinopyroxene cores from the Loolmurwak maar volcano. (b) Close-up of small pelletal lapilli from the Mianmoja Hill tuff cone. Note that the small lapilli in (b) have cores of melilite-laths similar to the structure seen in (a).

REFERENCES
Brooker, R.A., Kohn, S.C., Holloway, J.R. & McMillan, P.F. 2001: Structural controls on the solubility of CO_2 in silicate melts: bulk solubility data. Chemical Geology, 174, 225-239.
Mattsson, H.B. 2012: Rapid magma ascent and short eruption durations in the Lake Natron–Engaruka monogenetic volcanic field (Tanzania): A case study of the olivine melilititic Pello Hill scoria cone. Journal of Volcanology and Geothermal Research, 247-248, 16-25.

3.8

Fe stable isotope fractionation in modern and ancient hydrothermal Fe-Si deposits

Kirsten Moeller[1,2], Ronny Schoenberg[3], Tor Grenne[4], Ingunn H. Thorseth[2] & Rolf B. Pedersen[2]

[1] *Institute of Geological Sciences, University of Bern, Baltzerstrasse 1, CH-3012 Bern, (Kirsten.Moller@geo.uib.no)*
[2] *Centre for Geobiology, University of Bergen, Allégaten 41, N-5007 Bergen*
[3] *Department of Geosciences, University of Tübingen, Wilhelmstrasse 56, D-72074 Tübingen*
[4] *Geological Survey of Norway, Leiv Erikssons vei 39, N-7040 Trondheim*

The possible role of microorganisms in the formation of ancient siliceous Fe deposits, such as banded iron formations (BIF), has been under debate over the past decades. Here, we compare Fe isotope variations in microbial Fe-Si precipitates from the Jan Mayen vent fields, North Atlantic, with those of Ordovician jasper beds from the Løkken ophiolite complex, Norway. Both deposits precipitated in the proximity of white smoker type hydrothermal vent fields and exhibit similar macro- and microscopic features. The modern deposits consist of individual stratified, laminated layers which are largely composed of branching, twisted filaments. DNA analyses confirmed the occurrence of the Fe-oxidising bacterium *Mariprofundus ferrooxydans*. The Ordovician jaspers are the recrystallisation product of an Fe-Si precursor gel, which formed as fall out sediment in a hydrothermal plume and cumulated around the venting site [1]. Micron-scale filamentous structures, concentrated in red hematite-rich laminea, are thought to be formed by Fe-oxidising bacteria, thus giving evidence for biological activity during formation of the Fe-Si gel [2].

Fe isotope variations from -2.09 to -0.66 ‰ in δ^{56}Fe were determined for the modern biological precipitates. A similar scatter in δ^{56}Fe values (-0.38 to +0.89 ‰) was also measured for the Ordovician jaspers. The data suggest that Fe isotope fractionation was caused by partial oxidation of hydrothermally derived $Fe(II)_{aq}$ and precipitation of siliceous ferrihydrite particles in both systems. The oxidation mechanism, i.e., inorganic or microbially induced, however, cannot be derived from the Fe isotope variations.

REFERENCES
[1] Grenne, T. & Slack, J. 2003: Bedded jaspers of the Ordovician Løkken ophiolite, Norway: seafloor deposition and diagenetic maturation of hydrothermal plume-derived silica-iron gels, Mineralium Deposita, 38, 625-639.
[2] Little, C.T.S., Glynn, S.E.J. & Mills, R.A., 2004: Four-Hundred-and-Ninety-Million-Year Record of Bacteriogenic Iron Oxide Precipitation at Sea-Floor Hydrothermal Vents, Geomicrobiology Journal, 21, 415-429.

3.9

Trace element partitioning along the liquid line of descent from olivine-tholeiite to granite

Nandedkar Rohit[1], Ulmer Peter[1], Müntener Othmar[2], Niklaus Hürlimann[2]

[1] *Institut für Geochemie und Petrologie, Clausiusstrasse 25, CH-8092 Zürich (rohit.nandedkar@erdw.ethz.ch)*
[2] *Institut de Sciences de la Terre, Bâtiment Géopolis, CH-1015 Lausanne*

In this experimental study, the isobaric fractional crystallization history of a cooling hydrous, primitive basaltic magma at intermediate to shallow crustal levels has been investigated. An end-loaded piston cylinder apparatus was used at 7kbar. The synthetic compositional equivalent of an olivine-tholeiitic dyke from the Adamello batholith (Northern Italy) was used as a starting material adding 3wt% of H_2O. This composition was prepared with oxides and hydroxides and 32 trace elements at 40ppm level. The experiments were conducted at NNO and cover a temperature range of 1170-700°C. Phases were analyzed by EPMA. The following crystallization sequence has been determined: olivine (ol) => clinopyroxene (cpx) => plagioclase (plg), spinel (sp) => orthopyroxene (opx), amphibole (amph), magnetite (mag) => apatite (ap) => quartz (qtz), biotite (bt). Over the last 200°C of fractionation, per-aluminous granitic liquids were produced. Trace element compositions were analyzed with an New Wave 193nm Excimer Laser coupled to a Sector field ICP-MS (Thermo Element XR) with a small spot size (5-10 µm), low frequencies (5Hz) and low energies 35-45%. Despite of the high sensitivity of the mass spectrometer and the low intensity of the laser, only short signals (~5sec) have been obtained. Due to the small grain size and to avoid mixed analyses, the measuring technique was changed in a way that several crystals (4-5) of the same mineral were analyzed in one sequence. The obtained signals within this sequence were cut together, resulting in a longer integration interval. Amphibole and plagioclase are stable phases from 1010-700°C allowing for a systematic assessment of trace element partitioning between mineral phase and the corresponding melt over a wide temperature range. Amphibole compositions vary from pargasite to magnesio-hornblende to cummingtonite. The compositions of feldspars are less variable at An84-80 over 150°C. However, at 860°C the An content starts to decrease to more albitic compositions finishing at An27 at the lowest temperature runs. Partition coefficients of REE's for both minerals display a ~10fold increase with decreasing temperature. The higher compatibility of trace elements in the fractionating amphiboles and plagioclases play a major role in determining trace element patterns of calc-alkaline granitoids.

Using microphenocrysts of amphibole and the bulk compositions of chilled margin of mafic dikes in the Adamello, the experimental partition coefficients of rare earth elements could be used to estimate crystallization temperatures for the amphibole (Hürlimann et al. 2011), suggesting that amphibole was a near-liquidus phase in some evolved dikes of the Adamello.

REFERENCES

Hürlimann N., Müntener O., Ulmer P. 2011: Trace-element partitioning in post-plutonic dike-suites S-Adamello (N-Italy). Abstract SGM, P4.4.

3.10

Fluid inclusion study in ore and gangue minerals from Main Stage veins at Butte, Montana.

Ortelli M.[1], Kouzmanov K.[1], Dilles J.H.[2] and Rusk B.G.[3]

[1] *Earth and Environmental Sciences, University of Geneva, 13 Rue des Maraîchers, Geneva, Switzerland*
[2] *Geosciences, Oregon State University, Wilkinson Hall 104, Corvallis, OR 97331-5506, USA*
[3] *Dept of Geology, Western Washington University, Bellingham, WA, 98225, USA*

In this study, we report new microthermometric measurements on fluid inclusions in ore minerals (enargite, sphalerite) and adjacent quartz from the Leonard mine, Butte district, Montana. At Butte porphyry Cu-Mo ("pre-Main Stage") mineralization is cut by large through-going "Main Stage" base-metal vein lodes. The Main Stage mineralization consists of intergrown sulfides (chalcocite, enargite, pyrite, ± bornite, covellite, sphalerite) and gangue minerals (quartz, carbonates). Previous fluid inclusion studies in quartz from Main Stage veins describe CO_2-bearing (0.2 to 1 mol%) liquid-rich fluid inclusions that homogenize to liquid at temperatures between 250° and 300°C, with salinities ranging from 1 to 4 wt% NaCl eq. and some rare vapor-rich fluid inclusions (Rusk et al. 2008).

Four quartz generations have been defined based on cathodoluminescence imaging (SEM-CL) in samples belonging to the Cu-rich zone of the Main Stage mineralization, from the Leonard mine. An early, high-luminescent quartz (quartz-I, Figs. 1a-b) constitutes the crystals' core and precedes a dark, poorly-crystallized quartz generation (quartz-II), which is related to the deposition of the enargite-pyrite assemblage (Fig. 1b). Low luminescent, black quartz (quartz-IV) crosscuts all quartz generations and is coeval to the deposition of a Cu-rich sulfide (covellite, bornite) assemblage.

Primary fluid inclusions in enargite (Fig.1e), studied by near-infrared (NIR) microscopy, are liquid-rich, rectangular to tube-like, trapped along growth zones and show similar T_h and salinity to quartz-II-hosted fluid inclusions (Figs.1c-g). Secondary fluid inclusions in enargite trapped along healed fractures are larger in size, have lower T_h (230-250°C) and distinctly higher salinity (5.1 ± 1.2 wt% NaCl eq.). Three primary fluid inclusion assemblages in the late sphalerite (Fig.1f) contain trapped chalcopyrite and homogenize between 300° and 330°C and have salinity of 4.4 ± 1.3 wt% NaCl eq. Following the deposition of the enargite-pyrite assemblage at temperatures of 260-280°C from a low-salinity fluid (2.4 ± 0.9 wt% NaCl eq.), a slight increase in salinity and homogenization temperature is registered in quartz-IV-hosted inclusions, whereas secondary fluid inclusions in enargite could indicate later mixing with a cooler fluid of even higher salinity (Fig.1g). Primary fluid inclusions in sphalerite, which is late in the paragenetic sequence at Leonard, are witnesses for the incursion of high temperature fluids with similar salinity at the late stage of vein formation. To better understand the fluid evolution and composition within the studied sequence Raman microspectrometry and LA-ICP-MS analyses of fluid inclusions will be performed.

Acknowledgements: This study was supported by the Swiss National Science Foundation (grant 20021-127123).

REFERENCES

Rusk, B., Miller, B.J., and Reed, M., (2008) Fluid-inclusion evidence for the formation of Main Stage polymetallic base-metal veins, Butte, Montana, USA. in Spenser, J.E., and Titley, S.R. (eds.), Circum-Pacific tectonics, Geologic Evolution, and Ore Deposits: Tucson, Arizona Geological Society, Digest 22, p. 573-581.

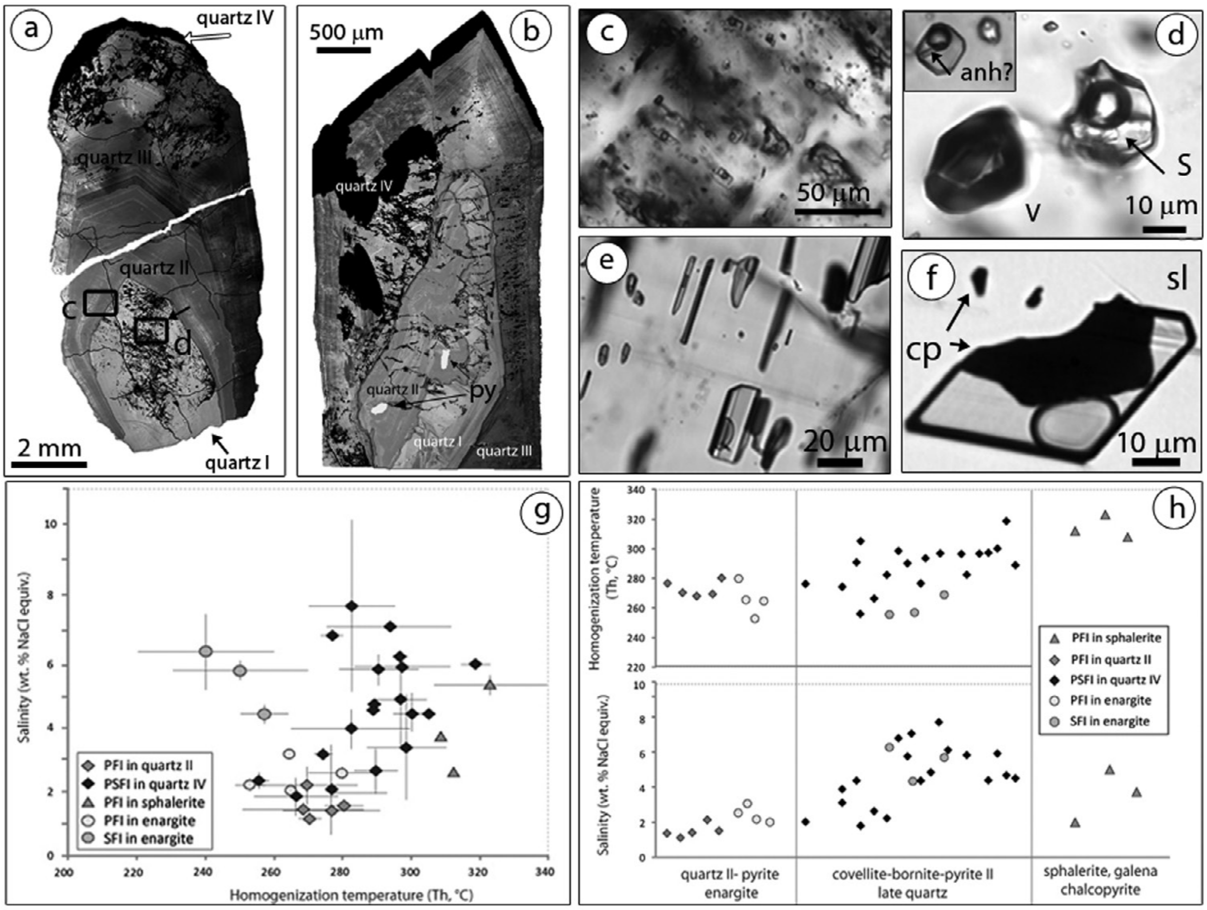

Figure 1. a-b) SEM-CL images of single quartz crystals. Multiple quartz generations are indicated: quartz-I (light-gray), quartz-II (medium-gray), quartz-III and late black quartz IV; c) Transmitted-light photomicrograph of primary liquid-rich fluid inclusions in quartz-II; d) Transmitted-light photomicrograph of vapor and liquid-rich polyphase fluid inclusions related to quartz-IV; e) Infrared transmitted-light photomicrograph of primary fluid inclusions in enargite; f) Transmitted-light photomicrograph of primary fluid inclusions in sphalerite with trapped chalcopyrite; g) Microthermometric data on 116 single fluid inclusions from 34 FIAs in quartz, enargite and sphalerite. Error bars correspond to the 1s standard deviation within the assemblage; h) Temperature and salinity evolution of fluid inclusion assemblages according to the paragenetic sequence. Abbreviations: PSFI – pseudo-secondary fluid inclusions, PFI – primary fluid inclusions, SFI – secondary fluid inclusions, anh-anhydrite, cp-chalcopyrite, py-pyrite, s-solid, sl-sphalerite, V-vapor.

3.11

Exotic mineralization at Chuquicamata, Chile: focus on the copper wad enigma

Marie-Caroline Pinget M.[1], Bernhard Dold[2], Lluís Fontboté[1]

[1] *Département de Minéralogie, University of Geneva, Rue de Maraîchers 13, Genève*
[2] *Geology Department, University of Chile, Plaza Ercilla 803, Santiago de Chile*

Supergene processes in porphyry copper deposits are important for their economic potential (Sillitoe, 2005). Meteoric fluids oxidize the upper part of the sulfidic deposit; oxidation of certain sulfide minerals, such as pyrite, produces sulphuric acid and lowers the pH, resulting in the mobilization of divalent metal cations like copper. Copper may re-precipitate more at depth, depending on the redox potential and pH conditions, as oxide or sulfide minerals enriching the primary ore. In certain cases, the supergene copper-rich fluids flow laterally and may precipitate downstream to form an exotic deposit.

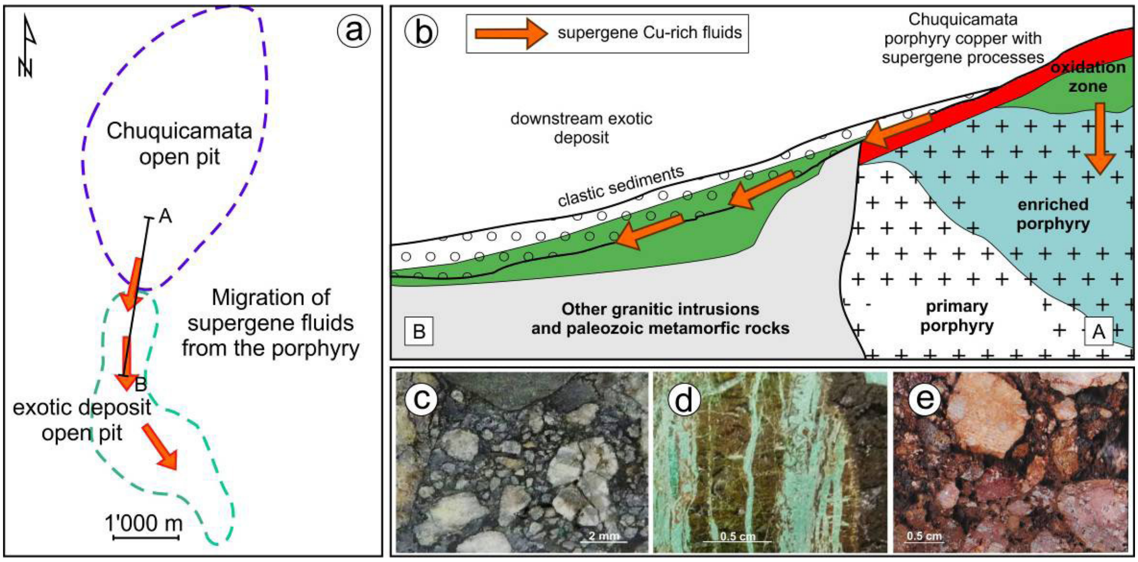

Figure 1. a. Location of the exotic deposit downstream of the Chuquicamata porphyry deposit. b. Schematic section across the Chuquicamata porphyry and its related exotic deposit. c. Gravels from the exotic deposit cemented with copper wad. d. Chrysocolla, atacamite, copper wad (brown) and copper pitch (black, right part) from the exotic deposit. e. Strongly altered gravels (kaolinite, alunite) from the central part of the exotic deposit.

At Chuquicamata, both in situ supergene enrichment and an exotic deposit are developed (Pinget et al., 2011, 2012). The exotic deposit extends 6 km to the south (Fig 1a), and contains of 3.63 Mt Cu (Ossandón, 2001), with grades typically between 0.7 and 1.5 Cu wt.%, and locally up to 15 wt.%Cu. In the central part of a mineralized paleochannel, the gravels and the bedrock are strongly altered (principally as kaolinite and alunite, Fig 1e), and contain virtually no Cu. Around this altered zone, copper mineralization is present, principally as chrysocolla, atacamite and "copper wad" as well as pseudomalachite, paracoquimbite, lebethenite and sampleite.
Despite its economic importance, copper-wad composition and structure are poorly known. The field term copper- wad includes dark brown to black powdery (in contrast to "copper- pitch" that is black shiny, Fig. 1d) copper-bearing material generally present as patina on fractures and rock surfaces and as cement of porous rocks (Fig. 1c). At Chuquicamata copper-wad occurs mainly in the external part of the exotic mineralization. Under an homogeneous appearance, XRD analyses indicate that copper- wad is a mixture between a poorly crystalline chrysocolla-like phase and other well crystallized minerals, principally atacamite, lebethenite, birnessite and gypsum. SEM backscattered electrons analyses reveal that the microscopic habitus of copper- wad can be very variable (Fig. 2 b-c).

The results achieved so far suggest that copper-wad s. str. is mainly the chrysocolla-like material. The compositional variability (Fig. 2a.) may be explained by the fact that copper-wad covers other minerals (like lebethenite in Fig. 2b) that cannot be discriminated during analysis.

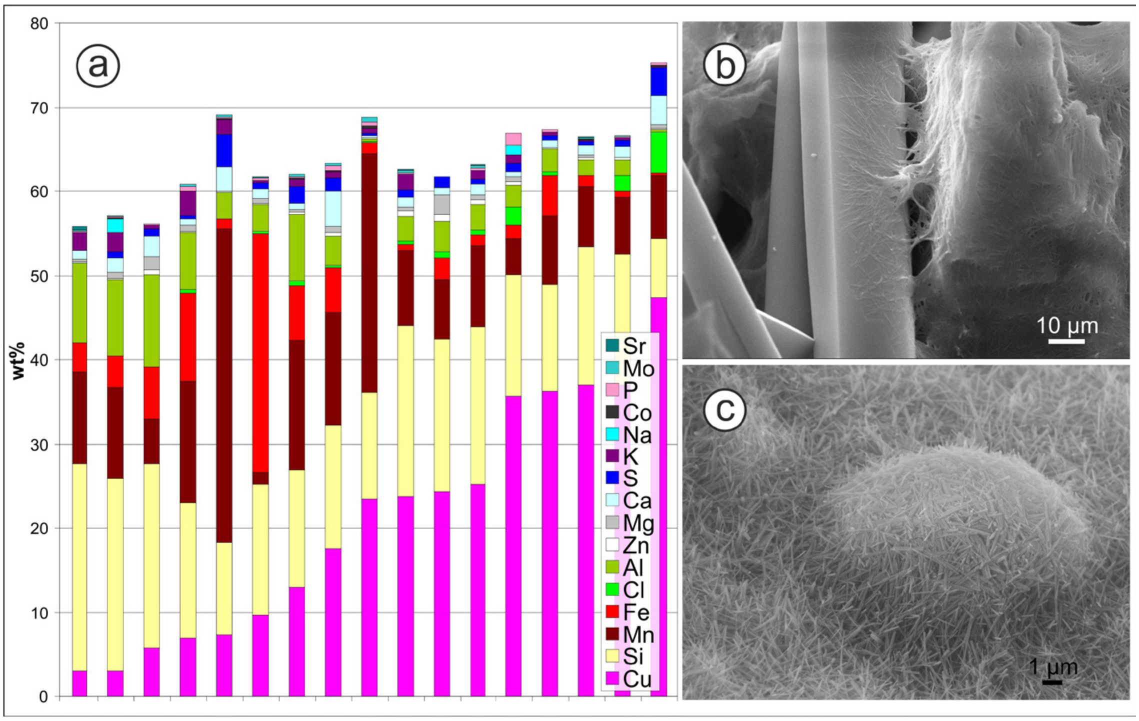

Figure 2. a.) Chemical analyses on copper-wad samples (XRF Uniquant) b-c.) Two examples of SEM backscattered electrons images on copper-wad. b.) copper-wad as flexible fibers covering a lebethenite crystal. c.) copper-wad needles forming a “film” that covers the substratum.

REFERENCES

Ossandón G, Fréraut R, Gustafson LB, Lindsay DD, Zentilli M (2001) Geology of the Chuquicamata Mine: A progress report. Economic Geology 96, 351-366.

Pinget MC, Fontboté L, Dold B, Ramirez F, Vergara M. 2011. The supergene enrichment at Chuquicamata revisited. In SGA Biennal Meeting No 11. Antofagasta, 823-825.

Pinget MC, Dold B, Fontboté L, Vergara M, Rojas de la Rivera J. 2012. Mineralogía de la mineralización exótica en Chuquicamata: nuevos avances. In 13th Congreso Geológico Chileno, Antofagasta, Chile, 37-39.

Sillitoe RH (2005) Supergene oxidized and enriched porphyry copper related deposits. Economic Geology 100th Anniversary Volume, 723-768.

3.12

First results of Barium isotope fractionation in scleractinian coral skeleton

Chloé Pretet[1], Thomas F. Nägler[2], Stéphanie Reynaud[3], Elias Samankassou[1]

[1] *Département de Géologie et Paléontologie, rue des Maraîchers 13, CH-1205, Genève, (chloe.pretet@unige.ch)*
[2] *Institut für Geologe, Baltzerstrasse 3, CH-3012 Bern*
[***]Centre scientifique de Monaco, Avenue Saint-Martin, 98000 Monaco

Here we present first measurements of barium isotope fractionation in scleractinian coral skeleton. Corals take part in the marine cycle of Ba and the Ba isotopic fractionation in the skeleton can provide informations about Ba cycling in shallow water. Ba in seawater is linked with paleo-productivity, given that Ba reacts like a nutrient in the water column. Prominent Ba sources to shallow marine environments are continental weathering and upwelling, both potentially influencing the oceanic cycle of Ba.

The Ba fractionation of natural (Bahamas/Florida) and cultured corals (CSM, Monaco), are compared to $Ba(NO_3)_2$ standard solution (± 0.1 ‰) and standard natural limestone BSC-CRM 393 (0.05 ± 0.2 ‰) (Bureau of Analysed Samples, Ltd., Middlesborough, England). The chemical method used was developped recently (Pretet et al., 2011). Measurements were performed using a $^{130}Ba/^{135}Ba$ double spike on Nu Instruments Multicollector ICP-MS following von Allmen et al. (2010) procedure.

The mean Ba isotopic fractionation in coral skeleton is 0.3 ± 0.2 and 0.6 ± 0.1 ‰ for cultured and natural samples, respectively. Statistic test reveals a significant difference between the sample sets (ANOVA: $p<0.01$). However, no significant differences were found between different cultured species (*Diploria strigosa*, *Acropora* sp., *Stylophora* sp., *Montipora* sp. and *Porites* sp.) Thus no species-specific fractionation could be found. The origin of the skeletal fractionation relative to standard can be linked to Ba incorporation in coral skeleton, or variations in seawater Ba isotopic composition, given the Ba residence time of 11 kyrs (Chan et al., 1976). The influence of diagenesis on the Ba isotopic composition was checked in 5 natural samples with varying calcite to aragonite ratios (0 to 0.3). No significant effect was observed.

These promising results encourage us to further investigate the Ba cycle and Ba fractionation on marine carbonate material. Currently we are working on the method for measuring Ba isotopic fractionation in seawater.

REFERENCES

Chan, L.H., Edmond, J.M., Stallard, R.F., Broecker, W.S., Chung, Y.C., Weiss, R.F., Ku, T.L., 1976, Radium and barium at GEOSECS stations in the Atlantic and Pacific. Earth and Planetary Sciences Letters 32, 258-267

Pretet, C., Nägler, T.F., Villa, I.M., Böttcher, M.E., Samankassou, E. 2011: Barium isotope fractionation in carbonates, 9th Swiss Geoscience Meeting, Abstract p.145, Zurich.

von Allmen, K., Böttcher, M., Samankassou, E., Nägler, F.T. 2010: Barium isotope fractionation in the global barium cycle: First evidence from barium minerals and precipitation experiments, Chemical Geology, 277, 70-77.

3.13

Experimental study of the sensitivity to shrink/swell behaviour of clayey soils in the Paris Basin

Tran Thanh Danh[1], Audiguier Martine[2], Cojean Roger[3],

Mines ParisTech, Centre de Géosciences, 77300 Fontainebleau, France
1 thanh-danh.tran@mines-paristech.fr; 2 martine.audiguier@mines-paristech.fr; 3 roger.cojean@mines-paristech.fr

In France since 1976, periods of prolonged drought accompanied by significant water deficits, have revealed a high vulnerability of constructions on clayey soils. This phenomenon is due to the shrink/swell properties of these soils. The mineralogical, microstructural, geotechnical and mechanical characteristics of three clayey formations in the Paris Basin were studied to highlight the contributions of the mineralogical composition and also the microstructure on the sensitivity of these soils to the shrinkage and swelling processes.

In this study, the Plastic clays of Sparnacian age, which exhibit no carbonate content, are compared to the Green clays of Romainville of Rupelian age and to the Blue marls of Argenteuil of Ludian age. Three distinct levels of Plastic clays of Sparnacian age were analyzed: a lower level, a medium level and a higher level. They differ in their clay content (<2µm) and proportion of clay minerals. It is more or less established that the microstructure of clayey soils partly controls the means of access (or withdrawal) of dipolar water molecules to adsorption sites on the surfaces of clay minerals (especially smectites). So, the characterizations of undisturbed samples and remoulded samples permit to identify the importance of the microstructure factors on the sensitivity of clayey soils to shrinkage and swelling processes. In fact, microstructure is partially or totally destroyed by the remoulding process in the laboratory.

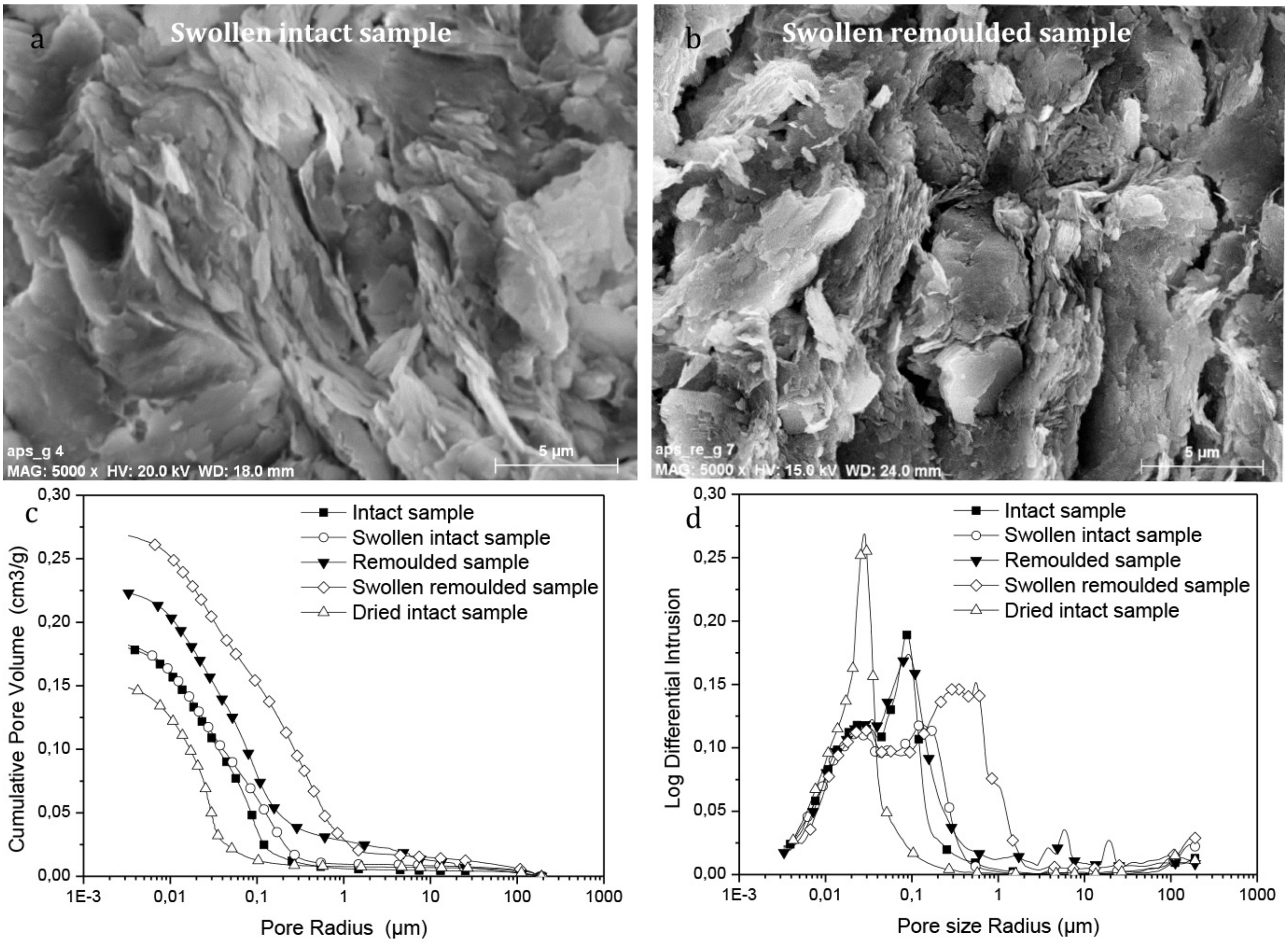

Figure 1. Analysis of microstructure of Plastic clays (higher level) by mercury porosimetry and scanning electron microscope.
a) Clay matrix of swollen intact sample
B) Clay matrix of swollen remoulded sample
C) Porosimetric curve
D) Derived porosimetric curve

Analyses of potential swelling by oedometer tests, analyses of mineralogical composition by X-ray diffraction, analyses of microstructure by mercury porosimetry and scanning electron microscope are presented. The corresponding results have confirmed the role of two families of factors in the processes of shrinkage and swelling of clayey soils: the mineralogical composition and the microstructure. Smectites and Illite-Smectite interstratified minerals promote swelling, which is not the case of Kaolinite. The swelling is counteracted by the presence of carbonates as well as quartz, the presence of these minerals limit the influence of clayey minerals. In the intact samples, the free swelling depends on the rate of carbonates or the rate of quartz. For a given percentage of carbonates or quartz, the swell sensitivity is greater for the remoulded soil than for the intact soil. In fact, the remoulding process destroys, at least partially, the elements of microstructures that counteract the swelling process. These elements of microstructure can be represented by carbonate bridges between clayey aggregates in carbonated clayey soils or clusters of quartz grains insensitive to swelling.

REFERENCES

Audiguier M. & Delage P. 1987: Etude microscopique et porosimétrique de sols fins naturels dans une perspective géotechnique. Actes de la VIIème Réunion Internationale de Micromorphologie des sols, Paris, juillet 1985, édité par N. Fedoroff, L.M. Bresson et M.A. Courty, 493-500, AFES.

Audiguier M., Geremew Z., Laribi S. & Cojean R. 2007: Caractérisation au laboratoire de la sensibilité au retrait-gonflement des sols argileux. Revue française de géotechnique, 120-121, 67-82.

Audiguier M., Geremew Z. & Cojean R. 2008: Relations entre les microstructures de deux sols argileux de la région Parisienne et leur sensibilité au retrait-gonflement. In J-P. Magnan, R. Cojean, Y-J. Cui, P. Mestat (eds.), SEC 2008, Symposium international Sécheresse et Constructions: 235-243. Paris: LCPC.

3.14

HP metamorphism in the Sesia Zone (Western Alps, Italy): Constraints on subduction dynamics of continental crust from in-situ U-Th-Pb dating of accessory minerals

von Niederhaeusern Brigitte[1], Engi Martin[1] & Rubatto Daniela[2]

[1] *Institut für Geologie, Universität Bern, Baltzerstrasse 1+3, CH-3012 Bern (vonniederhaeusern@geo.unibe.ch)*
[2] *Research School of Earth Sciences, Australian National University, Canberra*

The Sesia Zone, in the Western Italian Alps, comprises several continental slices derived from the Apulian margin and accreted to the orogen during the Alpine orogenic cycle. In the easternmost unit of the Sesia Zone, the so called Eclogitic Micaschist Complex (EMC), products of the Alpine high pressure metamorphism are remarkably well preserved; they reflect the oldest high pressure metamorphic overprint in the Western Alps. Geochronological and petrological data indicate that the Alpine high pressure metamorphic history involved several stages and the tectonic evolution for different slices of the EMC was unequal (Regis, 2012). The size, shape, and kinematics of the distinct crustal fragments that make up the Sesia Zone are still poorly constrained. The aim of the study is to delimit the geometry of these different tectonic blocks and to provide PTt-constraints on the early Alpine HP history of the Sesia terrane.

By combining in situ U-Th-Pb dating of accessory phases and detailed petrological and (micro-)structural analysis we can link the data to specific tectonometamorphic stages. Data from the SW part of the EMC are presented here:
- In a fine-grained orthogneiss, allanite shows up to 4 metamorphic growth zones that can be distinguished by texture, trace elements and age. In situ SHRIMP Th-Pb dating of these allanite zones yields two distinct metamorphic stages:
1) Allanite cores coexisting with omphacite are ~76 Ma old,
2) Allanite rims coexisting with albite yield ages around 61 Ma;
Intermediate growth zones, coexisting with phengite (3.5 Si), date between ~72 and 64 Ma. Detailed thermobarometric investigations are in progress to link these ages to specific P-T conditions.
- Zircon rims from a felsic eclogite and a carbonate-bearing mica schist, which can be related to HP assemblages, yield an age of ~ 78 -70 Ma and 74 Ma, respectively.

These new data reveal that a distinct HP stage occurred between ~78 and 74 Ma. Rubatto et al. (2011) demonstrated that the rocks in the central Sesia Zone experienced two HP stages between ~79 and 65 Ma. A first HP stage, dated between ~79 and 75 Ma, was immediately followed by decompression before a second HP stage took place around 65 Ma.
The oldest ages obtained during this study are consistent with the early high pressure ages in the central section indicating that these ages date the first high pressure peak. The allanite data further reflect a prolonged metamorphic evolution at elevated pressure conditions. The youngest age of 61 Ma records the exhumation to lower pressure-conditions. Ongoing petrological and microstructural analysis will link these new ages to the metamorphic evolution of this SW part of the Sesia block, and further constrain subduction and exhumation rates of the continental crust in the Western Alps.

REFERENCES

Regis, D. 2012. High-pressure evolution in the Sesia terrane (Italian Western Alps). PhD thesis, University of Bern
Rubatto,D., Regis, D., Hermann, J., Boston, K., Engi, M., Beltrando, M., McAlpine, S.R.B. 2011: Yo-yo subduction recorded by accessory minerals in the Italian Western Alps. Nature Geoscience 4(5), 338-342

P 3.1

Accessory Mineral Thermometers at High and Ultra-High Temperatures: a case study from the Ivrea-Verbano Zone.

Federico Galster, Othmar Müntener

Institut of Earth Sciences, University of Lausanne. Géopolis, 1015 Lausanne.

Ti-in-Zircon and Zr-in-Rutile are newly established thermometers calibrated both empirically and experimentally (e.g. Zack et al., 2004a; Ferry & Watson, 2007) and have been successfully applied as geothermometers at intermediate temperatures (400-650°C) in various geologic settings. However, the application of these thermometers to high and ultra-high temperatures (700-1100°C) is more problematic since investigations on small areas or even single samples result in a large set of temperatures. The difficulty in applying accessory mineral thermometers to high and ultra-high grade terranes is usually interpreted as related to diffusion during slow cooling after peak metamorphism, or to fluid-induced re-equilibration/recrystallisation during retrograde metamorphism.

We present preliminary data from the Ivrea-Verbano Zone (IVZ). The IVZ is a portion of the Sudalpine basement in northern Italy and southern Switzerland. It is interpreted as a fossil lower crustal section exhumed and tilted to its current position during the Alpine cycle after Variscan high-grade metamorphism and late Carboniferous and Permian magmatism.

The Ivrea zone consists of a heterogeneous metamorphic formation (the so-called kinzigite formation, mostly composed by paragneiss whose metamorphic grade ranges from amphibolite in the southeast to granulite conditions in the northwest) intruded by a Mafic Complex. The Mafic Complex consists essentially of gabbros and diorites with minor pyroxenites and ultramafic intercalations. The lower (northwestern) and the central part of the mafic complex are rich in metric to hectometric paragneiss septa (host-rock) originated from the kinzigite formation.

In Val Sesia, near Varallo, at the roof of the mafic intrusion the kinzigite formation consists of mica bearing (bt ± ms), orthopyroxene-free paragneiss. However, the paragneiss in the mafic complex are orthopyroxene bearing and almost free of mica, and display features of partial melting with a common paragenesis of qtz+fsp+opx+grt+accessory minerals. The amphibolites metamorphism in the kinzigite formation is interpreted as a result of a regional metamorphic event prior to the mafic intrusion (only partly obliterated by contact metamorphism close to the Mafic Complex) whiles the assemblages in the septa are interpreted as a result of thermal metamorphism during the gabbro emplacement. Therefore, the septa are the most promising rocks to provide constraints for the thermal budget of mafic magmas in the IVZ and, since they are quartz, zircon and rutile bearing, they offer the possibility to study the systematics of Ti-in-Zircon and Zr-in-Rutile thermometers.

Zircons and rutiles are investigated by LA-ICP-MS (magnetic sector-field spectrometer ELEMENT XR coupled with an ArF excimer ablation system NewWave UP-193). For Zr-in-rutile we apply the thermometer of Tomkins et al. (2007) assuming 8 kbar, for Ti-in-Zircon we apply the thermometer of Ferry and Watson (2007).

CL-images of zircon grains show complex patterns with inherited cores and metamorphic rims, the ages of homogeneous metamorphic rims obtained by LA-ICP-MS are close to ~280Ma, the ages of inherited cores vary between ~330Ma and >1Ga. Ti concentrations between the inherited core and the metamorphic rim of a single grain may vary, here we focus mostly on metamorphic rims.

Results indicate that the highest temperatures obtained by Ti-in-Zircon on metamorphic rims are close to 1000°C, while the lowest are around 850°C. Frequency diagrams display a bimodal temperature distribution, with a first peak around 880°C and a second around 980°C, this bimodal distribution is seen in some samples, others show only the lowest or the highest peak. The highest peak is observed mostly in rutile-poor samples, the lowest peak or bimodal distribution in rutile-rich samples.

Temperatures obtained by the Zr-in-Rutile thermometer are not correlated with grain size and only rarely decrease from core to rim. They show a bimodal distribution with a first peak around 750-800°C and a second peak around 950°C. This bimodal distribution is reproduced in some samples (in general, the same samples that showed the low temperatures by Ti-in-Zircon, see above); other samples show only the lowest peak (in general the same samples that showed the high temperatures by Ti-in-Zircon, see above).

Cr and Nb are used as discriminating proxy to distinguish between “metapelitic” and “metamafic” rutile (Zack et al., 2004b). The temperatures obtained from rutile with a “metapelitic” signature are clustered around the high and low temperature peak of frequency diagrams, in contrast rutile (even from the same sample) with a “metamafic” signature are clustered around the low temperature peak only. No rutile with Cr/Nb>1 gives temperatures above 900°C.
Rutile with zircon inclusions preserve the lowest temperatures, in general below 700°C and are interpreted as an effect of locally enhanced Zr diffusion during slow cooling after peak metamorphism.

Our preliminary data suggest a strong competition in controlling the distribution of Zr and Ti in rutile and zircon, respectively. A simple model of enhanced or inhibited post-peak diffusion should be replaced by a more complex model, where post-peak diffusion smoothes a previously established heterogeneous concentration of Zr (resp. Ti) in rutile (resp. in zircon), which in turn is a consequence of the changing activity and diffusion rates of Zr, Si and Ti during metamorphism and partial melting in the micro- and macroscale.

REFERENCES

Ferry, J., Watson, E., 2007: New thermodynamic models and revised calibration for Ti-in Zircon and Zr-in-Rutile thermometers. Contrib Min Petrol 154, 429-437

Tomkins, H.S., Powell, R., Ellis, D.J., 2007: The pressure dependence of Zr-in-rutile thermometer. J. Metamorph Geol 25, 703-713

Zack, T., Moraes, R., Kronz, A., 2004a. Temperature dependence of Zr in rutile: empirical calibration of a rutile thermometer. Contrib Min Petrol 148, 471-488

Zack, T., von Eynatten, H., Kronz, A., 2004b: Rutile geochemistry and its potential use in quantitative provenance studies. Sediment. Geol 171, 37-58

P 3.2

The Permian evolution of the internal Austroalpine units (Sesia Zone, Dent Blanche tectonic system): Constraints from in-situ U-Pb geochronology

von Niederhäusern Brigitte[1], Manzotti Paola[1], Cenki-Tok Bénédicte[2], Zucali Michele[3], Engi Martin[1], Rubatto Daniela[4], Darling James [5]

[1] *Institut für Geologie, Universität Bern, Baltzerstrasse 1+3, CH-3012 Bern (vonniederhaeusern@geo.unibe.ch)*
[2] *Géosciences Montpellier, Université de Montpellier 2, UMR5243, F-34095 Montpellier*
[3] *Dipartimento di Scienze della Terra "Ardito Desio", Università degli studi di Milano, via Mangiagalli 34, I-20133 Milano*
[4] *Research School of Earth Sciences, Australian National University, Canberra*
[5] *Department of Earth Sciences, Western University, Ontario, Canada.*

Permian extension in the Adriatic lithosphere was responsible for asthenosphere upwelling. This caused high temperature metamorphism at medium pressure and widespread partial melting, which led to upper crustal magmatic activity (e.g. Marotta and Spalla 2007). A metamorphic record of this process is preserved in the Austroalpine and Southalpine portions of the Alpine chain, which were not significantly affected by Alpine metamorphism. In the Western Alps, Permian metamorphism has long been suggested, but so far not reliably dated, whereas the timing of magmatic activity is well constrained.

In this study, new geochronological data (U-Pb dating on metamorphic and igneous zircon) are presented to fill some of the gaps in the current knowledge on the pre-Alpine metamorphic evolution of the two most classic and relevant Austroalpine units in the Western Alps, i.e. the Sesia zone and the Dent Blanche tectonic system.

In the SW part of the Sesia Zone, within the II DK unit, upper amphibolite to granulite-facies metamorphism was dated at ~277 Ma and at ~270 Ma. HT metamorphism is also recorded in the most internal unit of the Sesia zone (eclogitic micaschist complex): Metamorphic zircon from a metagabbro and an orthogneiss yield ages of ~ 276 Ma and ~274 Ma, respectively. The metababbro was subsequently exhumed to shallow crustal levels and intruded by felsic and intermediate dikes (Rebay and Spalla, 2001). One of these dikes was dated at ~264 Ma.

Within the Valpelline Series of the Dent Blanche tectonic system, three stages of amphibolite- to granulite-facies metamorphism are now evidenced by our new data: at ~287 Ma, ~274 Ma, and ~263 Ma. These stages of metamorphic overprinting clearly postdate the Variscan metamorphic cycle, which occurred around 350 Ma and was also recorded in our study, normally by the oldest U-Pb ages found.

Together with petrological data (Manzotti and Zucali 2012, Pognante et al. 1988), the new age constraints suggest that the middle and lower crust of the Valpelline Series and of the II DK experienced an extended regime of high heat flow at Permian times, from 290 to 260 Ma. During that interval a protracted series of processes lead to partial melting, producing migmatites, numerous leucogranite layers and pegmatite dikes. HT metamorphism is also recorded in the most internal unit of the Sesia zone, the Eclogitic Micaschist Complex. Dating of an andesitic dike that intruded a metagabbro after exhumation to shallow crustal levels, indicates that at least parts of these Permian lower crustal rocks must have been exhumed by the late Permian, predating the initiation of Jurassic rifting by tens of millions of years.

REFERENCES

Manzotti, P. & Zucali, M. 2012: The pre-Alpine tectonic history of the Austroalpine continental basement in the Valpelline unit (Western Italian Alps). Geological Magazine, 1-20.

Marotta A.M. & Spalla M.I. 2007: Permian-Triassic high thermal regime in the Alps: Result of late Variscan collapse or continental rifting? Validation by numerical modelling. Tectonics 26: TC 4016.

Pognante, U., Talarico, F., Benna, P. 1988: Incomplete blueschist re-crystallization in high-grade metamorphics from the Sesia-Lanzo unit (Vasario-Sparone subunit, Western Alps): A case history of metastability. Lithos 21, 129-142.

Rebay, G. & Spalla, M.I. 2001: Emplacement at granulite facies conditions of the Sesia – Lanzo metagabbros: an early record of Permian rifting? Lithos 58, 85-104.

P 3.3

Thermal structure and metamorphic evolution of the Piemont-Ligurian metasediments in the northern Western Alps

Negro François[1], Bousquet Romain[2], Vils Flurin[3], Pellet Clara-Marine[1], Schaub Jeanette[2]

1 Centre d'Hydrogéologie et de Géothermie (CHYN), Univ. de Neuchâtel, Emile-Argand 11, CH-2000 Neuchâtel (francois.negro@unine.ch)
2 Institut für Geowissenschaften, Universität Potsdam, Germany
3 Department of Earth Sciences, University of Bristol, UK

In the Western Alps, the Piemont-Ligurian oceanic domain recorded blueschist to eclogite metamorphic conditions during the Alpine orogeny. This domain has been classically divided in two zones (Combin and Zermatt-Saas), with contrasted metamorphic evolution, and separated by a major tectonic contact, known as the Combin fault. We present in this study new temperature data in the Piemont-Ligurian metasediments based on Raman spectroscopy of carbonaceous material (RSCM thermometry). We show that metamorphic record is very similar in the Piemont-Ligurian units with temperatures ranging from 420 to 530°C in the Combin zone and from 500 to 540°C in the Zermatt-Saas zone. These data demonstrate that there is no major temperature gap across the Combin fault. Moreover, we show that there is an increasing gradient of temperature towards the base of the Combin zone. Analysis of metamorphic assemblages and estimated temperatures points to a more pervasive retrogression in the Combin zone. Such thermal structure can be explained by a juxtaposition of Piemont-Ligurian units at depth that shared a common late metamorphic evolution. The heating observed in the Combin zone can be interpreted as the result of heat advection across the Combin fault or to an increase of the thermal gradient due to the incorporation of basement units in the orogenic prism during exhumation of high-pressure metamorphic units.

P 3.4

Serpentinization and fluid-rock interaction in mafic and ultramafic seafloor: Constraints from Ligurian ophiolite sequences

Vogel Monica[1], Früh-Green Gretchen[1], Schwarzenbach Esther[2], Boschi Chiara[3]

[1] Institute of Geochemistry and Petrology, ETH Zürich, Claussiusstr. 25, CH-8092 Zürich (monica.vogel@erdw.ethz.ch)
[2] Faculty of Geosciences, Virginia Tech, Blacksburg, USA
[3] Institute of Geoscience and Earth Resources, CRN Pisa, Italy

The Bracco-Levanto ophiolitic complex (Eastern Liguria) represents one of the largest and better-exposed ophiolitic successions in the Northern Apennines. It is considered to be a fragment of heterogeneous Jurassic lithosphere that records a tectono-magmatic and alteration history similar to that documented in a number of oceanic core complexes along the Mid-Atlantic Ridge (MAR), such as the Atlantis Massif at 30°N. Structural and petrological studies on these rocks provides constraints on the metamorphic/deformation phases connected to the formation and hydrothermal alteration of Jurassic oceanic lithosphere (Menna, 2009) and allow comparisons to present-day oceanic systems.

We present a comparative study of deformation processes and fluid-rock interaction in modern oceanic hydrothermal system, such as the Lost City Hydrothermal Field (LCHF) hosted in ultramafic rocks on the Atlantis Massif, and the Bracco-Levanto ophiolitic complex. A focus is on determining water-rock ratios and fluid flow paths during hydrothermal activity, and on processes leading to hydrothermal carbonate precipitation and the formation of ophicalcites, which are characteristic of the Northern Apennine ophiolite sequences. Our studies particularly allow us to test the hypothesis that the LCHF is a modern analogue for hydrothermal processes that produced ancient ophicalcites.

The mineralogical assemblages and textures in the Bracco-Levanto ophicalcites indicate a multiphase history of alteration. Oxygen Isotope and radiogenic strontium analysis have been performed on different vein generations. These data allow us to estimate formation temperatures and evaluate fluid-rock interaction during precipitation of carbonates that form a variable but extensive vein-network accompanied by serpentinization. Serpentinization continued with decreasing temperature during intense water circulation. Further we present bulk rock and mineral chemistry data of variably deformed serpentinite basement rocks of the Atlantic Massif and the Bracco-Levanto unit and compare these with the oxidized ophicalcites overlying the serpentinite, which have experienced higher water rock ratios.

REFERENCES

Menna, F., 2009, From magmatic to metamorphic deformations in a jurassic ophiolitic complex: the Bracco Gabbroic Massif, Easthern Liguria (Italy): Ofioliti, v. 34, no. 2, p. 109-130.

P 3.5

Residual liquid segregation and rhythmic magmatic layering by syn-magmatic shear in the Punta Falcone intrusion (Sardinia, Italy)

Hauser Anne-Cécile[1], Bussy François[1]

[1] *Institute of Earth Sciences, University of Lausanne, Dorigny, CH-1015 Lausanne (anne-cecile.hauser@unil.ch)*

The Punta Falcone is a small (200-300m x 600m) vertically layered Variscan gabbroic pluton built by successive injection of magmatic pulses at mid-crustal level. The Central zone of the complex, which is supposed to be the youngest one, is formed by plg-cumulus gabbros. No facies corresponding to an expulsed liquid could be found in the outcropping part of the system. On the other hand, hybrid rocks with mafic microgranular enclaves form dykes and brecciate the early gabbros.

Different types of magmatic planar structures occur throughout the complex. From the Central part towards the West the following structures were identified (fig 1):

1. Systematic continuous rhythmic layering with a regular spacing of 3cm in a cumulative part near the centre of the intrusion. Layering is defined by modal variations of amphibole (4-5mm big poikilitic Mg-hornblende grains around homogeneous plagioclase in the dark parts), and plagioclase (with thin albitic borders occurring together with some interstitial poikilitic quartz in the white layers). Mean orientation: 104/65.
2. Black planar structures ca. 4-5cm thick occur in the same facies as structures 1. They mainly consist of amphiboles; they are discordant and cut layering 1. The spacing of these zones is much more variable (between 20cm and 1m). Mean orientation: 117/83.
3. Sheared hybrid dykes in apparently isotropic gabbros. Other dykes of the same type in the same place are undeformed. Mean shear orientation: 097/50.
4. Thin white planes in a homogeneous gabbro ascribed to percolation of a more evolved liquid. Mean orientation: 123/86.
5. Somewhat diffuse rhythmic layering with cm scale. Mean orientation: 103/77.
6. Three different orientation sets can be identified on stereoplots: group I (structure 3) with the flattest dipping; an intermediate group II (structures 1 & 5) and group III (structures 2 & 4) with the steepest dipping. The angular difference between group I and group III is about 40°.

As structures (3) evidence syn-magmatic shearing, we infer shearing to be at least partly responsible for all other described structures. Shearing has to occur during/shortly after the injection of the magma when it is still a crystal mush. The residual liquid is expected to be extracted during this process, as illustrated in the centre of the intrusion. Layering textures suggest that the residual liquid escapes the system following regular planes. The parameters which control the observed regularity of extraction and thus of layering have to be further investigated.

Variation in orientation of the structures could be related to different processes, such as change of the local/regional stress field, rotation of the rocks because of the injection of new pulses displacing them, or conjugate shear zones. These processes could explain the presence of the two discordant structures (1 & 2) observed in the same facies close to the centre of the intrusion.

If cooling is too fast no structures will develop at all, as in the Eastern part, which is considered to be one or the earliest magma batches to emplace. The most central part does not show any structure as well. Cooling could have occurred in a period of quiescence towards the end of magmatic activity.

a) Magmatic layering & discordant bands (structures 1 & 2) b) Percolation planes (structure 4) c) Magmatic layering (structure 5)

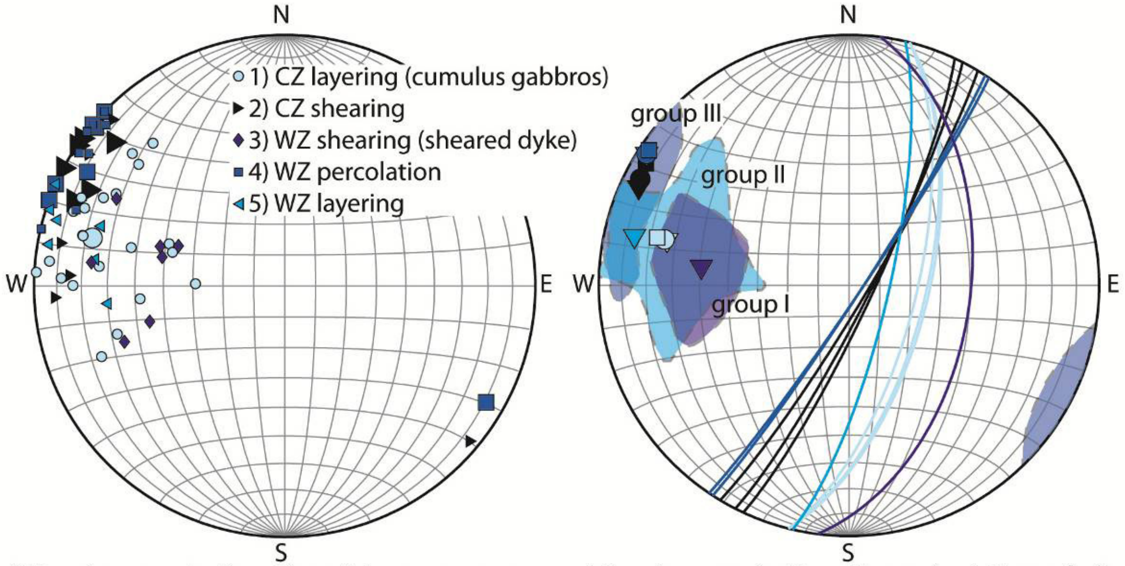

d) Equal area projection. Big points were measured directely on planar structure. Small points are calculated from two lineations.

e) Equal area projection. Mean orientations of: all points (triangle); big points counting double (circle); only big points (squares).

Figure 1: Magmatic structures and orientation of layering and shear zones.

P 3.6

Origin and emplacement of a clinopyroxenite body in the feeder-zone of an ocean island volcano (Fuerteventura, Canaries)

Tornare Evelyne[1], Bussy François[1]

[1] *Institute of Earth Sciences, Anthropole, University of Lausanne, CH-1015 Lausanne, Switzerland*

The PX1 or Pajàra pluton is a 22 Ma-old vertically layered gabbro-clinopyroxenite body outcropping in the exhumed basal complex of the Canarian Fuerteventura ocean island. It is interpreted as the shallow-level feeder-zone of an alkaline volcano. PX1 consists in five 50 to 100m-wide gabbroic sequences with a NNE-SSW orientation, alternating with clinopyxroxenite sequences. This general structure has been interpreted by Allibon et al. (2011) as sequential emplacement of basaltic magma pulses in a tectonically-controlled transtensional environment in a similar way as a sheeted-dyke complex. Clinopyroxenite sequences would represent truncated differentiation units from which residual liquids were squeezed out by local overpressure resulting from emplacement of subsequent magma pulses during peak magmatic activity. Alternatively, gabbroic sequences would represent non differenciated melts crystallized during more quiescent periods.

New detailed field observations could not establish any direct evidence of vertical or horizontal fractionation or layering in the clinopyroxenites. The latter appear more like a heterogeneous host-rock to the gabbroic dyke sequences than as discrete crystallization units. They are mainly composed of olivine-clinopyroxenites and wherlites crosscut by clinopyroxenitic pegmatite veins. In some places more evolved melts percolated through the clinopyroxenitic body as intergranular porous flow and also through open fractures resulting in dykes of various compositions. Olivine-rich enclaves of various shapes and sizes are also commonly observed within the clinopyroxenites. It is not yet clear whether these enclaves are in-situ dismembered cumulitic layers or lumps formed at deeper levels and brought up by subsequent magma batches. These observations appear to contradict the pyroxenite emplacement model by crystal-mush squeezing and truncated differentiation of Allibon et al. (2011). On the other hand, clinopyroxenes frequently exhibit chemical zonations which point to polybaric crystallization at different levels. Preliminary geochemical results also indicate a clear differentiation trend among clinopyroxenites. The most primitive sample is related to a large enclave of cumulitic dunite wrapped into clinopyroxenite. Our current interpretation is to consider PX1 as a clinopyroxenitic body resulting from emplacement of clinopyroxenite-wherlite mixed mushes, through which more differentiated alkaline melts percolated and gabbro dykes were injected.

REFERENCES

Allibon J., Bussy F., Lewin E., Darbellay B., (2011). The tectonically controlled emplacement of a vertically sheeted gabbro-pyroxenite intrusion: Feeder-zone of an ocean-island volcano (Fuerteventura, Canary Islands). Tectonophysics 500, 78-97.

P 3.7

Alkaline melts –peridotite reaction as the process responsible for the nephelinite-alkali basalt transition

Laetitia Rochat[1], Sebastien Pilet[1]

[1] *University of Lausanne, Switzerland. Laetitia.Rochat@unil.ch; Sebastien.Pilet@unil.ch.*

Alkaline lavas from continental volcanoes or oceanic islands are characterized by a compositional continuum from nephelinites to alkali olivine basalts and often to tholeiites. The trace-element patterns are generally similar for the various basic magmas from a single volcano, but with overall trace-element concentrations decreasing with decreasing alkalinity. The decrease of trace elements has been interpreted as an increase of the degree of partial melting of a common source [1]. We perform partial melting calculation to test this hypothesis for the cases of Cantal Massif (French Massif Central) and Iblean plateau (Sicily, Italy) alkaline series. These calculations show that even the nature of the source changes from peridotite to pyroxenite, the increase of the degree of partial melting of a common source is unable to explain the general decrease of trace-elements contents from nephelinite to alkali basalt. In addition, no lithologies potentially present in the mantle (peridotite ± CO_2, pyroxenite, …) seems able to produce the ~6 wt% SiO_2 variation observed in alkaline series by an increase of the degree of partial melting from ~2% to 10%, range predicted by the variation of Th or La in alkaline series.

An alternative to explain the nephelinite-alkali basalt transition is the partial melting of a heterogeneous source [2]. To test this hypothesis, we perform trace-elements simulation for the melting of a heterogeneous source including enriched mantle (EM) and pyroxenite (PX) embedded in depleted mantle (DM) [2]. Even the melt extraction depth and proportion of EM-DM-PX in the source could vary, no model has been able to produce the observed variations. A variation of depth at which the melt is extracted from the source could explain the variations observed for very incompatible elements but not for HREE. In addition such model predicts isotopic variations as function of the proportion of the melt coming from the different lithologies, variations that are in contradiction with the constant isotopic composition observed in Cantal and Iblean alkaline series.

A second alternative suggests that nepheline–alkali basalt transition could be linked to a reaction between alkaline melt and peridotite [3]. Reaction experiments at lithospheric pressure (0.8-2.5 GPa) [3, 4] have shown that key features of the major-element alkaline trend could be explained by interaction between nephelinitic melt and peridotite which generates a higher-Si melt plus ol via dissolution of opx from the peridotite. Here, we have calculated the effect of such reaction on the trace-element budget of alkaline lavas from Cantal massif and Iblean plateau. The opx dissolution induces a dilution of trace-elements which account for most of the variation observed between nephelinite to alkali basalt/tholeiite. Nevertheless, the best fit was obtained by combining melt-peridotite reaction with a slight increase of the degree of partial melting at which the initial nephelinitic melt is produced.

We conclude that the basanite–alkaline basalt transition more likely represents a reaction between low silica alkaline melt and peridotite rather than by an increase of the degree of partial melting of a common source.

REFERENCES

[1] Green (1970);
[2] Ito & Mahoney (2004);
[3] Pilet et al. (2008);
[4] Van den Bleeken et al. (2011).

P 3.8

PT-t evolution of migmatites from the region of Todtnau (southern Schwarzwald, southwest Germany)

Suter David, Franz Leander, de Capitani Christian

Mineralogisch-Petrographisches Institut, Bernoullistrasse 30, CH-4056 Basel
(d.suter@stud.unibas.ch), (leander.franz@unibas.ch), (christian.decapitani@unibas.ch)

The Schwarzwald is part of the Moldanubic Zone of the Hercynic fold belt of central Europe. The town Todtnau lies within the “central Schwarzwald gneiss complex” (CSGC) neighboring the “Badenweiler-Lenzkirch-zone”. The gneisses of the central and southern Schwarzwald experienced a complex thermal history in Variscan time with an early ultrahigh-temperature metamorphism followed by a pressure-dominated granulite-facies event and a LP/HT event leading to explicit anatexis of the rocks (see Kalt et al. 2000 and references within). Zircon dating reveal Variscan ages of about 330 Ma for this metamorphic overprint (Kalt et al. 1994; 2000). The aim of this study was a petrographic and thermobarometric investigation of metabasic and metapelitic migmatites from the southernmost part of the CSGC.

Samples were taken from 3 different locations around Todtnau. North-west of the town outcrops of metabasitic dictyonitic migmatites occur, which are intruded by small granite veins. The pristine rocks display only a slight metamorphic foliation and are cut by leucosome veins containing numerous hornblende crystals. Similar metabasic rocks crop out near the Todtnau cascades, however, they often display a distinct metamorphic foliation and fold textures. The third location lies northeast of Todtnau and is dominated by a series of metapelitic migmatites. These rocks, which reveal a distinct metamorphic foliation and banding with mica-rich melanosomes and quartz-feldspar-rich leucosomes, are often strongly weathered.

Under the microscope, the metabasic migmatites display sections hardly affected by the melting (paleaosome), which bear the mineral assemblage garnet-clinopyroxene-biotite-plagioclase-quartz. In sections with dominant anatexis, garnet and clinopyroxene are resorbed and a growth of hornblende is observed; furthermore, quartz, plagioclase and K-feldspar are present. Using conventional thermobarometry, PT conditions of 750 (+-+50)°C and 1.03 (+- 0.19) GPa are derived for the relic mineral assemblage in the palaeosome (Fig. 1). These data are supported by calculations with the TWQ-program of Berman (1991) and equilibrium assemblage calculations with the isopleth thermobarometry using the Theriak/Domino-program of De Capitani & Brown (1987). PT-conditions during the anatectic melting were estimated at 700-800°C at 0.55-0.75 GPa using the Al- and Ti-contents in hornblende that formed in the leucosome (Fig. 1).

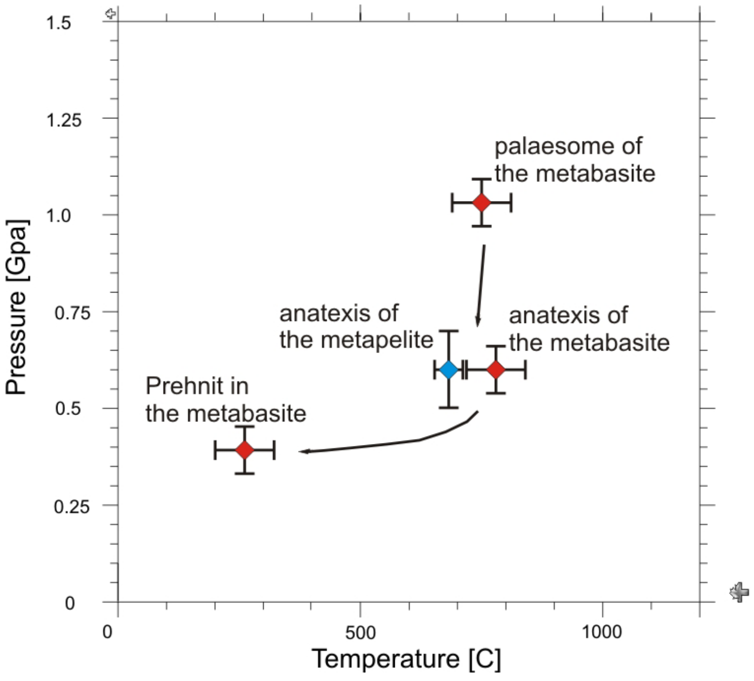

Fig.1: Assumed PT-path for the migmatites around Todtnau.

The metapelitic migmatites show a thorough anatectic overprint with leucosomes made up of K-feldspar, plagioclase and quartz while the melanosomes and palaeosomes contain additional sillimanite, Ti-rich biotite and rare garnet. Garnet-biotite thermometry combined with GASP barometry reveals PT-conditions of 700 (+-30)°C at 0.65-0.75 GPa, which is well in accord the results from the anatectic metabasic migmatites. Very similar results are achieved using the TWQ program. Equilibrium assemblage calculations with the Theriak/Domino program indicate a PT box ranging from 650-750°C at 0.3-0.8 GPa for the observed mineral assemblage in presence of anatectic melt (Fig.1).

Locally, the migmatites experienced a strong late hydrothermal overprint leading to an intense decomposition of the primary metamorphic minerals. In the metabasic rocks, mineral assemblage including prehnite and chlorite formed. Equilibrium assemblage calculations reveal PT-conditions of 200-350°C at <0.45 GPa for this overprint (Fig. 1). The timing of this last hydrothermal event is not constrained; it may have occurred during the late Palaeozoic magmatism or during the formation of the Rhine graben.

REFERENCES

Berman, R.G. (1991), Thermobarometry using multi-equilibrium calculations: a new technique, with petrological applications, in Quantitative methods in petrology: an issue in honor of Hugh J. Greenwood, edited by T.M. Gordon, and R.F. Martin, Canadian Mineralogist, 29, 833–855.

De Capitani, C., and T.D. Brown (1987), The computation of chemical equilibrium in complex systems containing non-ideal solutions, Geochimica et Cosmochimica Acta, 51, 2639–2652.

Kalt A., Altherr R., Hanel M. (2000), The variscan basement of the Schwarzwald, Berichte der Deutschen Mineralogischen Gesellschaft. 2000; 2,1-43.

Kalt A, Grauert B., Baumann A. (1994), Rb-Sr and U-Pb isotope studies on migmatites from the Schwarzwald (Germany): constraints on isotopic resetting during Variscan high-temperature metamorphism. J Metam Geol 12; 667-680

P 3.9

Fe^{3+}/Fe^{2+} ratios in minerals and bulk of metamorphic rocks: Mössbauer spectroscopy, wet chemistry and high resolution XANES on the blueschists of Syros and Sifnos (Cyclades, Greece)

Hunziker Daniela[1], Reusser Eric[2], Grolimund Daniel[3], Lottermoser Werner[4], Burg Jean-Pierre[1]

[1] *Geological Institute, ETH Zürich, Sonneggstrasse 5, CH-8092 Zürich (daniela.hunziker@erdw.ethz.ch)*
[2] *Institute of Geochemistry and Petrology, ETH Zürich, Clausiusstrasse 25, CH-8092 Zürich*
[3] *Swiss Light Source, Paul Scherrer Institute, CH-5232 Villigen*
[4] *University of Salzburg, Hellbrunnerstrasse 34, A-5020 Salzburg*

Ferric/ferrous iron ratios influence pressure and temperature estimations in metamorphic petrology. Any thermobarometric recalculation requires bulk and mineral iron values; however they are often scarcely known and have to be either estimated or pure ferrous systems be assumed. We intend to create a data base for blueschist minerals that can be incorporated into solid solution models used for pressure/temperature recalculations.

To create standards and correlate wet chemistry and Mössbauer spectroscopy with micro-XANES, minerals with supposedly pure ferrous and ferric incorporation were analysed. In addition, focus was set on more complex sodic amphiboles incorporating both Fe^{2+} and Fe^{3+} because they define the stability field of blueschist facies metamorphism. Glaucophane iron ratios of different parageneses, protoliths and Fetot from the locus typicus Syros and from Sifnos blueschists were determined with Mössbauer spectroscopy to investigate the influence on iron oxidation state and coordination. The same glaucophane grains were analysed with micro-XANES looking at the iron k-alpha pre-edge structure to investigate Fe^{3+}/Fe^{2+} ratios in situ.

Pressure/temperature estimations with the software PERPLE_X using measured bulk ferric/ferrous iron ratios and estimated ratios are compared. Significant discrepancy is discussed along with the consequences and misinterpretations that unknown or assumed ferric/ferrous iron ratios may introduce in the burial and exhumation history of the Syros and Sifnos blueschists.

P 3.10

Geochemical investigation of fluid inclusions in fissure-quarzcrystals of the Meta-dolomites in the Binn-Valley, Wallis, Switzerland

Müller Fabian[1], Mullis Joseph[1]

[1] *Mineralogisch-Petrographisches Institut, University of Basel, Bernoullistrasse 30, CH-4056 Basel (fab.mueller@unibas.ch).*

The aim of this investigation is a comparison of several sulfosalt bearing mineral localities in dolomitic rocks of the Binn-Valley (Wallis, CH), in terms of their occurring fluids. The Lengenbach quarry is one of the most famous mineral collecting sites in Switzerland. In the last decades, numerous investigations on geology, mineralogy and ore formation for this mineralization were done. The richness of sulfosalt minerals and the occurence of Tl-sulfosalts is of specific scientific interest. The mineral deposit is located in Triassic meta-dolomites, underlayed by Jurassic schists (Bündnerschiefer). Over the dolomitic rocks different Pretriassic ortho- and paragneises occure (Hügi 1988). Due to the tectonic settings the primary stratigraphic sequence of the rocks is reversed. Beside the Lengenbach quarry, other sulfosalt bearing deposits are known, situated within dolomitic rocks. The most famous are Reckibach and Turtschi. The localities Reckibach and Turtschi show considerable differences in their element dominances refered to the sulfosalt- and sulfide minerals. The outcrop Turtschi shows a Sb-Bi-dominance whereas Reckibach is clearly Ag-dominated. The Lengenbach quarry in addition is characterized by the occurence of Tl-sulfosalts and shows the largest mineral diversity of all outcrops (Graeser 1965).

Quartz crystals from alpine fissures are the hostmineral of the investigated fluid inclusions. Differentiated inclusion petrography and microthermometric investigations are the basis of this work. It enables to evaluate the succession, approximated composition and density of the fluid inclusions. With the help of a Raman-Microprobe it was possible to determine occurring daughter minerals (halite, calcite, sphalerit) and dissolved volatile species (H_2O, CO_2, H_2S). The qualitative composition of high-saline fluid inclusions were derived by SEM, analysing the perecipated solids after decrepitation.

The investigations show a clear fluid evolution, beginning with CO_2-rich fluid inclusions (Fig.1) too H_2O-rich inclusions (Fig.2). On two localities it was possible to determine high-saline fluid inclusions (Fig.3) which formed between the CO_2- an H_2O-rich fluid inclusions populations. It seems that the well developed sulfosalt-crystals in the fissures are the result of mobilization processes of preexisting sulfosalt precipitation within the dolomitic rocks more or less close to the fissure Systems. The occurrence and geochemistry of the ore penetration indicate a Sedex-formation (Knill 1993) for the different localities.

REFERENCES

Graeser S. (1965): Die Mineralfundstellen im Dolomit des Binntales. Schweiz. Min. Petr. Mitt., Band 45, Heft 2, 601-791.

Hügi M. (1988): Die Quarze der Mineraliengrube Lengenbach und ihre Einschlüsse. Unpublizierte Lizentiatsarbeit (Phil. nat. Fakultät Uni Bern, Mineralogisch- petrographisches Institut).

Knill M.D. (1996): The Pb-Zn-As-Tl-Ba-deposit at Lengenbach, Binn Valley, Switzerland. Beiträge zur Geologie der Schweiz, Geotechnische Serie, Lieferung 90.

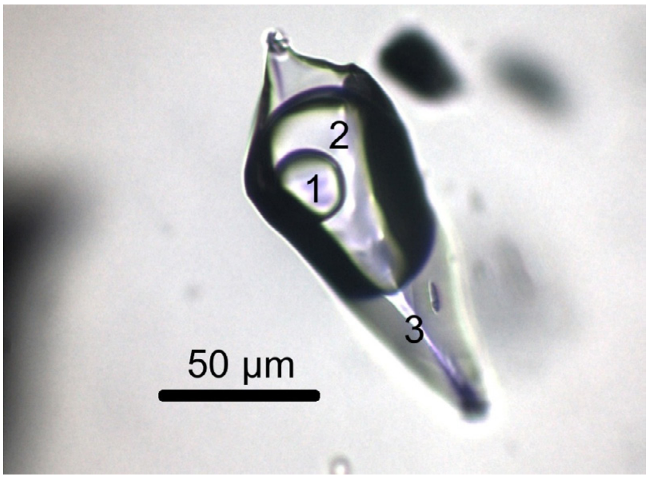

Figure 1: CO_2-rich fluid inclusion.
1: CO_2 (vapour), 2: CO_2 (liquid), 3: H_2O (liquid).

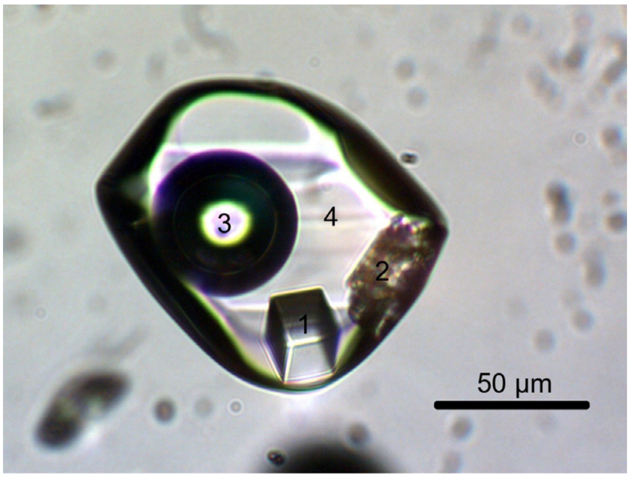

Figure 2: Salt-rich fluid inclusion.
1: NaCl (solid), 2: Calcite (solid), 3: H_2O/CO_2(vapour), 4: H_2O (liquid).

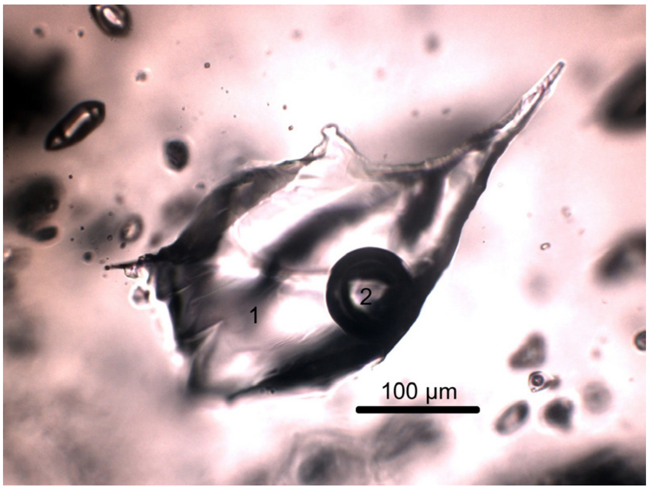

Figure 3. H_2O-rich fluid inclusion.
1: H_2O (liquid), 2: H_2O (vapour).

P 3.11

Retrograde fluid evolution and its impact on mineral precipitation. An example from an Alpine fissure of the Gotthard rail base tunnel between Amsteg and Sedrun, external part of the Central Alps.

Wolf Mathias*, Mullis Josef*

[1] *Mineralogisch-Petrographisches Institut, University of Basel, Bernoullistrasse 30,*
CH-4056 Basel (mathias.wolf@stud.unibas.ch)

Alpine fissures represent small hydrothermal systems in which the fluid evolution and mineral precipitation during retrograde conditions can well be investigated.

The present study is focused on a selected Alpine fissure, situated in the Central Aar granite of the Gotthard rail Tunnel. Its main topics are:
1. the evolution of the paleo- to the recent fluids (Bergwässer)
2. the evolution of the mineral assemblages due to changes in fluid composition and PT-conditions.

The Alpine fissure opened at 400 ±10° C and 3.5 to 3.8 kbar, due to compressional tectonics (Mullis, 2011).

Salinity of the mineralizing fluid evolved from 5.7 wt % NaCl equivalents in the earliest to < 3 wt % in the latest detected paleofluid. Recent fluids (Bergwasser) investigated by Bucher and Seelig (2010) show a bulk salinity of 0.27 wt %. This fluid evolution has been interrupted by a short input of a markedly higher saline fluid containing up to 8.7 wt % NaCl equivalents.

Several mineral assemblages formed during retrograde conditions: First the precipitation of biotite, epidote and quartz (early assemblage) succeeded by albite, adularia and chlorite (intermediate assemblage). Due to enhanced tectonic activity, a short but well developed assemblage followed with at least 3 generations of anhydrite ($\delta^{34}S$ = 25.6 ‰), baryte and hematite, containing higher saline fluid inclusions. Mineralization ends with the precipitation of the zeolite minerals laumontite, chabasite, stellerite and stilbite (late assemblage).

Interpretation:

1. The decrease in salinity from early metamorphic fluids in more or less closed systems towards late lower saline fluids is well known (Mullis et al. 1994). This possibly indicates dilution by meteoric water. This is the object of ongoing work including stable isotope and ICP-MS investigations.

2. Tectonic activity affected the fissure system episodically. A few strong events enabled infiltration of external fluids, containing Triassic sulfur. Sulfur bearing fluids are interpreted to originate from overlying evaporites (above the crystalline rocks of the Aar massif), from where they migrated into the actual position of the Central Aar granite.

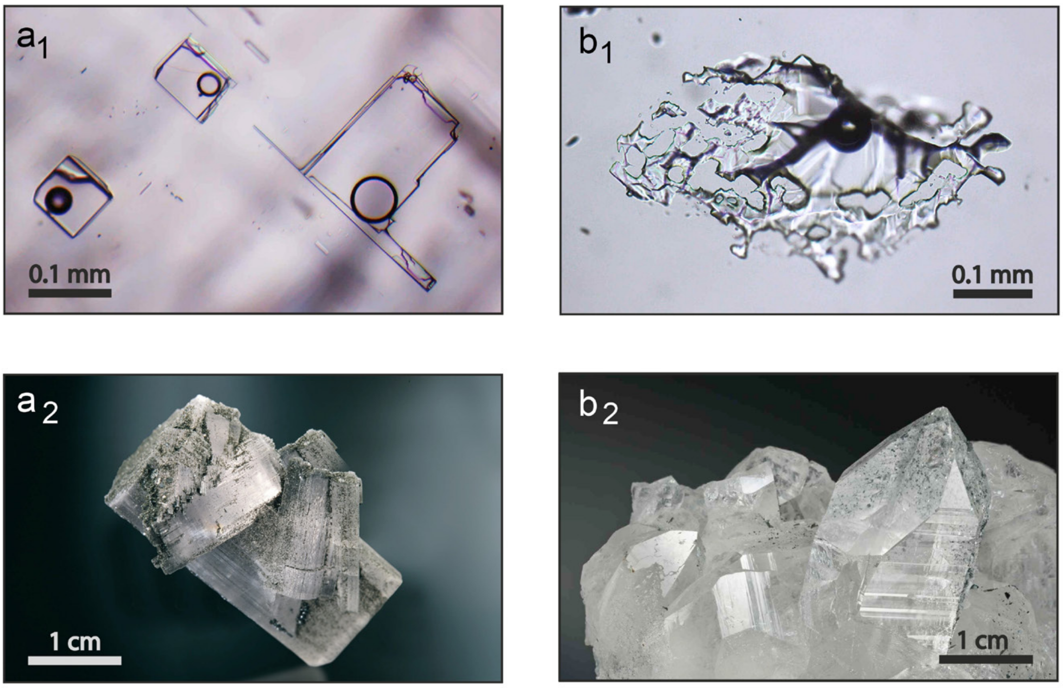

Figure 1. Earliest aqueous saline fluid inclusions (a_1 and b_1) in anhydrite (a_2) and quartz (b_2). Photos: a1 and b1 by Josef Mullis, a2 and b2 by Thomas Schüpbach.

REFERENCES

Mullis, J. 2011: Entstehung alpiner Zerrklüfte und Kluftminerale im Gotthard-Basistunnel, Abschnitt Amsteg-Sedrun und im Zugangs- und Kabelstollen von Amsteg. In: NEAT-Mineralien, Kristallschätze tief im Berg (Ed. by Amacher, P. & Schüpbach, T.). Verlag: GEO-Uri GmbH, Amsteg.

Mullis, J., Dubessy J., Poty, B. & O'Neil, J.1994: Fluid regimes during late stages of a continental collision: Physical, chemical, and stable isotope measurements of fluid inclusions in fissure quartz from a geotraverse through the Central Alps, Switzerland. Geochim. Cosmochim. Acta 58, 2239-2267.

Seelig, U. & Bucher, K. 2010: Halogens in water from the crystalline basement of the Gotthard rail base tunnel (central Alps). Geochim. Cosmochim. Acta 74, 2581-2595.

P 3.12

Experimental characterization of cement-bentonite interaction using core infiltration techniques coupled with 4D X-ray tomography

F. Dolder, U.K. Mäder A. Jenni

RWI, Institute of Geological Sciences, University of Bern, Baltzerstrasse 1-3, 3012 Bern, Switzerland
(florian.dolder@geo.unibe.ch, urs.maeder@geo.unibe.ch, andreas.jenni@geo.unibe.ch)

Deep geological disposal of radioactive waste foresee cementitious materials as reinforcement of tunnels, backfill, or as waste matrix. Bentonite, or sand-bentonite mixtures, are proposed as backfill material enclosing spent fuel drums, or as drift seals. The emplacement of cementitious material next to clay material generates an enormous chemical gradient in pore water, which drives diffusive transport. Laboratory studies and reactive transport modeling predict significant mineral alteration on both sides of interfaces, mainly resulting in a decrease of porosity in bentonite [2].

The goal of the project is to characterize and quantify the cement/bentonite skin effects spatially and temporally. The expected analytical data set will be amenable to interpretation by reactive transport modeling. The project focuses on the advective-diffusive transport domain, resolved at intermediate spatial scales. The experiment is carried out in a newly developed X-ray transparent core infiltration apparatus, which allow performing X-ray computed tomography scans (CT) [2] without interrupting the running core infiltration experiment (Fig. 2).

The experiment is performed on cylindrical bentonite samples, previously compacted and saturated (Fig. 1). A sample is then subjected to a confining pressure in order to simulate underground repository conditions. The infiltration of high-pH cement pore-fluids into the bentonite plug is expected to alter the mineral assemblage over time as an advancing reaction front. The related change in phase densities, porosity and local bulk density is tracked over time periodically by non-destructive CT scans. The resulting micrographs describe the “density” distribution in three dimensions and as a function of time. “Densities” are actually radiodensities calibrated with reference samples mounted in an identical apparatus (Fig. 2). After 1-2 years we will stop the experiment and subject the rock samples to post-mortem mineralogical and petrophysical analysis.

In the current experiment a compacted and saturated MX-80 bentonite is used as starting material. A confining pressure of 40 bar is applied. The infiltration fluid pressure is 20 bar, and the rate of discharge is on average 0.077 ml/day. The hydraulic conductivity of the bentonite is 1.12E-13 m/s at the beginning. The infiltrating fluid represents an ordinary Portland cement pore-water after a hydration time of 623 days (chemical composition after B. Lothenbach [3]).

First CT data show that X-ray computed tomography is a feasible tool to monitor ongoing infiltration experiments (Fig. 2). Using the reference samples, a bentonite density could be determined. The maximal voxel size of the scans is 0.10 mm. A pore-scale resolution is not required to track changes in a relatively homogenous medium with a large porosity and significant changes in X-ray attenuation during formation of mineral precipitates.

Acknowledgement
Financial support from Nagra is gratefully acknowledged. The Department of Forensic Medicine at University of Bern is acknowledged for providing time and technical support on their scanner.

REFERENCES

[1] Fernández R, Mäder U K, Rodríguez, M, Vigil de la Villa R and Cuevas J (2009). Alteration of compacted bentonite by diffusion of highly alkaline solutions. European Journal of Mineralogy 21, 725-735.
[2] Ketcham, R. A. and W. D. Carlson (2001). Acquisition, optimization and interpretation of X-ray computed tomographic imagery: applications to the geosciences. Computers & Geosciences 27(4): 381-400.
[3] Lothenbach, B. and F. Winnefeld (2006). Thermodynamic modelling of the hydration of Portland cement. Cement and Concrete Research 36(2): 209-226.

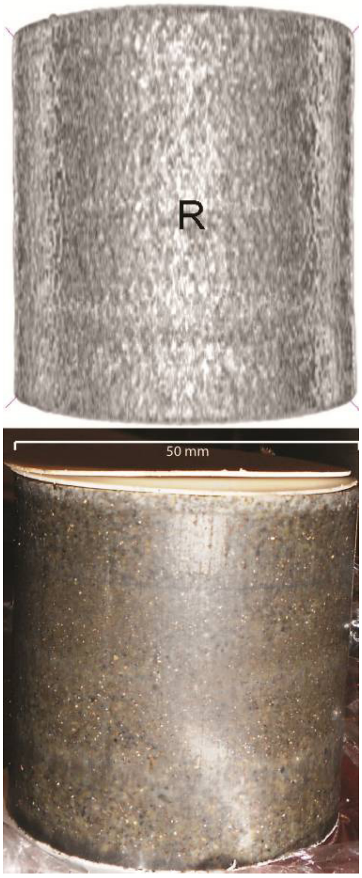

Figure 1. Two pictures of a bentonite sample. The upper image shows a CT scan and the lower one the original rock sample.

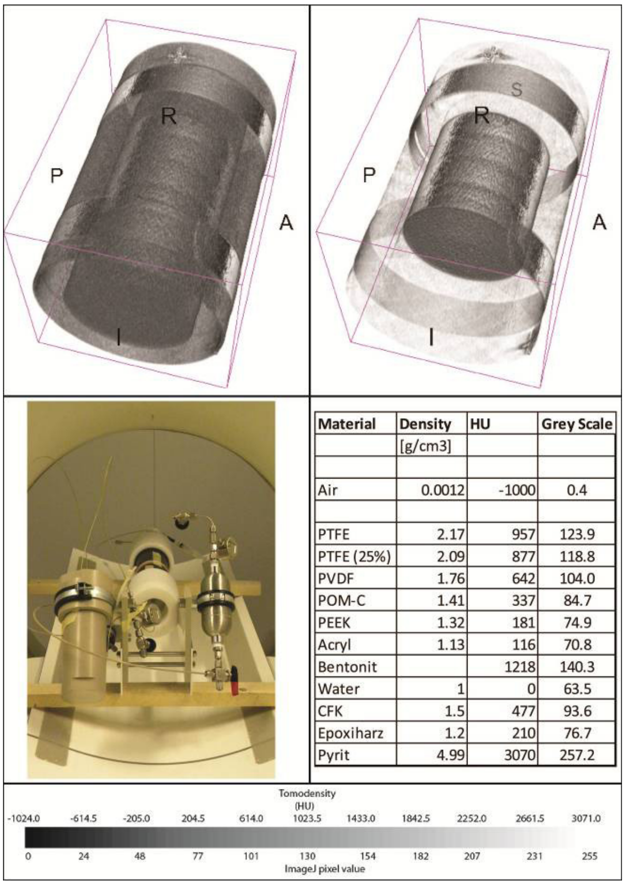

Material	**Density** [g/cm3]	**HU**	**Grey Scale**
Air	0.0012	-1000	0.4
PTFE	2.17	957	123.9
PTFE (25%)	2.09	877	118.8
PVDF	1.76	642	104.0
POM-C	1.41	337	84.7
PEEK	1.32	181	74.9
Acryl	1.13	116	70.8
Bentonit		1218	140.3
Water	1	0	63.5
CFK	1.5	477	93.6
Epoxiharz	1.2	210	76.7
Pyrit	4.99	3070	257.2

Figure 2. The two upper images are showing CT scans of the outer tube (left) and the bentonite specimen (right). The lower image is showing the mobile infiltration system in the CT scanner. The table and the gray-scale showing the relation between the radiodensity (HU) and the gray-scale values.

P 3.13

The enigmatic Songshugou complex (Qinling orogen, central China): mélange of high-pressure and (ultra) high-temperature metamorphic rocks?

Thomas Bader[1], Lifei Zhang[1], Leander Franz[2], Lothar Ratschbacher[3], Christian de Capitani[2]

[1] *Key Laboratory of Orogenic Belts and Crustal Evolution, MOE, School of Earth and Space Sciences, Peking University, Beijing 100871, China (thomas.bader@pku.edu.cn)*
[2] *Mineralogisch-Petrographisches Institut, Universität Basel, CH-4056 Basel*
[3] *Geologie, Technische Universität Bergakademie Freiberg, D-09599 Freiberg, Germany*

The ~25 × 5 km Songshugou complex abuts Devonian migmatites (P–T: 700-770 °C, 0.5-0.7 GPa) of the Qinling complex. It comprises a core of ultramafic rocks surrounded by amphibolite mylonites that host medium- to coarse-grained garnet-amphibolite and garnet-clinopyroxenite lenses. The latter underwent (ultra)high temperature metamorphism at 840-920 °C and 1.0-1.4 GPa (Zhang, 1999). Clinopyroxene-albite symplectites from these rocks were interpreted as relics of an earlier high-pressure stage, whose P–T conditions remain unknown (Zhang, 1999). Along a shear zone at the southern margin of the Songshugou complex, kyanite-bearing felsic granulite (peak P–T 800-900 °C, 1.3-1.6 GPa, Liu et al., 1996) and migmatitic, partly spinel- and corundum-bearing gneisses crop out. Herein, we focus on the garnet amphibolites, present new P–T data derived from garnet isopleth thermobarometry via DOMINO, and suggest a new model for the evolution of the Songshugou complex.

Samples 75282C and 75293E are composed of prograde zoned, ≤5 mm garnet porphyroclasts, mm-sized, light-greenish to greenish-brown, zoned amphiboles, and a mylonitic matrix of amphibole with subordinate plagioclase and quartz. Thermodynamic modeling in TNCKFMASH system points to quartz-eclogite facies conditions during garnet growth (Fig. 1), from 498 °C at 2.25 GPa to 530 °C at 2.54 GPa (sample 75293), and from 494 °C at 2.13 GPa to 510 °C at 2.44 GPa (sample 75282C). According to the calculation, garnet coexisted with omphacite, actinolite, lawsonite, phengite, quartz, and rutile at peak-pressure. During exhumation, omphacite and lawsonite were consumed and amphibole growth continued. Pronounced heating is reflected by steadily increasing Ti-contents in amphibole; Ti-in-amphibole thermometry (Colombi, 1988) applied to rims of large zoned amphibole prisms points to ~680 °C. Partial garnet-breakdown by formation of plagioclase-amphibole-quartz-coronas yielded similar conditions of 660-700 °C and 0.9-1.2 GPa by conventional thermobarometry (Bhadra & Bhattacharya, 2007; Colombi, 1988).

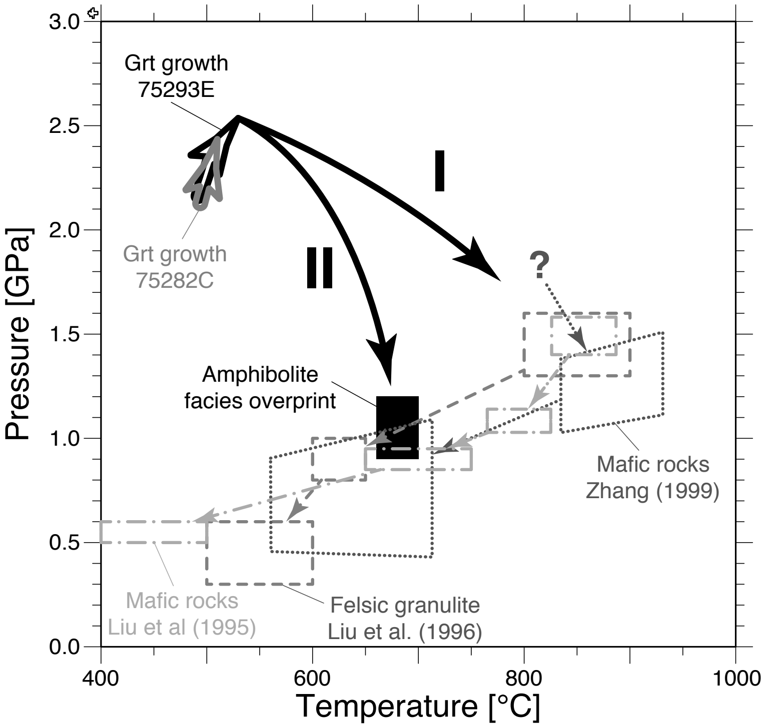

Figure 1. Published and new P–T estimates of mafic and felsic rocks from Songshugou complex.

It is debatable, which P-T path the two garnet amphibolites followed during exhumation, because nearby granulite-facies garnet clinopyroxenites also show relics of an earlier eclogite-facies metamorphism (Zhang, 1999), outlining P-T path I in Fig. 1. As our samples show no indications of granulite-facies metamorphism, this scenario does not apply to them and PT-path II in Fig. 1 is suggested. To account for these distinctly different P–T paths, we interpret the Songshugou metabasites as part of a tectonic mélange. The investigated samples stem from the downgoing slab, while the (U)HT garnet clinopyroxenite either represent a part of the overriding plate that was dragged to upper mantle depths or a different part of the downgoing slab that was exposed to distinctly higher temperatures during exhumation. The ultramafics stem from the upper mantle underneath the overriding plate. During their exhumation, all rocks were juxtaposed at P–T conditions of ~650-700 °C and ~1.0 GPa, as they have the amphibolite facies overprint in common.

REFERENCES

Bhadra, S. & Bhattacharya, A. 2007: The barometer tremolite + tschermakite + 2 albite = 2 pargasite + 8 quartz: Constraints from experimental data at unit silica activity, with application to garnet-free natural assemblages. American Mineralogist 92, 491-502.

Colombi, A. 1988: Métamorphisme et géochimie des roches mafiques des Alpes ouest-centrales (géopofil Viège Domodossola-Locarno). Ph.D. thesis, Universität Lausanne, 216 p.

Liu, L., Zhou, D., Dong, Y., Zhang, H., Liu, Y. & Zhang, Z. 1995: High-pressure metabasites and their retrograde metamorphic P-T-t path from the Songshugou area, Eastern Qinling Mountains. Acta Petrologica Sinica, 11, 127-136 (in Chinese with English abstract).

Liu, L., Zhou, D., Wang, Y., Chen, D. & Liu, Y. 1996: Study and implication of the high-pressure felsic granulite in the Qinling complex of East Qinling. Science in China Series D 39, Supplement, 60-68.

Zhang, Z.J. 1999: Metamorphic evolution of garnet-clinopyroxene-amphibole rocks from the Proterozoic Songshugou mafic-ultramafic complex, Qinling Mountains, central China. Island Arc 8, 259-280.

P 3.14

New data about regional metamorphism and magmatism of Khrami crystalline massif (the Caucasus, Georgia)

Giorgi Beridze[1], Ketevan Tedliashvili[1]

[1] *Alexsandre Janelidze Institute of Geology of Ivane Javakhishvili Tbilisi State University (giorgi.beridze@list.ru)*

The Khrami crystalline massif (KhM) represents a deeply eroded part of pre-Alpine basement of the Black sea – Central Transcaucasian terrane.

Among the pre-Alpine formations, that build up the KhM according to their age succession following major rock complexes are present: 1 – Precambrian gneiss-migmatite complex (GMC), 2 – pre-Variscian (Cambrian) basitic, 3 – Sudetian granitic and 4 – Late Variscian, volkcanigenic-sedimentary and quartz-porphyry – granite-porphyry complex (Khutsishvili, 1977; Gamkrelidze, Shengelia, 2005).

Two stages of regional metamorphism are identified within the KhM: prograde HT/LP (700-720°C, p<1.5 kbar) and retrograde (420-500°C, p 1.3-1.6 kbar).

The formation age of granites and basitic magmatism of the pre-Alpine basement of KhM was considered as Variscian for a long time. Based on special geological and isotope- geochronological investigation has been determined neo- Proterozoic age of initial rocks of GMC, Grenvilian prograde and Sudetian retrograde RM and Sudetian age of granites. La-ICP-MS U-Pb dating of two zircon crystals from paraplagiogneisses of GMC shows the age of RM 931±16 Ma.The average age of 28 crystals of zircon from granites and outer rims of the zircon from paraplagiogneisses corresponds to 325.6±2.6 Ma and covers interval 319-332±Ma.

Sudetian age of granites is firmly determined by geological data as well. In particular the age of developed on the periphery of KhM volcanigenic-sedimentary complex based on faunal and flora dating covers the interval from Visean till the late Bashkirian stage. To this time interval is related volcanic activity of quartz-porphyry and granite-porphyry composition. Their dikes inject postmetamorphic granites of KhM, accordingly the age limit of the latter couldn't be younger than Visean.

Geological, petrological and geochemical data as well as isotope-geochronological data enables to trace the stages of RM and granite formation and accordingly formation of pre-Alpine continental crust of KhM.

Basic mineral parageneses of Grenvile Regional Metamorphism – Crd+Bt+Qtz+Ort, Hbl+Bt+Pl+Qtz, Bt+Pl±Cum+Qtz while exposure of Sudetian phase of tectogenesis are emplaced by paragenesis Ms(Ser)+Chl+Ab±Mikr±Bt±Qtz, Ab+Chl+Mikr+Ep±Qtz+Car, Ab+Act+Chl+Ep±Qtz.

In GMC vein bodies of Cambrian (?) metagabbro are present which underwent only Sudetian RM and are injected by granites of the same age. The age of metabasites is apparently Cambrian (Shengelia, 2000; Gamkrelidze, Shengelia, 2001).

Isotope-geochronological data as well as existed geological, petrological and geochemical data enable to trace major stages of regional metamorphism and granite formation and accordingly formation of pre-Alpine continental crust of KhM.

On the first stage (1000 Ma and more) of formation of pre-Alpine continental crust of KhM takes place accumulation of terrigenous sediments (graywackes and pssamites) with minor amount of basic volcanites, that correspond to interplate and transitional between interplate and oceanic basalts. The source area for non-Proterozoic marine basin that provided it with clastic material, was located to the north from the basin and was built up by the rocks of subcontinental crust with low contetnt of K_2O. The total thickness of non-Proterozoic sheet is not less than 10 kbar.

On the second stage (1000-900 Ma) of crust-forming processes under suprasubduction conditions was formed of subcontinental or immature continental crust. As a result of Grenvilian RM (T=700-720°C, P,1.5 kbar), non-Proterozoic formations were transformed into plagiogneiss-plagiomigmatite complex. Plagiogneisses correspond to S-type granites and according to chemical and geochemical parameters belong to upper crust.

Cambrian metagabbroids occupied 25% of total volume of gneissimigmatite complex of KhM and caused basification of Grenvilian subcontinental crust.

According to geochemical data the most of Late Variscian granitoids belong to upper crustal type and are more comparable with S – type granitoids.

Simultaneously with formation of Late Variscian granitoids retrograde metamorphism (T≈420-500°C, P=1.3-1.6 kbar) and intensive rhiolitic volcanism takes place.

So, true continental crust in pre-Alpine basement of KhM is being formed during exposure of Late Variscian phase of tectogenesis. KhM was rich in leucocratic bodies of crustal-anatectical eutectoidal granites of different size.
It's significant, that great masses of all pre-Alpine rocks of different ages underwent intensive and almost total microclinization and are saturated by granitic material.

In the very end of Variscian orogenesis takes place unusually abrupt exhgumation of deeply burried parts of the earth crust, caused by izostatic and intensive erosion.

REFERENCES

Khutsishvili O.D. (1977). "Tectonic and formation history of Khrami crystalline massif." Proceedings of GI AS GSSR, vol. 56, 109p.

Gamkrelidze I.P., Shengelia D.M. (2005). "Precambrian-Paleozoic regional metamorphism, granitoid magmatism and geodynamics of the Caucasus." M. "Nauchni mir," 458 p.

Tedliashvili K.. Kvakhadze N., Maisuradze N., Beridze G. (2012). "Comparative characteristics of gneiss-migmatite complexes of the Black Sea - Centraltranscaucasian Tarrane. "Sciences and Technologies," #1-3. p. 30-36.

Shengelia D.M. (2000). "Mono- and polycycled regional metamorphism of the crystalline basement of the Caucasus." GI AS GSSR, New series, vol.115, p.282-289.

Gamkrelidze I.P., Shengelia D.M. (2001). "Conditions of the formation of magmatic rocks of Dzirula crystalline massif (the Caucasus)." Geotectonics, #1, p.60-72.

P 3.15

Elemental composition of a bangle shard from Harrappa, an Indus valley settlement

Kayani Saheeb-Ahmed

National University of Sciences and Technology, Islamabad-44000, Pakistan (saheebk@ceme.nust.edu.pk)

A terracotta bangle shard, collected from Harrappa, was tested for mineralogical and thermal characteristics and the results were reported by Kayani & Siddiqui in 2011. Although Harrappa is the most important site of Indus valley civilization yet little research has been carried out on terracotta jewellery unearthed at this site.

In order to complement the results of mineralogical and thermal testing, a brief research study has been carried out to determine the elemental composition of the components of the same bangle shard specimen using WD-XRF spectrometry analysis. (The testing was carried out at Geoscience Advance Research Laboratories, Islamabad, a facility maintained by Geological Survey of Pakistan.) Concentration of all major elements is included in the following table.

Element	Wt%
Si	46.845
Ti	0.712
Al	20.714
Fe	6.247
Mn	0.055
Mg	17.467
Ca	1.364
K	2.816
S	1.08

Loss on ignition (LOI) for above reported values is 2.7 wt%. As a consequence of the limitation imposed by the type of equipment used, no data on trace elements is available. However, the values of major elements for the tested specimen are comparable with the results of similar tests reported by Kumar et al. in 2006 (for Harrappan era pottery specimens only). Their pottery specimens were collected at Sanghol, another Indus valley site located near the city of Chandigarh in present day India. Minor variations may exist depending upon nature of the local soil.

REFERENCES

Kayani, S. A., Siddiqui, R. U. H. 2011: Mineralogical and thermal analyses of a bangle shard from Harrappa, an Indus valley settlement in Pakistan. Scientific Annals of Alexandru Ioan Cuza University (Geology Series), 57, 69-73.

Kumar, A., Garg, M. L., Singh, N., & Vijayan, V. 2006: Elemental analysis of potteries using energy dispersive X-ray fluorescence technique. Indian Journal of Pure & Applied Physics, 44, 300-307.

P 3.16

Geochemistry of Silurian Niur Sandstones in Tabas Block, Central Iran

Zohreh Nowrouzi[1], Reza Moosavi Harami[1], Asadolla Mahboubi[1], Mahammad Hossein Mahmoodi Gharaie [1] & Farzin Ghaemi[1]

[1] Ferdowsi University of Mashhad, Faculty of Science, Geology Department, IR-9177948974, Mashhad, Iran (Z_Novroozi85@yahoo.com)

An integrated petrographic and geochemical study of sandstone portions of Silurian Niur Formation, Central Iran was carried out to infer their provenance and tectonic setting. This study is based on the petrography (40 rock samples) and geochemistry (12 rock samples) analysis from one stratigraphic section in Derenjal Mountains in Northwestern Tabas block.

Modal analysis data of 40 medium sand size and well sorted samples reveal most of quartz composed of monocrystalin grains with straight to slightly undulos extinction but there are about 3% polycrystalin quartz. These monocrystalin and polycrystalin quartz grains with rutile needle inclusions can be derived from felsic igneous rocks of a craton interior setting.

On the basis of the framework composition and geochemistry (major and trace elements) data, the sandstones are classified as quartzarenite, sublitharenite, and subarkose types. Petrographic studies reveal that these sandstones contain quartz, feldspars and fragments of sedimentary rocks.

The detrital modes of these sandstones indicate that they were derived from recycled orogen and stable cratonic source. Major and trace element contents of them are generally depleted (except SiO_2) relative to UCC (Upper Continental Crust) which is mainly due to the presence of quartz and absence of other Al-bearing minerals.

Modal composition and discrimination diagrams based on major as Roser & Korsh(1988, Fig.1a) and Bhatia (1983, Fig.1b) also trace element concentrations, such as Ti, La, Th, Sc and Zr, and Bhatia & crook (1986, Fig.2) diagram, suggest a felsic igneous source rock and quartzose polycyclic sedimentary provenance in a passive continental margin setting. Furthermore high Zr/Sc values in these sandstones, considered as a sign of recycling, which can be related to effects of the Caledonian orogeny in Central Iran.

The results of this study suggest that the main source for these sandstones was likely located in Tabas block in Central Iran as an upplifted basin. Paleoweathering conditions indicated by modal compositions and Al_2O_3+K_2O+Na_2O% versus SiO_2 bivariate of these sandstones. Our studies suggests humid conditions for source area.

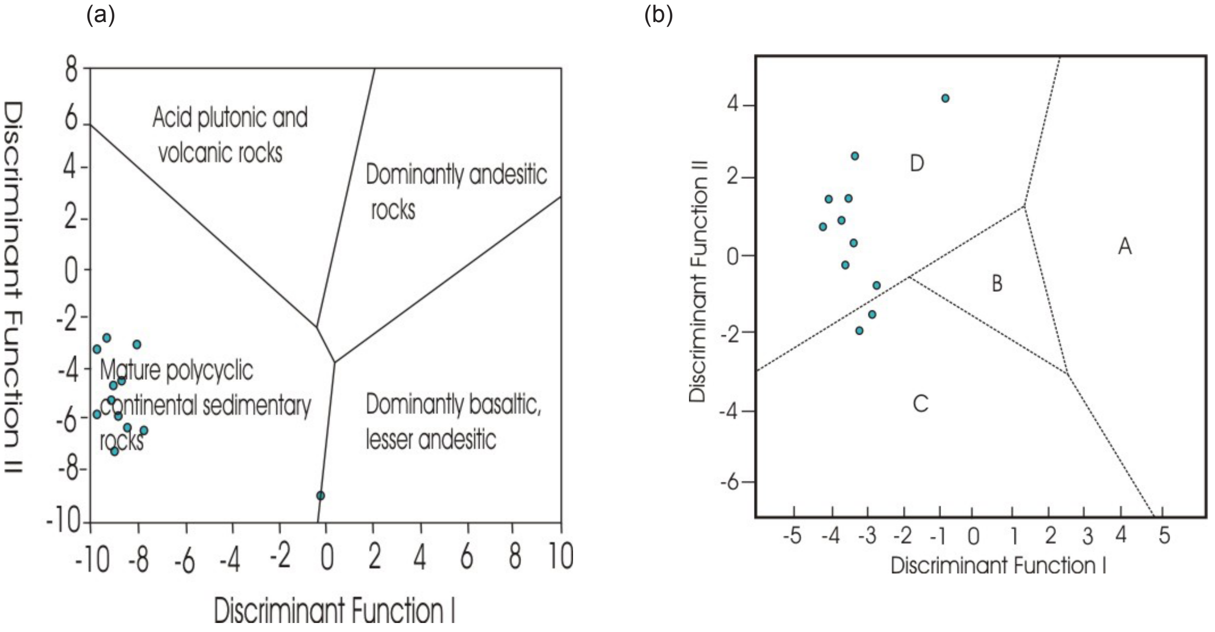

Figure 1. Plots of the major element composition of the Silurian Niur Sandstone member on the (a) different provenances discrimination diagram of Roser and Korsch (1988) and (b) tectonic setting discrimination diagram of Bhatia (1983). A=oceanic island arc; B=continental island arc; C=active continentalmargin; D=passive continental margin.

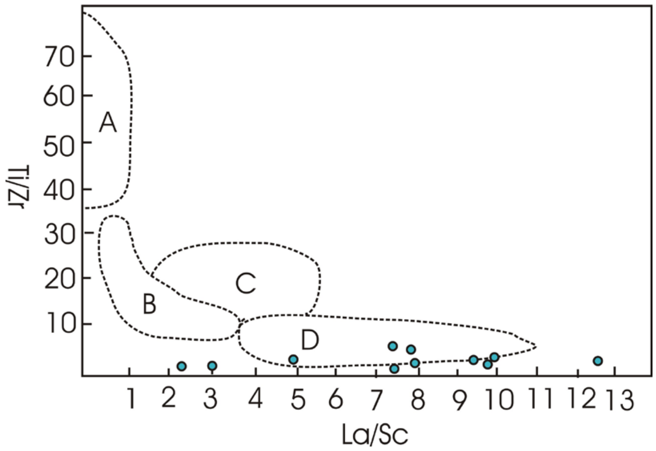

Figure 2. Trace element compositionof the sandstones from Niur Formation on the triangleand bivariate tectonic setting discriminationdiagramsof Bhatia and Crook (1986). A=oceanic island arc; B=continental island arc; C=active continentalmargin; D=passive continental margin.

REFERENCES

Bhatia, M.R. 1983: Plate tectonics and geochemical composition of sand-stones. J. Geol. 91, 611–627.

Bhatia, M.R., Crook, K.A.W., 1986. Trace element characteristics of gray-wackes and tectonic setting discrimination of sedimentary basins.Contrib. Mineral. Petrol. 92, 181–193.

Roser, B.P., Korsch, R.J. 1988. Provenance signatures of sandstone–mud-stone suites determined using discriminant function analysis of major-element data. Chem. Geol. 67, 119–139.

P 3.17

Early Palaeozoic tectonic process in north-western Gondwana as revealed by zircon hafnium isotope analysis: tectonic switching along an active margin

Van der Lelij Roelant[1], Spikings Richard[1], Gerdes Axel[2] & Ulianov Alexey[3]

[1] *Section of Earth and Environmental sciences, University of Geneva, Rue des Maraîchers 13, 1205 Genève (roelant.vanderlelij@unige.ch)*
[2] *Institut für Petrologie, Geochemie und Lagerstättenkunde, Universität Frankfurt am Main, Altenhöferallee 1, D-60438, Germany*
[3] *Institut de Minéralogie et Géochimie, Université de Lausanne, Anthropole, CH-1015 Lausanne*

An increasing number of global plate reconstructions for the lower Palaeozoic, place the southern Rheic Ocean passive margin in the Northern Andes, across present day Venezuela, Colombia and Ecuador. These reconstructions are based upon the hypotheses that: a) the lower Palaeozoic position of these terranes was outboard of the Colombian Andes basement and b) Ordovician tholeiites exposed in Mexico record a rift to drift transition during the opening of the Rheic Ocean (e.g., Keppie et al., 2008 and references therein). However: a) these units are separated from South America by the intervening Caribbean Plate, and their lower Palaeozoic position is speculative; b) the same basement complexes have also been interpreted as a tectonic assemblage of Early and Late Palaeozoic high pressure belts formed in convergent margin settings (e.g., Vega-Granillo et al., 2009 and references therein); and c) these models seem to ignore all existing data and working hypotheses from Northern Andean geology, which predict Ordovician accretionary orogenesis, rather than rifting (e.g., Restrepo-Pace and Cediel, 2010).

The study of basement rocks exposed in the Northern Andes of Venezuela and Colombia should be a less controversial basis for understanding the tectonic history of northern South America. We present new, in-situ zircon Lu-Hf isotopic and U-Pb geochronological which place new constraints on the tectonic settings of the Northern Andes in the Early Palaeozoic.

The Northern Andes host Precambrian basement overlain by Middle to Late Cambrian metasedimentary units whose detrital zircon signature suggests a Gondwanan provenance. Metamorphism of these units to upper amphibolite facies and deformation together with early Ordovician orthogneisses suggests metamorphism may have culminated at ~470 Ma. Middle Ordovician to latest Silurian granitoids are mostly undeformed, have continental arc geochemistry, and Hf isotopic data shows a much more juvenile input in the magmatic source after ~470 Ma.

Zircons from a Felsic tuff associated to a VMS deposit and marine sedimentary rocks from the western Mérida Andes in Venezuela, yield a late Ordovician age. The development of a marine basin suggests crustal thinning, and the common association of post-Archaean VMS deposits to back-arc or intra-arc settings suggests that the middle Ordovician shift to less crustal magmatism was accompanied by extension driven by slab roll-back. Subsequent Late Ordovician to Silurian magmatism rapidly became more crustal, which may suggest a period of crustal thickening driven by compression.

Due to their very similar geological histories, isotopic trends, and detrital zircon signatures, we propose that the basement rocks exposed in the Santander Massif of Colombia and the Mérida Andes of Venezuela do not define separate allochthonous terranes as previous authors have suggested. Instead, these basement blocks followed similar histories on the north western Gondwanan margin since at least the Cambrian.

Intense Lower Palaeozoic deformation and magmatism, followed by an absence of Devonian – middle Carboniferous magmatism in Colombia and Venezuela, are features shared with the central and southern Andes of Peru, Chile and Argentina (Bahlburg et al., 2009), where tectonic switching may also have been the modus operandi in the lower Palaeozoic (Miller and Söllner, 2005). This suggests a similar tectonic setting along the same active margin.

Collectively, these findings strongly suggest that the north-western corner of Gondwana was host to an active margin. Therefore, the southern passive margin of the Rheic Ocean was situated eastwards from the basement rocks exposed in the Northern Andes.

REFERENCES

Bahlburg, H., Vervoort, J.D., Du Frane, S.A., Bock, B., Augustsson, C., and Reimann, C., 2009, Timing of crust formation and recycling in accretionary orogens: Insights learned from the western margin of South America: Earth-Science Reviews, v. 97, no. 1-4, p. 215–241.

Keppie, J.D., Dostal, J., Miller, B.V., Ramos-Arias, M.A., Morales-Gámez, M., Nance, R.D., Murphy, J.B., Ortega-Rivera, A., Lee, J.W.K., and Housh, T., 2008, Ordovician-earliest Silurian rift tholeiites in the Acatlán Complex, southern Mexico: Evidence of rifting on the southern margin of the Rheic Ocean: Tectonophysics, v. 461, no. 1-4, p. 130–156.

Miller, H., and Söllner, F., 2005, The Famatina complex (NW Argentina): back-docking of an island arc or terrane accretion? Early Palaeozoic geodynamics at the western Gondwana margin: Geological Society, London, Special Publications, v. 246, no. 1, p. 241.

Restrepo-Pace, P.A., and Cediel, F., 2010, Northern South America basement tectonics and implications for Palaeocontinental reconstructions of the Americas: Journal of South American Earth Sciences, v. 29, p. 764–771.

Vega-Granillo, R., Calmus, T., Meza-Figueroa, D., Ruiz, J., Talavera-Mendoza, O., and López-Martínez, M., 2009, Structural and tectonic evolution of the Acatlán Complex, southern Mexico: its role in the collisional history of Laurentia and Gondwana: Tectonics, v. 28, no. 4, p. TC4008.

P 3.18

Accessory ilmenorutile of diamondiferous terrigenous rocks of South Timan in the north-east borderland of the East-European platform.

Grakova, O.V.

Institute of Geology, Komi Science Centre, Ural branch of The Russian Academy of Sciences, Syktyvkar, Republic of Komi, Russia (ovgrakova@geo.komisc.ru)

The diamond-bearing terrigenous rocks is located in the Timan ridge in the north-east borderland of the East-European platform. The geological history of the Timan there was a huge break in sedimentation which was in the early Paleozoic. It promoted of wide manifestation of rock weathering processes so that there was a concentration of a number of useful minerals. There are unique on reserves of a deposit of bauxites and the titanium, and perspective show of rare, nonferrous and noble metals, diamonds and many other mineral resources.

The problem of a diamond content of Timan is the center problem of explorer more than 50 years. But the question of conditions of their formation, placement and a structure remains a subject of discussions. In spite of the long mineralogical study of this stratigraphical subdivision, there is still no answer to two important questions: 1 – whether the productive formations are sedimentary rocks; 2 – if the productive deposits of the Pizhma series are a secondary collector, as it was traditionally thought, where are provenances of Timanian diamonds?

Individual indicator minerals is important in determining the conditions of formation of diamond-bearing terrigenous deposits in the Timan problematic genesis. As featured typomorphic ilmenorutile we can select the specific conditions of formation and history of the further development of minerals.

Microprobe analysis ilmenorutile of diamondiferous terrigenous mid-devonian deposits, composed of sandstones with gritstone and clay bands, showed that the basic components of the mineral are niobium, tantalum, titanium and iron, there are the following admixture element: tungsten, vanadium, tin, manganese and scandium. According to available data [1] we can conclude that we are dealing with the decay products ilmenorutile. From the ratio of $(Nb_2O_5 + Ta_2O_5) / TiO_2$ they are similar to ilmenorutiles typical of granitic pegmatites, in Ta_2O_5/Nb_2O_5 ratio they similar to be ilmenorutiles beryl-columbite albitization granitic pegmatites. According to the content to V they refer to ilmenorutile of carbonatites, Sn contain ilmenorutiles of pegmatites.

According to the results of the study the author comes to the conclusion, that the rocks of Asyvvoj relate to secondary deposits. Ilmenorutile formation passed in different conditions, basically it is connected with granitice pegmatites, but there are some admixture elements connected with carbonatites.

REFERENCES

Grakova O. V. Accessory ilmenorutile of diamondiferous mid-devonian rocks of South Timan // the Bulletin Of In. geology of Komi NC UrO of the Russian Academy of Sciences, 2011. N° 10. P. 11–13.

Grakova O. V. Mineralogy of diamond-bearing terrigenous rocks in the north-east borderland of the East-European platform // 14 – international EMPG conference. Kiel, 2012. P. 69.

Katelya (Grakova), O.V. Minerals of diamond-bearing rock of the Pizhma series of the Middle Timan. // The Syktyvkar mineralogical collection. Syktyvkar, 2007. N° 35. P.81-88. (Institute of Geology, Komi Science Centre, Ural branch of The Russian Academy of Sciences. V. 122).

P 3.19

Exocontact Metamorphism in Klich Gabbro-diorite Intrusive

Kristine Vardanashvili [1], Nikoloz Maisuradze[1]

[1] Alexsandre Janelidze Institute of Geology of Ivane Javakhishvili Tbilisi State University (qristinav@yahoo.com)

The Klich gabbro-dioritic intrusive participates in the make-up of the crystalline core of the Greater Caucasus and is exposed in the limits of the Pass subzone of the Main Range zone. The exposure of the intrusive is fixed in the eastern part of mountainous Apkhazeti, in headwaters of the river Kodori, covering about $10km^2$. According to different authors the intrusive is represented by "eye-shaped" biotite-hornblende bearing and biotitic orthogneisses (Somin, 1971), or by gabbros and gabbrodioritic orthogneisses (Javakhishvili, 1979). According to our data, the most widespread among the rocks composing the Klich intrusive are hornblende bearing and weakly biotitized gneissose diorites, and relatively less spread are their last marginal members – gabbros and especially quartz-diorites. The rocks including the intrusive are represented by the rocks of Gwandra suite of Buulgen series, which underwent regional metamorphism corresponding to the staurolite facies connected with the Late Baikalian orogenic cycle. In the Late Paleozoic time, the Gwandra suite rocks together with the rocks composing the Klich intrusive, underwent prograde regional metamorphism connected with the Bretonian phase of the Variscan orogeny, which corresponds to the andalusite-sillimanite pressure type and temperature conditions of biotite-muscovite bearing gneissic facies (Shengelia, Ketskhoveli, 1982; Shengelia, 2000).

According to K_2O/Na_2O-SiO_2 diagram figurative points of the Klich gabbro-dioritic intrusive are disposed in Na-, K-Na- and Na-MORB series. In $FeO^{*}/MgO-SiO_2$ and AFM diagrams they occupy the calc-alkaline and tholeiitic fields, but in $Na_2O+K_2O-SiO_2$ diagram they correspond to the calc-alkaline only.

According to ACM and AFM binary diagram figurative points of the studied rocks arranged predominantly near the fields of MAR and basic cumulates and in Ti/Cr-Ni diagrams they occupy an IAT field.

In Ce/Pb-Ce, Sm/Yb-Ce/Sm diagrams the figurative points indicating the rocks composing the Klich intrusive occupied the MORB, IOB and MORB+IOB fields. According to Th/Y-Nb/Y, Th/Yb-Ta/Yb and La/Nb-Ti diagrams their content corresponds to the MORB. In the Th/Yb-Nb/Yb diagram the points are distributed in the area of the depleted mantle, but in Rb/Y-Nb/Y diagram they correspond to the middle and lower crust formations.

Spider diagrams of the Klich gabbro-dioritic intrusive rocks are characterized by low angle of inclination and positive Eu minima that is indicative of typical mid-acidic rocks.

Thus, from petrochemical and geochemical study of the Klich gabbro-diorite gneisses it has been established that composition of the intrusive:

1. varies between gabbro-diorites and quartz diorites;
2. corresponds to weakly differentiated low potassium series;
3. is characterized by low ratio of K_2O/ Na_2O.

In the contact zone of the Klich intrusive and the enclosing metapelitic crystalline schist the products of contact metamorphism, massive metamorphic rocks-felses are spread. 10-30m wide stripe of felses is spread around the intrusive, into the gorges of the river Klich and its right tributary the Achapara river. As a result of thermic metamorphism, in the exocontact of the intrusive are developed following parageneses: $Cor+Grt\pm Sill(Andl)\pm Spi$, $Sill+Bt\pm Spi\pm Qtz$, $Cor+Spi\pm Qtz$, there are established reactions: $St+Qtz\rightarrow Cor+Grt\pm Andl(Sill)\pm Spi+H2O$, $Ms+St+Qtz\rightarrow Sill+Bt+H_2O$, $St\rightarrow Cor+Spi$, $St\rightarrow Andl(Sill)+Spi$ and is fixed $Andl\rightarrow Sill$ inversion in them. Felses are represented in the contact zone 1-5m of the Klich intrusive by cordierite-sillimanite-spinel parageneses; in 5-20m from contact area there have developed stable mineral association of garnet-biotite-sillimanite-andalusite; in 20-90m^{-s} they are substituted more low–temperature mineral parageneses – stavrolite-biotite-andalusite-garnet.

Felse has an exotic mineral composition, as there are fixed both relicts (stavrolite, muscovite, quartz, andalusite) and newly originated minerals (cordierite, garnet, sillimanite, spinel, biotite). These rocks are very nice: black-yellowish-pinky inclusion make harmonious pattern against the grey background. Physical-chemical characteristic of these rocks; completely meet the requirement of facing stone raw material, they correspond to the (A d) I class of quality of ornamentality. Felse belongs to the most stable group of rocks and can be used for interior and exterior lining.

REFERENCES

Javakhishvili Sh.I. (1970). Schists of the southern Slope of the greater Caucasus. Proc. of GIAS GSSR. Vol. 24, 194.

Somin M.L. (1971). Prejurassic basement of the Greater Rouge out Southern Slope of the Great Caucasus. Moscow "Nauka" 245.

Shengelia D.M., Ketskoveli D.M. (1982). Low and moderate pressure metamorphism in Abkhazia. Proc. of GIAS GSSR. Vol. 78, 206.

Shengelia D.M. (2000). Mono-and polycycle regional metamorphism of crystalline basement of the Caucasus. Proc. of of GIAS GSSR. New ser.vol.115, 282-299.

P 3.20

Metamorphism of the polarural precambrian rocks

Ulyasheva Natalia

Institute of Geology Komi Science Centre Ural Division Russian Academy of Scienses, Pervomayskaya 54, Syktyvkar (nsulasheva@geo.komisc.ru)

There are blocks of the Early Proterozoic crust in the north of the Urals represented by deeply metamorphosed amphibolites, schists, and gneisses of the harbeysky complex. Petrographic and micromineralogical studies of amphibolites and amphibole schists allowed to distinguish several generations of mineral formations using a scanning electron microscope JSM – 6400.

In massive and weakly foliated amphibolites major rock – forming minerals are green amphibole of the pargasite – hastingsite series, oligoclase, and andesine. Quartz grains, clinozoisite and chlorite are rare, the last one often replaces amphibole at the edges. Garnet (high – calcium pyrope – almandine), clinozoisite, biotite, chlorite, and muscovite are distributed along with blue – green and light green amphiboles of the series pargasite – hastingsite in foliated amphibolites. Albite forms porphyroblasts and also is presented in the form of tabular grains in the intergranular space. Chlorite and muscovite are developed perpendeculary to the schistosity and often replace garnet, indicating their later forming. Schists were found in local areas and were divided into mainly amphibole, quartz – amphibole, garnet – muscovite – chlorite – clinozoisite – amphibole, and garnet – glaucophane – albite species with the presence of bluish – green, light green amphiboles of the pargasite – hastingsite series, and pale green actinolite.

As a result the minerals parageneses formed under different thermobaric conditions were distinguished. They are pargasite – hastingsite + oligoclase (andesine), pargasite – hastingsite + albite + garnet, pargasite – hastingsite + albite + garnet + clinozoisite, garnet + glaucophane, actinolite + chlorite + clinozoisite, muscovite + chlorite + clinozoisite + quartz. Calculations of thermodynamic parameters of the amphibolites metamorphism were performed using the TPF program developed by A. N. Konilov, A. A. Grafchikov (Institute of Experimental Mineralogy, Chernogolovka), and based on a system of agreed goetermometers and geobarometers, in which the minerals compositions are used in a variety of mineral associations. We applied plagioclase – amphibole (Holland & Blundy 1994; Jaques et al. 1982), garnet – amphibole (Lavrentyeva & Perchuk 1989; Powell 1985; Wells 1979) geotermometers, and also amphibole (Hammarstrom & Zen 1986; Hollister et al. 1987; Schmidt 1991) and plagioclase – amphibole (Fershtater 1990) geobarometers. As a result it was found that temperatures generally range from 600 to 7900 in accordance with the pargasite – hastigsite + oligoclase mineral assemblage, in rare cases they are lower. The pressure is 5,5 – 10,0 kbar in the massive and weakly foliated amphibolites. Conditions of the amphibole and plagioclase metamorphism from these rocks correspond to high stages of moderate pressure amphibolite facies.

The garnet – containing parageneses of foliated amphibolites correspond to low stages of metamorphism amphibolite and epidote – amphibolite facies (T 480 – 6400) of increased pressures (P 8 – 12 kbar). The rocks were exposed to low temperature changes in the epidote – amphibolite and green schist facies conditions in local areas. Thus the harbeysky complex rocks experienced a polimetamorphism in conditions of the moderate pressure high temperature amphibolites, epidote – amphibolite facies, and low – temperature changes.

Was supported by program of fundamental research Russian Akademy of Scienses N° 12-И-5-2022 und youth project Ural Division of RAS № 11-5-НП-43.

REFERENCES

Fershtater, G. B. 1990: Empirical plagioclase – hornblende barometer. Geochemistry, 3, 328.

Hammarstrom, J.M. & Zen, E. An. 1986: Aluminium in hornblende: an empirical igneous geobarometer. Amer. Mineral., 71, 1297–1313.

Holland, T. & Blundy, J. 1994: Non-ideal interactions in calcic amphiboles and their bearing on amphibole-plagioclase thermometry. Contrib. to Mineral. and Petrol., 116, 433–447.

Hollister, L. S., Grisson, G. C., Peters, E. K. et al. 1987: Confirmation of the empirical correlation of Al in hornblende with pressure of solidification of calc-alkaline plutons. Amer. Mineral., 72, 231–239.

Jaques, A. L., Blake, D. H., Donchak, P. J. T. 1982: Regional metamorphism in the Selwyn Range area, north-west Queensland. BMR J. of Austral. Geol. and Geophys., 7–3, 181–196.

Lavrentyeva, I. V., Perchuk, L. L. 1989: Experimental study of amphibole-garnet equilibrium <calcium-free system>. Dokl. Akad. Nauk USSP, 306–1, 173–175.

Powell, R. 1985: Regression diagnostics and robust regression in geothermometer / geobarometer calibration: the garnet-clinopyroxene geothermometer revisited. J. of Metamor. Geol., 3, 231–243.

Schmidt, M. W. 1991: Experimental calibration of the Al-in-hornblende geobarometer at 6500 C, 3.5-13.0 kbar. Terra abstracts, 3–1, 30.

Wells, P. R. A. 1979: P-T conditions in the Moines of the Central Highlands, Scotland. J. Geol. Soc. London, 136, 663–671.

P 3.21

The Madneuli polymetallic deposit, Bolnisi district, Georgia: Evidence for a magmatic input in a submarine, transitional hydrothermal system.

Stefano Gialli [1], Robert Moritz [1], Nino Popkhadze [2], Vladimer Gugushvili [2], Ramaz Migineishvili [2], Jorge Spangenberg [3]

[1] *Earth and Environmental Sciences, University of Geneva, Switzerland*
[2] *A. Djanelidze Institute of Geology, Tbilisi, Georgia*
[3] *Institute of Mineralogy and Geochemistry, University of Lausanne, Switzerland*

The Late Cretaceous Madneuli polymetallic deposit is located in the Bolnisi district, southern Georgia and hosted by a volcanogenic sedimentary subaqueous sequence. The Bolnisi district is located in the Somkheto-Karabakh island arc of the Lesser Caucasus, which extends towards the West in the Eastern Pontides, Turkey. The origin of the Madneuli deposit is controversial. In order to constrain its genesis, we have undertaken a detailed study of ore paragenesis and alteration combined with a stable isotope investigation.

Two different ore types are recognized at the Madneuli deposit (Fig. 1):

a) A subvertical stockwork part, constituted mainly of pyrite, chalcopyrite and sphalerite with enargite in the core of the system. Quartz and abundant barite are the main gangue minerals. A stratiform, massive sulfide orebody and sandstone lenses cemented by barite are located on the top of the stringer zone; the massive sulfide body is characterized by a sphalerite, galena, chalcopyrite, pyrite and tennantite-tetrahedrite assemblage. The alteration halo surrounding this ore zone is composed of a strongly silicified core, grading out into a quartz-sericite-pyrite zone and an outer quartz-chlorite-sericite zone. Drilling has intersected a Late Cretaceous granodiorite to quartz-diorite porphyry intrusion 800-900 m below this ore zone.

b) Subvertical pyrite-chlorite-hematite-gold±chalcopyrite veins occur on the eastern flank of the open pit and are mainly mined for gold. Native gold is associated with telluriumbismuthite contained in pyrite, or as intergrowths with hypogene hematite. Silicified platy calcite occurs locally and documents boiling conditions. The alteration assemblage is formed by quartz-chlorite-pyrite and confined to the immediate proximity of the veins.

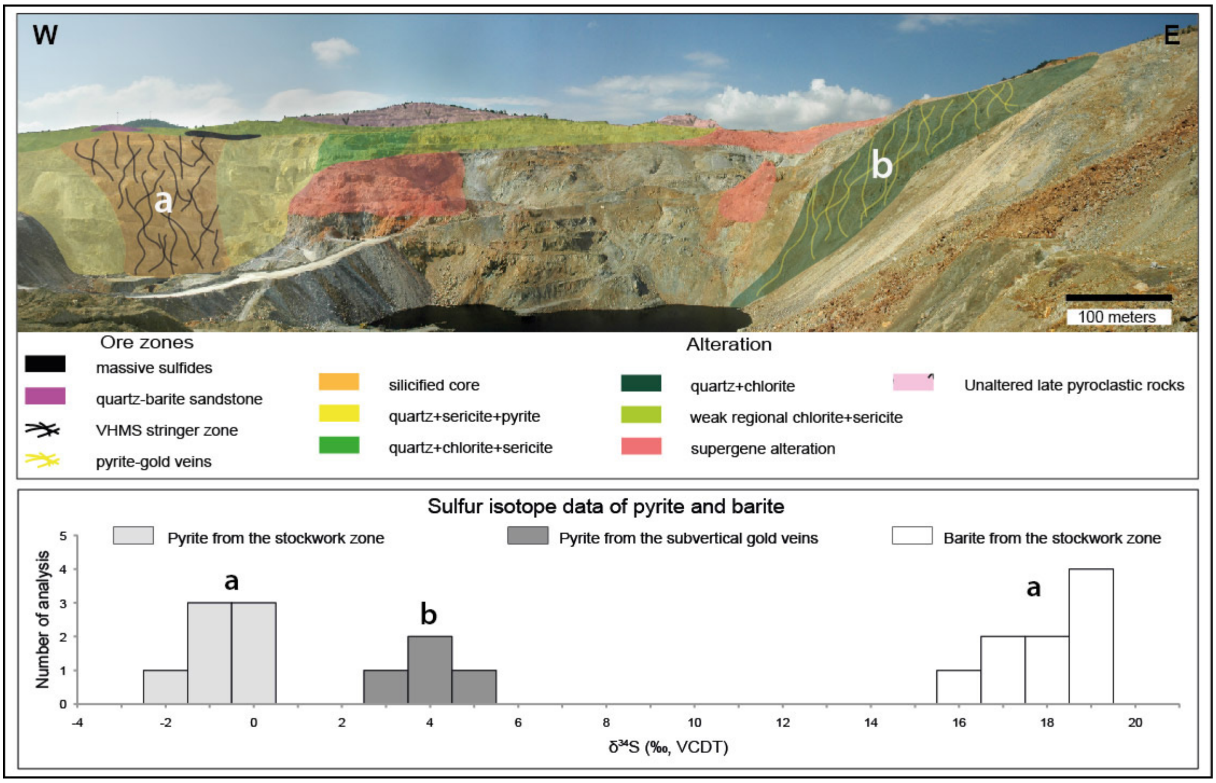

Fig. 1 – Correlation between ore zones, hydrothermal alteration distribution and sulfur isotopic composition of pyrite and barite in the Madneuli open pit.

Pyrite from the stockwork and massive sulfide orebodies has $\delta^{34}S$ values from -2 to 0‰, and pyrite from the gold-bearing subvertical veins has $\delta^{34}S$ values between +3 and +5‰. Barite from the stockwork area has $\delta^{34}S$ values between +16 and +19‰. Our results, except the negative pyrite values from the stockwork orebody, are consistent with those obtained in other studies for Late Cretaceous VHMS deposits in the Eastern Pontides.

The combined field, petrographic and isotope data, show that the Madneuli ore deposit consists of the tight spatial association of two ore forming events: one which forms the subvertical stockwork (Fig. 1 zone a), and an event interpreted as epithermal responsible for the subvertical veins in the eastern flank (Fig. 1 zone b).

The negative sulfur isotope values in pyrite and the presence of enargite in the stringer zone (Fig. 1 zone a) could be attributed to a magmatic input, akin to interpretations proposed for submarine mineralizing systems in the Western Pacific. The Madneuli ore deposit reflects transitional ore formation processes under shallow submarine to emerging conditions in a rifting volcanic arc.

P 3.22

The Gedabek epithermal Cu-Au deposit, Lesser Caucasus, Western Azerbaijan: geology, alterations, petrography and evolution of the sulfidation fluid states.

Hemon Pierre[1], Moritz Robert[1] & Ramazanov Vagif[2]

[1] *Earth and Environmental Sciences, University of Geneva, Switzerland (hemon.pierre@gmail.com)*
[2] *Baku State University, Azerbaijan*

The Gedabek-Karadagh ore district is one of the main producing mining districts of Western Azerbaijan, and is the largest porphyry-epithermal ore field of the country. It belongs to the Lesser Caucasus, located in the central part of the Tethyan metallogenic belt. It is emplaced within the Jurassic-Cretaceous Somkheto-Karabakh magmatic arc, resulting from the subduction of the Tethys Ocean along the Eurasian margin (Sosson et al., 2010).

The Gedabek ore deposit has been exploited since the 19th century, first for copper and silver, and nowadays for gold by open pit mining. This deposit is still controversial, and previously, it was classified as a porphyry deposit, and more recently as a high-sulphidation epithermal deposit. The ore body consists of a flat lens-shaped silicified-body emplaced between Middle Jurassic andesitic volcanoclastic rocks and a Late Jurassic granodiorite. Several generations of mafic to intermediate dikes, as well as dikes with a breccia texture, crosscut the volcanoclastic rocks and the granodiorite. Their relationship with the mineralizing process is still unclear.

This study aims at constraining the tectonic setting of the deposit using lithogeochemistry of the various magmatic country rocks, characterizing the hydrothermal alteration and the ore paragenesis, as well as the nature of the fluids involved in the ore formation processes.

Lithogeochemistry based on immobile elements suggests a sub-alkaline magmatic setting with basaltic to andesitic compositions. Our study questions the primary magmatic nature of the so-called “quartz-porphyry” intrusion, which hosts the main orebody, and rather suggests that this rock is the product of extensive silicification. Field observations reveal a strong lithological control (more permeable horizons) for silicification processes, as well as the propylitic alteration, within bedded pyroclastic rocks. X-Ray diffraction analyses revealed a late argilic alteration crosscutting the silicified body with the presence of dickite and kaolinite.

A preliminary petrologic study allowed us to distinguish two main mineralization events. An early pervasive silicification composed of microcrystalline quartz and adularia, associated with disseminated pyrite and low ore grades. A later semi-massive to veins or veinlets minerazation composed mainly of sphalerite and chalcopyrite, and subsidiary fahlore, galena and arsenopyrite. Chalcocite and covellite are spatially associated with chalcopyrite and sphalerite, and are attributed to secondary enrichment of hypogene origin, as indicated by the presence of some enargite.

Rare native gold has been observed associated to the second event. But ICP-AES analyses yield a strong correlation between Au, Bi and Te, distinctly higher than between Au and Ag. It suggests an association of Au and Ag mainly with Te-Bi enriched minerals rather than in electrum or native gold. Variable but high contents of volatile elements (Te, Se, Hg, Sb, As) are consistent with a shallow epithermal environment.

Petrological observations and microprobe measurements of the FeS content of sphalerites indicate an intermediate state of the fluids, within a quartz-adularia-sericite-calcite deposit, with an evolution from lower toward higher sulfidation state (Einaudi et al., 2003; Simmons et al., 2005; Sillitoe & Hedenquist, 2003).

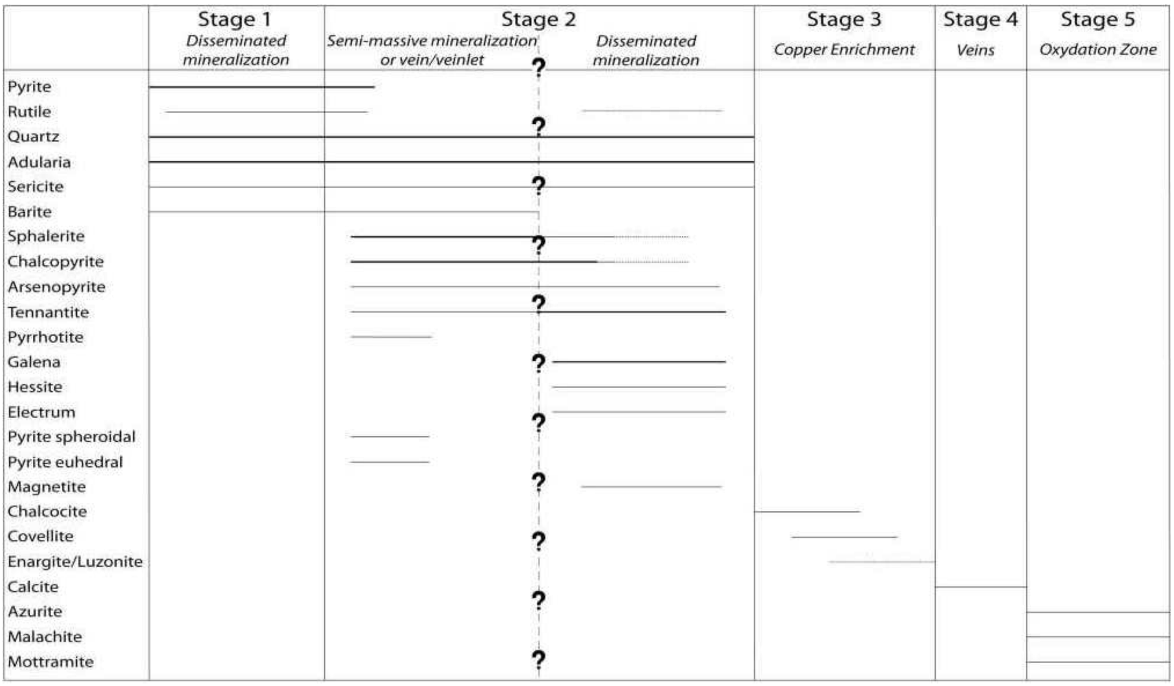

Figure 1. Paragenetic sequence from the Gedabek ore deposit; Thick bars: dominant minerals; Thin bars: Minor mineralization; Doted bars: Rare to uncertain.

REFERENCES

Einaudi, M.T., Hedenquist, J.W. & Inan, E.E. 2003: Sulfidation state of fluids in active and extinct hydrothermal systems: Transitions from porphyry to epithermal environments. SEG Special Publication, 10.

Sillitoe, R.H. & Hedenquist, J.W. 2003: Linkages between volcanotectonic settings, ore-fluid compositions, and epithermal precious metal deposits. SEG Special Publication, 10.

Simmons, C.F, White, N.C. & John, D.A. 2005: Geological characteristics of epithermal precious and base metal deposits. Economic Geology, 100th Anniversary Volume, 485-522.

Sosson et al. 2010: Subductions, obduction and collision in the Lesser Caucasus (Armenia, Azerbaijan, Georgia), new insights. Geological Society of London, Special Publication, 340, 329-352.

P 3.23

Present copper-rich "gel" formation in the giant porphyry copper deposit of Chuquicamata (northern Chile)

Lambiel Frédéric[1], Bernhard Dold[2] & Lluís Fontboté[3]

[1] *Institut de Minéralogie et Géochimie, University of Lausanne, Bâtiment Anthropole, CH-1015 Lausanne (frederic.lambiel@unil.ch)*
[2] *FCFM-Departamento de Geología, Universidad de Chile, Plaza Ercilla 803, Santiago de Chile, Chile (bdold@ing.uchile.cl)*
[3] *Earth and Environmental Sciences, University of Geneva, Rue des Maraîchers 13, CH-1205 Genève (Lluis.Fontbote@unige.ch)*

In the frame of a project focused on supergene processes in the Chuquicamata deposit (Pinget et al., 2011 and 2012), copper-rich "gel" crusts that are presently precipitated in the exotic deposit of Mina Sur, south of the Chuquicamata porphyry deposit (Fig. 1A, 1B), are studied.

The "gels" are precipitated from moderately saline waters containing up to several 100 mg Cu/l. Three groups of copper-rich "gels" (up to 61% Cu in weight, Table 1) have been distinguished according to the pH of the waters from which they precipitate. In "gels" formed from waters with pH between 5.8 and 6.0, posnjakite ($Cu_4 (SO_4)(OH)_6$), brochantite ($Cu_4(SO_4)(OH)_6$), malachite ($Cu_2(CO_3)(OH)_2$) and possibly dioptase $CuSiO_2(OH)_2$ were identified using XRF, XRD, SEM and ESEM analyses. In "gels" precipitating from waters with pH between 7.2 and 7.7, devilline ($CaCu_4(SO_4)_2(OH)_6{*}3(H_2O)$) is mainly present. A third group of "gels" consists mainly of atacamite ($Cu_2Cl(OH)_3$) and were precipitated of water with a pH of 5.7. In addition to the above copper minerals, the "gels" contain also gypsum, a not yet identified sodium sulphate, and halite (Fig. 2A). The sodium sulphate occurs as lenticular crystals (Fig. 2A) and as efflorescent aggregates (Fig. 2B).

Table 1 : Semi quantitative analyses of "gel" sampled at Mina Sur (XRF, using UniQuant,in wt-%). Part of the aluminium content may be due to clay particles transported in suspension and incorporated in the gel crusts.

Gels sample	pH	Na2O	MgO	Al2O3	SiO2	MnO	Fe2O3	P2O5	K2O	CaO	SO3	Cl	Cu	Zn
2Nord	7.2 to 7.7	b.d.	0.3	5.3	1.7	0.1	0.5	b.d.	0.3	2.4	15.7	1.3	57.5	0.1
2Sud	7.2 to 7.7	b.d.	0.8	1.4	6.2	0.1	1.1	b.d.	0.8	5.4	19.8	1.6	49.4	0.5
7C1	5.8 to 6.0	5.2	2.3	3.1	3.5	0.1	0.8	b.d.	0.9	7.4	23.4	3.3	39.1	0.4
7C2	5.8 to 6.0	b.d.	1.0	3.0	2.3	0.1	0.7	b.d.	0.8	6.9	21.7	3.4	47.1	0.4
EX2	5.7	b.d.	b.d.	2.7	2.8	0.1	0.4	0.3	0.1	0.5	2.5	13.4	61.6	0.1

(b.d. = below detection limit)

The possibility of using the precipitation mechanisms of the present copper gels as analogue for the formation of copper minerals in the exotic Mina Sur is examined.

Acknowledgements
The project is carried out with funding of the Swiss National Science Foundation (grant 129988) and of the Fondation A. Lombard, and with the support of the Geology Department of the Chuquicamata mine (CODELCO). Help of M. Dadras, Neuchâtel (ESEM), and of P. Vonlanthen and T.Adatte, Lausanne (SEM and XRD) is acknowledged.

REFERENCES

Pinget M.C., Fontboté L, Dold B, Ramirez F, Vergara M. 2011: The supergene enrichment at Chuquicamata revisited. Proceedings 11th SGA Biennal Meeting, Antofagasta, Chile, p. 823-825.

Pinget M.-C., Dold B., Fontboté L., Vergara M., Rojas de la Rivera J. (2012). Mineralogía de la mineralización exótica en Chuquicamata: nuevos avances. Proceedings 13th Congreso Geológico Chileno, Antofagasta, Chile: 37-39.

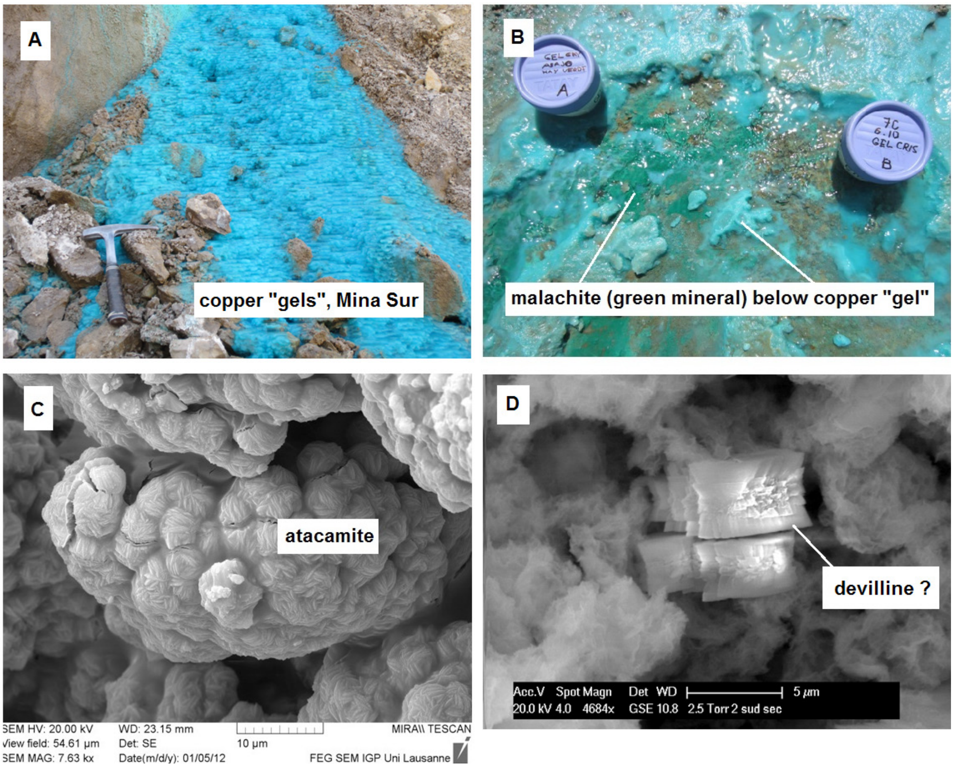

Figure 1 : A) Outcrop of copper rich "gel" being precipitated from water with pH between 7.2 and 7.7 (Mina Sur). B) Malachite overgrown by copper "gel" precipitated from water with pH between 5.8 and 6.0 .C) SEM photograph of atacamite precipitated from a water with pH of 5.7. D) ESEM photograph of "gel" with a probable devilline aggregate

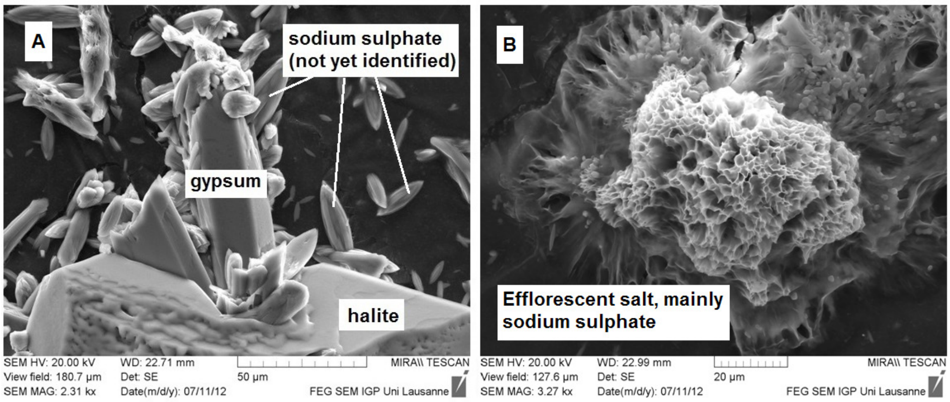

Figure 2: Phases formed by drying gels formed from water with pH between 7.2 and 7.7. Microscope observation shows that the phases precipitate in the following order: gypsum, sodium sulphate and halite.

P 3.24

New mineralogical and fluid inclusion genetic constraints for Archean batholith-hosted gold veins at the Lac Herbin deposit, Val-d'Or, Canada

Rezeau Hervé[1], Moritz Robert[1], Beaudoin Georges[2], & Gobeil Claude[3]

[1] *Section des sciences de la Terre et de l'Environnement, Université de Genève, Rue des Maraîchers 13, 1205 Genève*
[2] *Département de géologie et de génie géologique, Université Laval, Québec, Canada*
[3] *QMX Gold Corporation, exploration office, Val-d'Or, Québec, Canada*

The Val-d'Or district is a major quartz-tourmaline-carbonate gold-bearing vein field, which occurs in the Archean Abitibi greenstone belt, Superior province, Canada. The district underwent regional greenschist to amphibolite metamorphism and the mineralized veins post-date metamorphism. The Lac Herbin mine consists of a network of parallel steep reverse faults, hosted by the synvolcanic Bourlamaque granodiorite batholith. There are two related vein sets: subvertical veins in ductile shears with banded textures formed by one or more episodes of filling, and subhorizontal veins in extensional fractures between shear zones with typical open-space filling textures. Veins are surrounded by zoned alteration envelopes consisting of an outer zone of cryptic alteration characterized by a chlorite-carbonate-white mica assemblage, and an inner zone of visible alteration characterized by a carbonate-white mica-albite. This study presents detailed mineral paragenetic and fluid inclusion study of a gold deposit hosted by the Bourlamaque batholith in the Val-d'Or district.

The paragenetic sequence is typical for the Val-d'Or district, characterized by a vein filling deposition of carbonate, tourmaline, pyrite, pyrrhotite +/- chalcopyrite, sphalerite and cobaltite, chlorite, sericite and quartz. Pyrite contains inclusions of gold, chalcopyrite, tellurobismuth, pyrrhotite and cubanite. However, most of the gold, chalcopyrite and tellurobismuth associated with Ca-Fe-Mg-Mn-bearing carbonates were deposited into fractures in deformed pyrite, but the two types of gold have similar Au/Ag ratios (90/10). The gold-tellurobismuth filling fractures in pyrite at Lac Herbin are reminiscent and could illustrate the process described by Frost et al. (2002), who interpret them as a result of melt coexisting with hydrothermal fluids.

Fluid inclusion petrography outlines five fluid inclusion types in quartz: (1) three-phase L-L-V (H_2O-CO_2) ; (2) two-phase CO_2-rich ; (3) high temperature two-phase H_2O-rich ; (4) low temperature three-phase saline and (5) low temperature two-phase H_2O-rich. Inclusion types 1 and 2, which occur together, were described in other studies from the Val-d'Or district, whereas the timing of type 3 remains uncertain. Inclusion types 1 and 2 are arranged in three dimensional clusters unrelated to fractures in quartz crystal whereas type 3 are observed both alone in quartz crystal and in healed fractures. They post-date inclusion types 4 and 5 which are only related to fractures.

In terms of an exploration guide, the presence of chalcopyrite is a good indicator for auriferous mineralization, in addition to the well-constrained regional structural setting.

REFERENCES

Frost B. R., Mavrogenes J. A. and Tomkins A. G. 2002: Partial melting of sulfide ore deposits during medium- and high-grade metamorphism. Canadian Mineralogist, 40, 1-18.

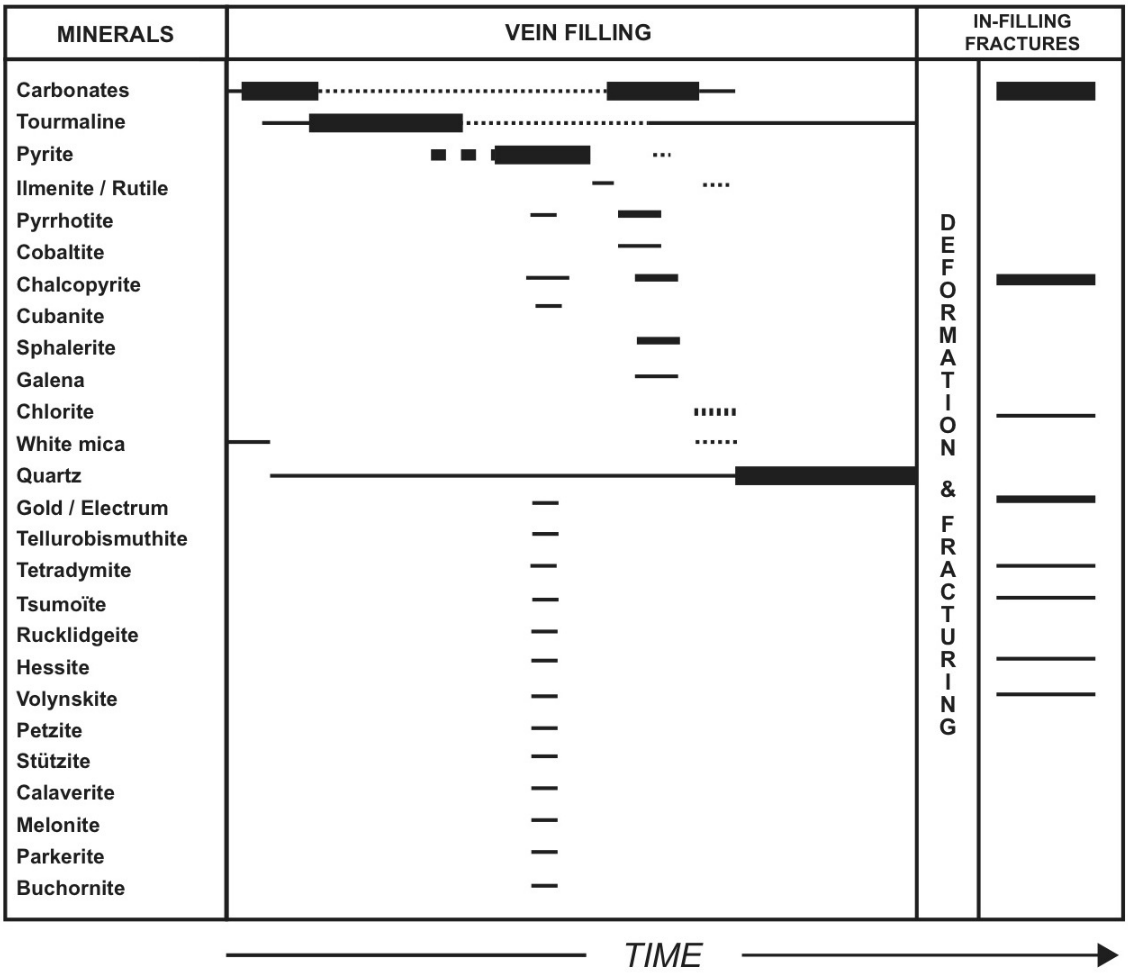

Figure 1. Paragenesis sequence recognized in the Lac Herbin deposit.

P 3.25

Reactivation of fault zones in Precambrian crystalline basement and the location of stratabound, sandstone-hosted Pb-Zn deposits along the front of the Scandinavian Caledonides.

Nicolas Saintilan[1], Michael B. Stephens[2], Lluís Fontboté[1], Erik Lundstam[3]

1University of Geneva, Department of Earth and Environmental Sciences, Mineralogy Department, Rue des Maraîchers 13, 1205 Genève, Switzerland (nicolas.saintilan@unige.ch)
2Geological Survey of Sweden (SGU), Box 670 SE-751 28 Uppsala, Sweden
3Boliden Mineral AB, SE-776 98 Garpenberg

Non-stratiform yet stratabound, sandstone-hosted Pb-Zn deposits and minor occurrences are known along the front of the Scandinavian Caledonides over a distance of more than 1000 km and include the Laisvall and Vassbo deposits. Mineralisation is emplaced in the Ediacaran-Cambrian autochthonous sedimentary rocks beneath the Caledonian thrust nappes resting unconformably on top of Precambrian crystalline basement, as well as in the lowermost allochthonous units.

The present study is part of a broader project aiming to assess the role of the basement, the migration flow path, the driving force, the precipitation mechanism, and the age of mineralisation in a structurally-constrained geological frame. It is based on abundant drilling and mine data as well as on existing and new geochemical data.

In this work we present data aiming to understand the structural and tectonic controls of the ore distribution at the Laisvall stratabound Pb-Zn deposit, hosted in autochthonous sandstone. Magnetic lineaments, which correspond to geological features in the Precambrian crystalline basement, were identified in airborne magnetic data. Magnetic maxima match the main regional geological trends (N-S to NNE-SSW and NW-SE trends) in the Precambrian basement (rock units, ductile deformation zones and foliation). There is a correlation between some magnetic minima and faults in the Precambrian basement (e.g. the Hornavan fault). A similar correlation between certain magnetic minima and faults in the Ediacaran-Cambrian sedimentary cover rocks was revealed by geological modelling of the Laisvall deposit in 3D space. The magnetic maxima show inflection areas that correspond to locations where their trend changes from NNE-SSW to NW-SE. Mineralisation at Laisvall is closely associated with such inflection areas as shown by ore grade modelling.

In addition, and in order to examine the possibility of an analogue feeder for Laisvall-type deposits, a detailed structural analysis was conducted on the Åkerlandet Pb-Zn-Ba-F vein deposit hosted in the Precambrian crystalline basement.

Airborne magnetic data and 3D modelling of ore grades and geology suggest that mineralisation is related to faults in the Precambrian crystalline basement. These data are consistent with the hypothesis that faults provided channelways during mineralisation after deposition of an aquitard on top of the host rock. The faults were active during Ediacaran-Cambrian sedimentation. Current work is examining the possibility that ore is related to extensional domains along the faults.

REFERENCES

Lilljequist, R. 1973: Geological map of the Laisvall area, Southern Norbotten, Swedish Lappland. Scale 1:50,000. Sveriges Geologiska Undersökning (SGU), Serie C nr 691.

Rickard, D.T., Willdén, M.Y., Marinder, N.E. & Donnelly, T.H. 1979: Studies on the genesis of the Laisvall sandstone lead-zinc deposit, Sweden. Econ. Geol., v.74, p.1255-1285.

Willdén, M.Y. 1980: Paleoenvironment of the autochthonous sedimentary rocks sequence at Laisvall, Swedish Caledonides. Doctoral thesis, Stockholms Universitets Geologiska Institutionen.

P 3.26

Isotope composition of lacustrine vapour of Lake Geneva

Decrouy Laurent[1], Bourquard Maël[1] & Vennemann Torsten [1]

[1] *Institut des sciences de la Terre, Université de Lausanne, Geopolis, CH-1015 Lausanne (laurent.decrouy@unil.ch)*

The measurement of isotope compositions of water ($\delta^{18}O$ and $\delta^{2}H$) has become a routine in many fields of Earth science such as hydrology, hydrogeology, and (palaeo)climatology. Yet, the evolution of the isotope composition of water vapour in continental settings is still poorly known. It has clearly been established that the original isotope composition of continental water vapour is controlled by the meteorological conditions during evaporation above the oceans and that the subsequent evolution is mostly controlled by condensation and rainout as the air mass travels across the continent. However, for air masses that have a low amount of moisture, the evapotranspiration above the continents has a strong influence on its isotope composition. This is particularly valid above big lakes where a significant proportion of moisture comes from the evaporation of surface water. As most of these air masses do not produce rain in the location of evaporation, the evolution of the isotope composition of this contribution has rarely been studied. Isotopic analysis of atmospheric vapour may, however, help scientists to better understand the influence of big lakes on the regional climate. It may also provide a better estimate of lake water loss through evaporation.

A preliminary study on the isotope composition of water vapour in the region of Lake Geneva was conducted in 2011 and 2012. A method was developed to sample water vapour and to analyse its isotope composition. The final aim of the project is to estimate the influence of evaporation of lake water on the atmospheric water vapour, to describe the isotopic fractionation during evaporation, and to estimate the influence of evaporation on the isotope composition of water in Lake Geneva.

Atmospheric water vapour was sampled with 2 l vacuum-sealed bottles. Samples were collected from a sailing boat at approximately 4 km south of Lausanne. For each sampling, 3 to 5 samples were collected along an elevation profile (0.3 to 10 m above water surface) to sample the 'lacustrine atmosphere'. In addition, 1 to 3 samples were collected on land at different sites (Echichens 470 m alt., Sauvabelin Tower 700 m alt., and Cugy 700 m alt.) to sample the 'free atmosphere'. For each sample, relative air humidity and temperature were measured. Surface lake water was also sampled and its temperature recorded. Water was then extracted from each bottle in the laboratory using a vacuum line. One bottle provided between 5 to 30 µl depending on the humidity. For the measurement of the isotope composition of water vapour, subsamples of 1.5 µl were injected manually into a Picarro L2102-i WS-CRDS system. For each sample, 8 injections were done and the last 5 used to calculate the values. Analytical errors are estimated to be 0.2 ‰ and 1.0 ‰ for $\delta^{18}O_{vapour}$ and $\delta^{2}H_{vapour}$, respectively. The isotope composition of water vapour originating from evaporation of surface lake water ('lake vapour') was calculated using the isotope composition and temperature of surface lake water, relative humidity measured just above the lake surface, and fractionation factors given in Majoube (1971) and Merlivat (1978).

Most samples show that the lacustrine atmosphere contains more water vapour and has lower water vapour isotope composition than the free atmosphere (Figure 1). Besides, calculated values for lake vapour are substantially depleted in the heavy isotopes compared to the atmospheric values. While air moisture increases near the water surface, the isotope composition of water vapour above the lake surface is homogenous from 0.3 to 10 m. Higher values were measured during summer while lowest values were measured during winter.

Lower values for lacustrine atmosphere are interpreted as being due to the addition of lake vapour to the free atmosphere. Based on oxygen isotope results, the contribution of water evaporated from the lake to the lacustrine atmosphere is estimated to range between 34 and 57 %. Because of the very dynamic behaviour of atmospheric processes, further studies including continuous measurements of water vapour are needed to better understand the influence of evaporation on the regional atmosphere and the evolution of surface lake water.

REFERENCES

Majoube, M. 1971: Fractionnement en oxygène-18 et en deuterium entre l'eau et sa vapeur. Journal of Chemical Physics, 10, 1423-1436.

Merlivat, L. 1978: Molecular diffusivities of H2 16O, HD16O and H2 18O in gases. Journal of Chemical Physics, 69, 2864-2871.

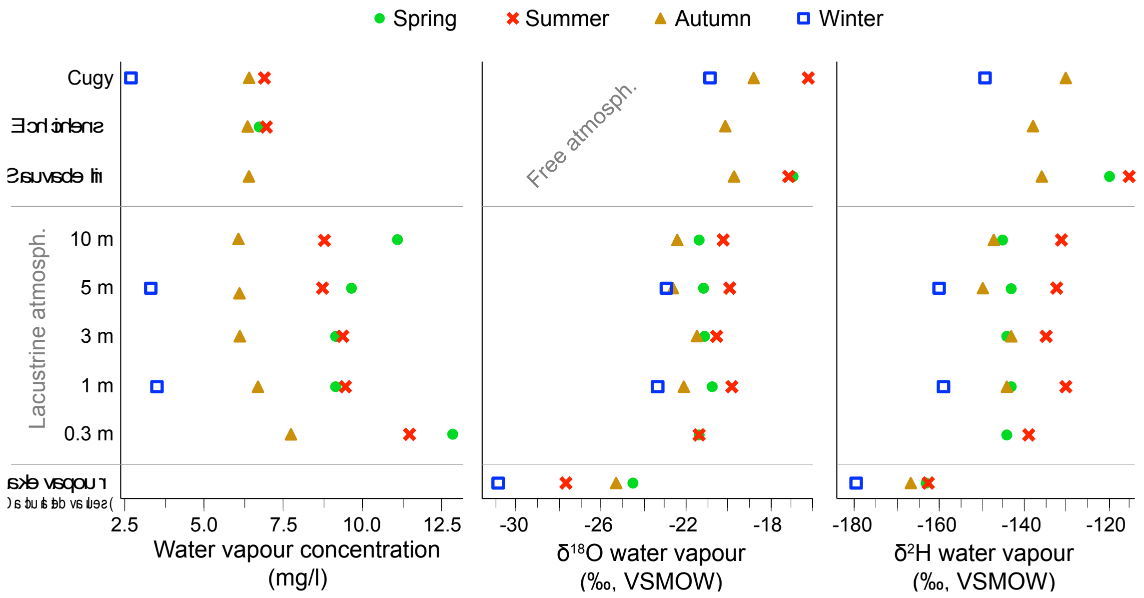

Figure 1. Concentration and isotope composition of atmospheric water vapour measured along elevation profiles above the lake surface and at different sites on land. Values calculated for water vapour originating from the evaporation of surface lake water (lake vapour) is also illustrated for comparison.

P 3.27

Thermal ionisation mass spectrometric determination of the $^{40}K/^{39}K$ ratio

Maria O. Naumenko[1], Klaus Mezger[1], Thomas F. Nägler[1], Igor M. Villa[1,2]

[1] *-Institut für Geologie, Universität Bern, Switzerland*
[2] *-Università di Milano Bicocca, Italy*

The isotope ^{40}K is radioactive and undergoes β- decay to ^{40}Ca (ca. 89.3%) and electron capture to ^{40}Ar (ca. 10.7%). Both decays can potentially be used as dating systems. The most commonly used branch is the decay of ^{40}K to ^{40}Ar because it can yield highly precise ages. Both decay schemes rely on the knowledge of the ^{40}K branching ratio and the natural ^{40}K abundance.

A ^{40}K abundance of 0.011672±41 % was measured on terrestrial material [1]. The relative uncertainty of 0.35 % has not been improved since. Recent improvements in the precision of mass spectrometric measurements have led to the situation that the uncertainties on the K decay constant and the abundance of ^{40}K are a major source of uncertainty on the measured ages. A more precise definition of the ^{40}K decay constant was attempted by different research groups within the last decade [2-9] but the goal of obtaining 0.1 % relative uncertainty on K-Ar ages for geological materials, as requested by the EARTHtime initiative, has not been achieved yet. In order to improve on this situation we studied the abundances of the K isotopes in terrestrial standards.

A ThermoFischer Triton+ thermal ionisation mass spectrometer was used for K isotope ratio measurements of the NIST SRM 918b K standard loaded on Ta filaments with 0.1M phosphoric acid. Three techniques were applied: (A) dynamic measurement with in-run normalisation to the IUPAC value $^{41}K/^{39}K=0.072168$; (B) a simple total evaporation procedure; (C) the “NBL-modified” total evaporation [10]. The ^{40}K ion beam was measured in a Faraday cup with a 1E12 Ω resistor; ^{39}K and ^{41}K were collected in Faraday cups with 1E11Ω resistors. Amplifier gains were intercalibrated by supplying fixed voltages off-line. Different measurement techniques were combined with different loading procedures. We also tested ionisation yields for the evaporation procedures (B) and (C).

Our measured $^{40}K/^{39}K$ ratios are statistically indistinguishable from those reported by [1] but have lower uncertainties. Techniques A, B and C gave 1 standard error of 0.07%, 0.2%, and 0.14%, respectively.

REFERENCES

1. Garner E.L. et al. (1975) J.Res.Natl.Bur.Stand.79A, 713-725.
2. Min K. et al. (2000) Geochim. Cosmochim. Acta 64, 73-98.
3. Nägler T.F., Villa I.M. (2000) Chem. Geol. 169, 5-16.
4. Kwon J. et al. (2002) Math.Geol. 34, 457-475.
5. Grau Malonda A., Grau Carles A. (2002) Appl. Radiat. Isot. 56, 153-156.
6. Kossert K., Günter E. (2004) Appl.Radiat.Isot.60, 459-464.
7. Krumrei T.V. et al. (2006) Chem.Geol. 227, 258-273.
8. Renne P.R. et al. (2010) Geochim. Cosmochim. Acta 74, 5349-5367.
9. Schwarz W.H. et al. (2011) Geochim. Cosmochim. Acta 75, 5094-5096.
10. Richter S., Goldberg S.A. (2003) Int. J. Mass Spect. 229, 181-197.